

**STRUCTURE RHEOLOGY OF
POLYETHYLENE OXIDE SOLUTION**

A Thesis

**Submitted to the College of Engineering
of Al-Nahrain University in Partial Fulfillment
of the Requirements for the Degree of
Master of Science in
Chemical Engineering**

by

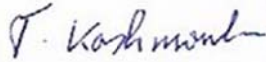
**ESTABRAQ SAAD K. AL-GERTAN
B. Sc. in Chemical Engineering 2009**

Gumada Al-Ulla
April

1433
2012

Certification

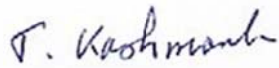
I certify that this thesis entitled "**Structure Rheology of Polyethylene Oxide Solution**" was prepared by **Estabraq Saad Kamil** under my supervision at Al-Nahrain University/ College of Engineering in partial fulfillment of the requirements for the degree of Master of Science in Chemical Engineering.

Signature: 
Name: Prof. Dr. Talib B. Kashmoula
(Supervisor)
Date: 21/5/2012

Signature: 
Name: Asst. Prof. Dr. Basim O. Hasan
(Head of Department)
Date: 2/5/2012

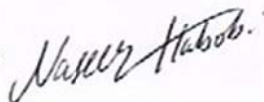
Certificate

We certify, as an examining committee, that we have read this thesis entitled "Structure Rheology of Polyethylene Oxide Solution", examined the student (Estabraq Saad Kamil) in its content and found it meets the standard of thesis for the degree of Master of Science in chemical Engineering.

Signature: 

Name: Prof. Dr. Talib B. Kashmoula
(Supervisor)

Date: 2 / 5 / 2012

Signature: 

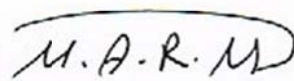
Name: Asst. Prof. Dr. Naseer A.
Al-Habobi
(Member)

Date: 2 / 5 / 2012

Signature: 

Name: Asst. Prof. Dr. Khalid A. Sukkar
(Member)

Date: 8 / 5 / 2012

Signature: 

Name: Asst. Prof. Dr. Muhannad
A.R. Mohammed
(Chairman)

Date: 2 / 5 / 2012

Approval of the College of Engineering

Signature: 

Name: Prof. Dr. Muhsin J. Jweeg
(Dean)

Date: 3 / 5 / 2012

Abstract

Intrinsic viscosities, condition for the transition from particle to network solution (critical molecular weight), viscoelastic properties, and drag reduction have been studied for polyethylene oxide in water which is widely used in industrial applications. The polyethylene oxide (PEO) samples had two different structures, the first one was linear and covers a wide range of molecular weight of (1-8000) kg/mol and the other one was branched and had molecular weights of 0.55 and 40 kg/mol.

Intrinsic viscosities and Huggins constants have been determined for all types at 25°C using a capillary viscometer. It was found that the values of Mark-Houwink parameters (K and a) increase with increasing the molecular weight for both types linear and branched PEO. Measurements of critical molecular weight and viscoelastic properties have been carried out for the linear PEO samples in water at 25°C using a rotational rheometer for different concentration. It was found that the critical molecular weight decreases with increasing the concentration and for the viscoelastic properties the obtained relaxation times explain the different efficiency in drag reduction for high and low molecular weight polyethylene oxide samples: only high molecular weights samples > 1000 kg/mol exhibit relaxation times high enough to be effective for vortices inhibition.

Measurements of drag reduction have been carried out for the high molecular weights by using a special self-developed set-up with dimensions to obtain turbulent flow. It was found that the amount of PEO required to reduce the friction factor during the flow decreases with increasing molecular weight.

List of Contents

Contents	Page
Abstract	I
List of Contents	II
Notations	V
List of Tables	IX
List of Figures	XIII
Chapter One : Introduction	
1.1 Polyethylene Oxide	1
1.2 Viscoelastic Properties	5
1.3 Drag Reduction	6
1.4 Purpose of the Present Work	7
Chapter Two : Literature Survey	
2.1 Structure Rheology	8
2.2 Intrinsic Viscosity	9
2.2 Review of Polyethylene Oxide Intrinsic Viscosity	11
2.3 The Network Solution (Semi-dilute and Concentrated Solution)	13
2.4 Viscous and Elastic Responses	15
2.5 Response of the Maxwell and Voigt Elements	17
2.6.1 Transient Response: Stress Relaxation	17
2.6.2 Transient Response: Creep	20
2.6.3 Dynamic Response: Loss and Storage Moduli	22
2.7 Bead-Spring Model	24
2.8 Shear Rate Dependence of Viscosity	26
2.9 Shear Thinning of Polymer	27

2.10	Review of Viscoelastic Properties of Polyethylene Oxide	28
2.11	Drag Reduction Phenomenon and Applications	31
2.12	Review of Polyethylene Oxide as Drag Reduction Agent	37

Chapter Three : Experimental Work

3.1	Materials	39
3.2	Dissolving Process	39
3.3	Operating Procedure	43
3.4	Calculations	58

Chapter Four : Results and Discussions

4.1	Introduction	61
4.2	Intrinsic Viscosity of Polyethylene Oxide in Water	61
4.2.1	Intrinsic Viscosity Measurements for Group A Samples at 25 °C	61
4.2.2	Intrinsic Viscosity Measurements for Group B Samples at 30 °C	65
4.2.3	Intrinsic Viscosity Measurements for Group B Samples at 25 °C	70
4.2.4	Intrinsic Viscosity Measurements for the Branched Polyethylene Oxide at 25 °C	74
4.3	The Transition from Particle to Network (Critical Molecular Weight)	78
4.4	Viscoelastic Properties of Polyethylene Oxide	81
4.4.1	The Flow Behavior of Polyethylene Oxide	82
4.4.2	Creep Diagram of Polyethylene Oxide	84
4.4.3	Graessley Diagram of Polyethylene Oxide	85
4.4.4	Storage and Loss Modulus and Maxwell and Bead-Spring Model	87
4.5	Drag Reduction	94

Chapter Five : Conclusions and Recommendations

5.1	Conclusions	104
5.2	Recommendations	106
	References	107
	Appendix A	
	Intrinsic Viscosity	A-1

Notations

Symbols	Notations	Units
A_2	Second Virial Coefficient	mL.mol/g ²
A_3	Third Virial Coefficient	mL.mol/g ²
a	Mark-Haowink Constant	
a_0, a_1, b_0, b_1	Constant in Equation (2.24)	
b	Blend Composition	(dm ³ .kg ⁻¹) ²
Δb	Polymer Blend	(dm ³ .kg ⁻¹) ²
C	Concentration	g/mol
$[C]$	Intrinsic Concentration	ppm
DR	Drag Reduction	
$\%DR$	Percentage Drag Reduction	
DR_{max}	Maximum Drag Reduction	
$[DR]$	Intrinsic Drag Reduction	
e_θ	The Azimuthal Direction	
f	Frequency	Hz
G	Shear Modulus	Pa.
G^*	Complex Shear Modulus	Pa.
G'	Storage Modulus	Pa.
G''	Loss Modulus	Pa.
$\hat{G}, \hat{\eta}$	Amplitudes of Shear Modulus and Viscosity in Equation (2.5)	
J	Creep Compliance	1/Pa.
K	Mark-Haowink Constant	ml/g
k'	Huggins Constant	
k''	Kraemer Constant	
$k\Box$	Schulz-Blaschke Constant	

M_{wt}	Molecular Weight	g/mol
M_c	Critical Molecular Weight	g/mol
M_e	Entanglement Molecular Weight	g/mol
p	Pressure	Pa.
Re	Reynolds Number	
R_G	Radius of Gyration	nm
R	Universal Gas Constant	8.134 J/mol
r	Radios	cm
T	Temperature	°C
t_o	Flow time of Pure Solvent	s
t	Flow Time of Solution	s
U	Velocity	1/min
u	Rotational Speed	1/min

Greek Letters

$[\square]$	Intrinsic Viscosity	ml/g
η	Viscosity of Solution	ml/g
η_o	Viscosity of Pure Solvent	ml/g
η_0	Zero Shear Viscosity	Pa. s
η_r	Relative Viscosity	
η_{sp}	Specific Viscosity	
η_{red}	Reduced Viscosity	ml/g
μ	Dynamic Viscosity	cP
ρ	Density	g/cm ³
τ	Torque	μ Nm
ν	Kinematics' Viscosity	cps

σ	Shear Stress	Pa. s
σ_{\square}	Characteristic Relaxation Time (Maxwell Model)	s
σ_R	Relaxation Time	s
$\dot{\sigma}$	Time Derivative of Shear stress	s
γ	Strain	
γ_0	Zero Shear Rate	1/s
$\dot{\gamma}$	Shear Rate	1/s
$\dot{\gamma}_c$	Critical Shear Rate	1/s
ω	Angular Frequency	1/s
Ω_e	The Domain Filled by the Fluid	
Δ_e	Anisotropic Laplacian	

Subscripts

0	at Time = 0
o	Without Polymer Additives
c	Critical
e	Entanglement
r	Relative
sp	Specific
red	Reduced
R	Relaxation time
G	Gyration

Abbreviations

DR	Drag Reduction
FDA	Food and Drug Administration
NSE	Neutron Spin-echo
PEG	Polyethylene Glycol
PEO	Polyethylene Oxide
PIB	Polyisobutylene
POE	Polyoxiethylene
RDA	Rotating Disk Apparatus
SANS	Small-angle Neutron Scattering
SCA- <i>n</i>	4-sulfonic calix[<i>n</i>]arene
VTF	Vogel-Tammann-Fulcher

List of Tables

Table	Title	Page
3-1	Dissolving Times of PEO Solutions for Dilute Concentrations	41
3-2	Dissolving Times of PEO Solutions for Concentrated Concentrations	42
3-3	Dissolving Times of PEO Solutions for Drag Reduction	43
4-1	Specific and Reduced Viscosity of 1 kg/mol Molecular Weight PEO at 25 °C	62
4-2	Specific and Reduced Viscosity of 3 kg/mol Molecular Weight PEO at 25 °C	62
4-3	Specific and Reduced Viscosity of 10 kg/mol Molecular Weight PEO at 25 °C	63
4-4	Specific and Reduced Viscosity of 20 kg/mol Molecular Weight PEO at 25 °C	63
4-5	Specific and Reduced Viscosity of 35 kg/mol Molecular Weight PEO at 25 °C	64
4-6	Specific and Reduced Viscosity of 100 kg/mol Molecular Weight PEO at 30 °C	66
4-7	Specific and Reduced Viscosity of 300 kg/mol Molecular Weight PEO at 30 °C	66
4-8	Specific and Reduced Viscosity of 1000 kg/mol Molecular Weight PEO at 30 °C	67
4-9	Specific and Reduced Viscosity of 4000 kg/mol Molecular Weight PEO at 30 °C	67
4-10	Specific and Reduced Viscosity of 8000 kg/mol Molecular Weight PEO at 30 °C	68
4-11	Calculated Molecular Weight and Intrinsic Viscosity of	69

Group B of PEO Samples at 30°C	
4-12	Specific and Reduced Viscosity of 99 kg/mol Molecular Weight PEO at 25 °C 70
4-13	Specific and Reduced Viscosity of 370 kg/mol Molecular Weight PEO at 25 °C 71
4-14	Specific and Reduced Viscosity of 110 kg/mol Molecular Weight PEO at 25 °C 71
4-15	Specific and Reduced Viscosity of 460 kg/mol Molecular Weight PEO at 25 °C 72
4-16	Specific and Reduced Viscosity of 8000 kg/mol Molecular Weight PEO at 25 °C 72
4-17	Specific and Reduced Viscosity of 0.55 kg/mol Molecular Weight PEO at 25 °C 74
4-18	Specific and Reduced Viscosity of 40 kg/mol Molecular Weight PEO at 25 °C 75
4-19	Intrinsic Viscosity of PEO Solution with Different Molecular Weights at 25°C 76
4-20	Huggin's constant and Mark-Houwink Parameters of PEO in Water at 25°C 78
4-21	Zero Shear Viscosity of 1% PEO Solution at 25°C 79
4-22	Zero Shear Viscosity of 5% PEO Solution at 25°C 80
4-23	Relaxation Time for Different Concentration of PEO Solution at 25°C 91
4-24	Torque's Values of PEO Solutions at (23.3-23.8 °C) 95
4-25	Percentage Drag Reduction of PEO Solutions at (23.3-23.8 °C) 96
4-26	Maximum Drag Reduction of PEO Solutions at (23.3-23.8 °C) 99
4-27	Intrinsic Drag Reduction of PEO Solutions at (23.3-23.8 °C) 99

4-28	Drag Reduction's Values of PEO Solutions at (23.3-23.8°C)	100
4-29	Intrinsic Concentration of PEO Solutions at (23.3-23.8 °C)	103
A-1	Linear Polyethylene Oxide of Molecular Weight 1 kg/mol with Water at Temperature 25°C, Time of Water = 256.41 sec	A-1
A-2	Linear Polyethylene Oxide of Molecular Weight 3 kg/mol with Water at Temperature 25°C, Time of Water = 256.41 sec	A-1
A-3	Linear Polyethylene Oxide of Molecular Weight 10 kg/mol with Water at Temperature 25°C, Time of Water = 256.41 sec	A-2
A-4	Linear Polyethylene Oxide of Molecular Weight 20 kg/mol with Water at Temperature 25°C, Time of Water = 256.41 sec	A-2
A-5	Linear Polyethylene Oxide of Molecular Weight 35 kg/mol with Water at Temperature 25°C, Time of Water = 180.67 sec	A-3
A-6	Linear Polyethylene Oxide of Molecular Weight 99 kg/mol with Water at Temperature 30°C, Time of Water = 256.15 sec	A-3
A-7	Linear Polyethylene Oxide of Molecular Weight 370 kg/mol with Water at Temperature 30°C, Time of Water = 256.15 sec	A-4
A-8	Linear Polyethylene Oxide of Molecular Weight 1100 kg/mol with Water at Temperature 30°C, Time of Water = 256.15 sec	A-4
A-9	Linear Polyethylene Oxide of Molecular Weight 4600 kg/mol with Water at Temperature 30°C, Time of Water = 256.15 sec	A-5
A-10	Linear Polyethylene Oxide of Molecular Weight 8000 kg/mol with Water at Temperature 30°C, Time of Water = 256.15 sec	A-5
A-11	Linear Polyethylene Oxide of Molecular Weight 99 kg/mol with Water at Temperature 25°C, Time of Water = 289.22 sec	A-6
A-12	Linear Polyethylene Oxide of Molecular Weight 370 kg/mol with Water at Temperature 25°C, Time of Water = 303.022 sec	A-6
A-13	Linear Polyethylene Oxide of Molecular Weight 1100 kg/mol	A-7

- with Water at Temperature 25°C, Time of Water = 289.22 sec
- A-14 Linear Polyethylene Oxide of Molecular Weight 4600 kg/mol A-7
with Water at Temperature 25°C, Time of Water = 303.022 sec
- A-15 Linear Polyethylene Oxide of Molecular Weight 8000 kg/mol A-8
with Water at Temperature 25°C, Time of Water = 289.22 sec
- A-16 Branched Polyethylene Oxide of Molecular Weight 0,55 A-8
kg/mol with Water at Temperature 25°C, Time of Water =
289.22 sec
- A-17 Branched Polyethylene Oxide of Molecular Weight 40 kg/mol A-9
with Water at Temperature 25°C, Time of Water = 285.95 sec

List of Figures

Figure	Title	Page
1-1	The Synthesis of Polyethylene Oxide	1
1-2	Biocompatible Multiarm Starpolymers	5
2-1	Logarithmic Plot of $[\eta]$ vs. M (Schematic)	10
2-2	Relationship Between Apparent Viscosity and (a) Concentration at Constant Molecular Weight; (b) Molecular Weight at Constant Concentration	14
2-3	Relationships of Polymer Chains in Solution at Different Concentration Regions. (a) Dilute Solution Regime, (b) Transition Regions, (c) Semi-Dilute Regime	14
2-4	The Chain Element Concept	15
2-5	Illustration of (a) The Maxwell Element and (b) The Voigt Element	17
2-6	Creep Experiment: (a) presetting a constant shear stress at time $t=0$ results in a time dependent strain $\gamma(t)$ and compliance $J(t)$ as shown in (b) for a viscoelastic liquid as described by the Maxwell model. The stress σ_0 is removed at some later time. For a real viscoelastic Sample, the shape of the $\gamma(t)$ and $J(t)$ curves is shown in (c). There from the slope at long measuring times, we can obtain the zero shear viscosity η_0	21
2-7	Normalized Dynamic Moduli G' and G''	24
2-8	Scheme of the Bead-Spring Model	24
2-9	Schemes of Flow and Viscosity Curves with Different Flow Behavior (a) Shear Thickening Behavior (b) Shear Thinning Behavior	26

2-10	Shear Thinning of Polymer Melts and Concentrated Polymer Solutions	27
2-11a	Rheology Data for the PEO Sample with $M_w = 932$ kg/mol Measured at Temperature $T = 378$ K. Black Squares Belong to the Storage Modulus, Red Circles to the Loss Modulus	30
2-11b	Rheology Data for the PEO Sample with $M_w = 610$ kg/mol Measured at Temperature $T = 348$ K. Black Squares Belong to the Storage Modulus, Red Circles to the Loss Modulus	31
2-12	Extensional Flow	36
3-1	Viscometric Measurement System	44
3-2	Schott Ubbelohde Capillary Viscometer	45
3-3	Water Bath with Viscometer	46
3-4	USD200 Rotational Rheometer	47
3-5	Rotational Rheometer Geometries (a) Cone/Plat (b) Double Gap	48
3-6	Set-up of Cone/plat Measurements	49
3-7	Drag Reduction Geometry	56
3-8	Drag Reduction Container	57
3-9	Schott Ubbelohde Capillary Viscometer	58
3-10	$\frac{\eta_{sp}}{c}$ or $\frac{\ln \eta_r}{c}$ vs. Concentration	59
4-1	Reduced Viscosity vs. Specific Viscosity for Group A of PEO Samples at 25°C	64
4-2	Reduced Viscosity vs. Specific Viscosity for Group B of PEO Samples at 30°C	68
4-3	Reduced Viscosity vs. Specific Viscosity for Group B of PEO Samples at 25°C	73
4-4	Reduced Viscosity vs. Specific Viscosity for Branched PEO	75

	Samples at 25°C	
4-5	log (Molecular Weight) vs. log (Intrinsic Viscosity) for Different PEO in Water at 25°C	77
4-6	log (Molecular Weight) vs. log (Zero Shear Viscosity) for 1% PEO Solutions at 25°C	79
4-7	log (Molecular Weight) vs. log (Zero Shear Viscosity) for 5% PEO Solutions at 25°C	80
4-8	Flow Curve for 1% PEO Solutions at 25°C	82
4-9	Flow Curve for 5% PEO Solutions at 25°C	82
4-10	Creep Diagram for 5% PEO Solutions at 25°C	84
4-11	Graessley Diagram for 1% and 5% PEO Solutions at 25°C	85
4-12	Shear Moduli vs. Frequency of 5% PEO Solutions of Different Molar Mass at 25 C. Red and Open Symbols: Storage Modulus; Blue and Filled Symbols: Loss Modulus	87
4-13	Shear Moduli vs. Frequency of 1% PEO Solutions of Different Molar Mass at 25 C. Red and Open symbols: Storage Modulus; Blue and Filled Symbols: Loss Modulus	88
4-14	Shear Moduli vs. Frequency of 0.2% and 0.05% PEO Solutions of Different Molar Mass at 25 C. Red and Open Symbols: Storage Modulus; Blue and Filled Symbols: Loss Modulus. Due to the Low Viscosity all Measurements were performed with a Double Gap Geometry Z1	90
4-15	Calculated Relaxation Time Due to the Rouse Model for Different Molecular Weights and Concentrations. The Horizontal Lines at 10 ms and 100 s Correspond to the Highest and Lowest Frequency Which can be measured in the Frequency Sweep	92

4-16	Percentage Drag Reduction vs. Concentration of PEO Solutions at (23.3-23.8 °C)	98
4-17	C/DR vs. Concentration of 8000 kg/mol PEO Solutions at (23.3-23.8 °C)	101
4-18	C/DR vs. Concentration of 4600 kg/mol PEO Solutions at (23.3-23.8 °C)	101
4-19	C/DR vs. Concentration of 1100 kg/mol PEO Solutions at (23.3-23.8 °C)	102
4-20	C/DR vs. Concentration of 370 kg/mol PEO Solutions at (23.3-23.8 °C)	102

Chapter One

Introduction

1.1 Polyethylene Oxide (PEO)

The ethylene oxide monomer is nothing more than an epoxide ring. Two corners of the molecule consist of -CH₂- linkages. The third corner is oxygen, -O- as shown in figure 1-1^[1].

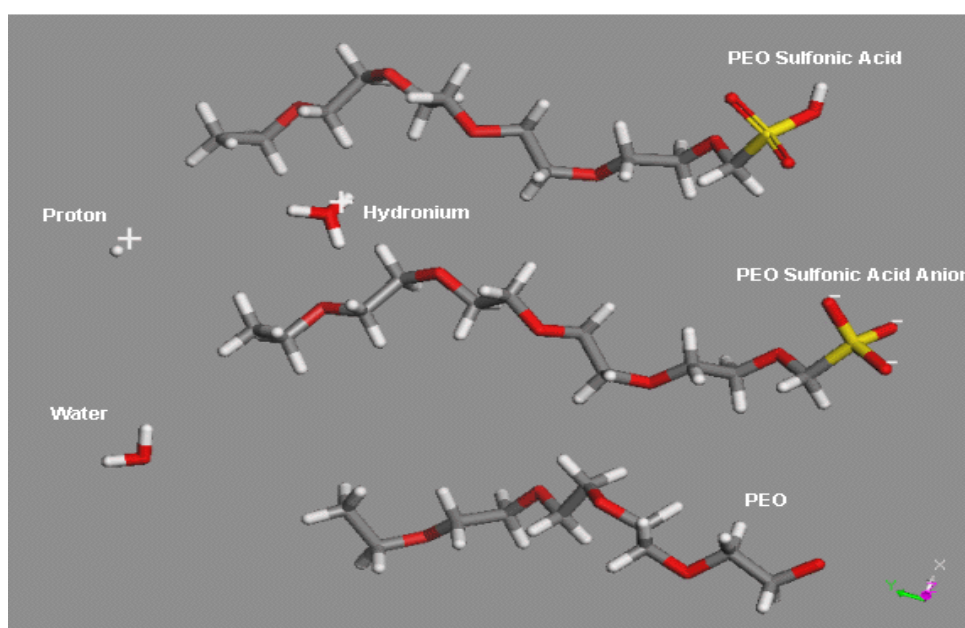


Figure 1-1 the Synthesis of Polyethylene Oxide ^[1].

In the presence of a catalyst the monomer forms a chain having the repeat unit -CH₂-CH₂-O-. With a molecular formula of ^[2]:



Factors that make PEO wet-end chemistry puzzling include (a) the fact that it can be used as a retention aid even though it is nonionic, (b) the fact that its performance is highly dependent on its shear history, and (c) the fact that it needs the presence of lignin or certain phenolic "cofactor"

additives to achieve its best effect as a flocculant and retention aid. Observations of PEO behavior suggest that the molecular chains are initially tangled with each other and that this tangling is somehow essential for effective flocculation. PEO is usually received as dry granules. These need to be dispersed with care, using a dilution ratio of at least 100 and avoidance of excessive shear ^[1].

It has also been known as polyethylene oxide (PEO) or polyoxyethylene (POE), or polyethylene glycol (PEG) depending on its molecular weight, and under the tradename Carbowax. The three names PEO, POE, or PEG are chemically synonymous, but historically PEG has tended to refer to oligomers and polymers with a molecular mass below 20,000 g/mol, PEO to polymers with a molecular mass above 20,000 g/mol, and POE to a polymer of any molecular mass ^[2]. PEO and PEG are commercially available over a wide range of molecular weights from 300 g/mol to 10,000,000 g/mol. While PEO and PEG with different molecular weights find use in different applications and have different physical properties (e.g., viscosity, elasticity) due to chain length effects, their chemical properties are nearly identical. Different forms of PEO are also available dependent on the initiator used for the polymerization process, the most common of which is a monofunctional methyl ether PEO (methoxypoly(ethylene oxide)), abbreviated mPEO. Lower - molecular - weight PEOs are also available as purer oligomers, referred to as monodisperse, uniform or discrete. Very high purity PEO has recently been shown to be crystalline, allowing determination of an x-ray crystal structure ^[3]. Low molecular weight ($M_{wt} < 1,000$) PEOs are viscous and colorless liquids, while higher molecular weight PEOs are waxy, white solids with

melting points proportional to their molecular weights to an upper limit of about 67°C^[4], and a flash point of (182-287°C)^[2].

Polyethylene oxide, being a polyether, strongly hydrogen bonds with water. It is non-ionic and undergoes salting-out effects associated with neutral molecules in solution of high dielectric media. Salting-out effects manifest themselves in depressing the upper temperature limit of solubility, and in the reducing the viscosity of both the dilute and concentrated solutions of the polymers^[5].

Polyethylene oxide is also freely soluble in acetonitrile, in ethylene dichloride, in trichloroethylene, and in methylene chloride. Heating may be required to obtain solutions in many other organic solvents. It is insoluble in aliphatic hydrocarbons, and in ethylene glycol^[5].

Poly (ethylene oxide) (PEO) is one of the most intensely studied polymers in current materials science and biotechnology because of not only its unique behaviors in solution but also its wide applications^[6, 7].

The key properties of PEO are its soft semi-crystalline thermoplastic that displays a lot of interesting properties and finds many applications due to the wide range of molecular weight in which it is commercially available (10^2 – 8×10^6 g/mol), chemical stability, solubility both in water and many organic solvents, non toxicity, rapid clearance from the body, lack of immunogenicity and a Food and Drug Administration (FDA) approval for internal consumption. Films of high molecular weight PEO are tough, ductile, heat-sealable, and because of their high degree of crystallization, resist well to atmospheric moisture^[8].

PEOs are also available with different geometries. Branched PEOs have three to ten PEO chains emanating from a central core group. Star PEOs

have 10–100 PEO chains emanating from a central core group. Comb PEOs have multiple PEO chains normally grafted to a polymer backbone^[9].

Architectures based on nonlinear PEO have recently become a focus of scientific interest, due to their branched structures and unique rheological property^[10], and their intriguing potential for biomedical and pharmaceutical applications, for instance as multivalent PEGylation reagent. Also, it has recently found increasing use as a conducting medium in light-weight, high energy polymer batteries^[11], as well as for solid polymer electrolytes^[21]. Star-shaped PEOs bear multiple functional end groups adjustable by the number of arms and thus exhibit higher attachment capacity and higher capability for ion-complication in comparison with their linear analogues, combined with reduced degree of crystallization^[13].

Two fundamentally different approaches for the synthesis of star polymers can be distinguished: the ‘arm-first’ and the ‘core-first’ procedure. The ‘arm-first’ strategy relies on deactivation of living PEO chains by reaction with multifunctional electrophiles. In this manner well-defined star polymers with defined molecular weight of the arms and predetermined functionality can be synthesized. For instance, grafting onto cyclophosphazenes resulted in six- and twelve-arm PEO stars^[14]. Multiarm PEO-stars have also been prepared by attachment of PEO chains to different types of dendrimers. The ‘arm-first’ approach, however, requires additional separation of the resulting star-shaped polymer from the linear ‘arms’, which commonly have to be used in excess. Moreover, the arms in such star polymers can only be functionalized via protected functional initiators. In contrast, by the ‘core-first’ approach the growing polymer chains introduce multiple alkoxides that can be functionalized subsequent to the polymerization^[15].

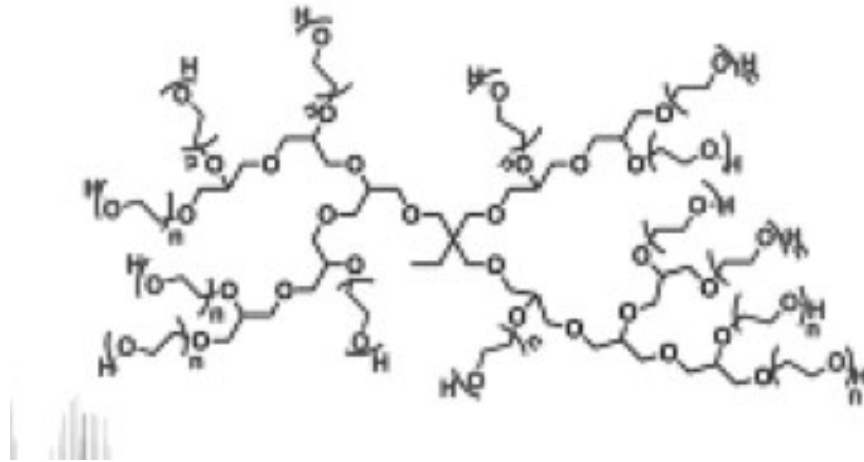


Figure 1-2 Biocompatible Multiarm Star polymers ^[15].

1.2 Viscoelastic Properties

There are two extreme cases for mechanical behavior of samples: in one side there are pure liquids, like water or oil, which can be described by Newton's law of liquids. On the other side there are pure solids like steel or stone, which are described by Hooke's law. Pure solids show an instantaneous stress response on deformation. In between of these extreme cases, there exists a broad range of viscoelastic samples which exhibit a nontrivial time dependence of the stress response on deformation or vice versa ^[16, 17]. Important classes of such materials include polymers and polymer solutions, surfactant solutions, and biological materials, among others, which are characterized by complex structures with multiple characteristic time and length scales. One of the most important descriptors of these properties is the complex shear modulus $G^*(\omega)$, which is measured in the frequency domain ω . The real part $G'(\omega)$ describes the elastic (storage) property of the system, while the imaginary part $G''(\omega)$ is a measure of the viscous (loss) behavior. The dependence of G' and G'' on the frequency gives insight into

the molecular structure of the system. Additionally, the ability to measure the mechanical response of a material to an applied shear strain has a variety of potential applications, especially in biology, where the mechanical properties of the cells and intracellular matter are of utmost importance ^[18].

1.3 Drag Reduction

The main objective of drag reduction is to reduce the fluid mechanical force known as “drag,” which is exerted on an engineering system improving its efficiency. There are passive and active techniques to reduce the drag ^[19]. The passive techniques do not require any energy input to flow; only installation and maintenance costs are involved. The rib lets and large eddy breakup devices fall into this category. However, the maximum drag reduction is limited up to 10%. The active techniques require certain energy input. However, level of drag reduction achieved is up to 80%. Among all the techniques, additions of minute amount of high molecular weight polymers and surfactants have been very active area of research ^[20].

High molecular weight polymers ($>10^5$) are very effective drag reducers ^[21], several attempts have been made to enhance the drag reduction effectiveness (DRE) and mechanical stability of polymer drag reducers. In general, homopolymers, alternate copolymers, graft polymers, and polyelectrolytes and polysaccharides from natural and microbial resources are efficient drag reducers in water, organic solvents, and crude oil. The extent of drag reduction increases with the molecular weight and length of the polymers, and so does their susceptibility to flow-induced degradation ^[22-24].

1.4 Purpose of the Present Work

- Determination of the intrinsic viscosity for Polyethylene Oxide which are used in previous literature either as drag reduction agent or viscosity index improver in water.
- Calculate the Mark-Houwink parameters were calculated for different molecular weights for polyethylene oxide in water at 25°C.
- Determination of the value of critical molecular weight, and describe the behavior of polyethylene oxide solution.
- Determination of viscose and viscoelastic properties of polyethylene oxide solutions and description with Maxwell and Bead-Spring models parameters.
- Determination of the drag reduction variables for polyethylene oxide solutions depending on concentration and molecular weight of PEO.

Chapter Two

Literature survey

2.1 Structure Rheology

Rheology is the study of the deformation and flow of matter. The rheological properties of a liquid are dominant features that can be quantified to characterize its behavior, and the response of a liquid to a forced shearing flow is the basis for determining the specific rheological properties of a given liquid. General qualitative terms used to describe these properties are viscoelastic, Newtonian, nonNewtonian, thixotropic and dilatant. Quantitative parameters used are viscosity, elasticity, shear rate, shear strain, and shear stress. The broadest view of liquid rheology is obtained by using oscillatory flow at a selected frequency because both viscous and elastic properties are revealed. Steady flow reveals only viscous properties. Values of shear stress, shear rate, and shear strain are primary parameters for quantitative specification of both the flow condition and the liquid response. It is from these quantities that the components of the viscoelastic modulus, the viscosity and the elasticity (or alternately the loss and storage moduli) are obtained. These numbers form the basis for quantitative specification of the liquid's properties for quality control or other applications^[25].

In addition to the quantitative specification above, it is useful to have a concept of the microstructure of a liquid, since that is the underlying physical basis for its rheological properties. A liquid with isotropic structure is one with perfectly random microstructure organization; in an anisotropic liquid the microstructure has a preferential directional orientation. The organization of the structural elements determines the way the liquid will

flow, and microstructural organization is influenced by three distinct flow factors ^[25]:

1. A liquid at rest (no flow) is isotropic.
2. Flowing liquid may become anisotropic.
3. Flow induced anisotropy decays when flow is stopped ^[25].

2.2 Intrinsic Viscosity

The viscosity of a polymer solution (η) is higher than that (η_o) of the pure solvent at a specified temperature and the increase in medium viscosity on dissolving the polymer in the solvent is a function of both molecular weight and concentration of the polymer solute ^[26].

If the polymer solution is very dilute, then the viscosities of the solvent and the solution at a given temperature would be proportional to their flow times in a given capillary viscometer such that the relative viscosity η_r expressed by the ratio (η / η_o) would be given by the flow time ratio (t / t_o), where t_o is the flow time of a given volume of the solvent and t is the flow time of the same volume of solution respectively. The parameter called specific viscosity, η_{sp} as defined by $\eta_{sp} = (\eta - \eta_o) / \eta_o = (t - t_o) / t_o$, where specific viscosity per concentration equal to reduced viscosity, and intrinsic viscosity is ^[26]:

$$[\eta] = \lim_{c \rightarrow 0} \eta_{red} \quad (2.1)$$

Intrinsic viscosity $[\eta]$ may be regarded as a measure of the specific hydrodynamic volume of a dissolved polymer at infinite dilution $C \rightarrow 0$ ^[27]. The intrinsic viscosity measured in a specific solvent is related to the molecular weight M , by the Mark –Houwink equation ^[28, 29].

$$[\eta] = KM^a \quad (2.2)$$

Where K and a are Mark-Houwink constants that depend upon the type of polymer, solvent, and the temperature of the viscosity determinations [28]. The unit of intrinsic viscosity is an inverse concentration [30].

A plot of $\log [\eta]$ vs. $\log M$ usually gives a straight line, the slope of this line is the "a" value and the intercept is equal to the log of the "K" value as shown in figure 2-1 [28].

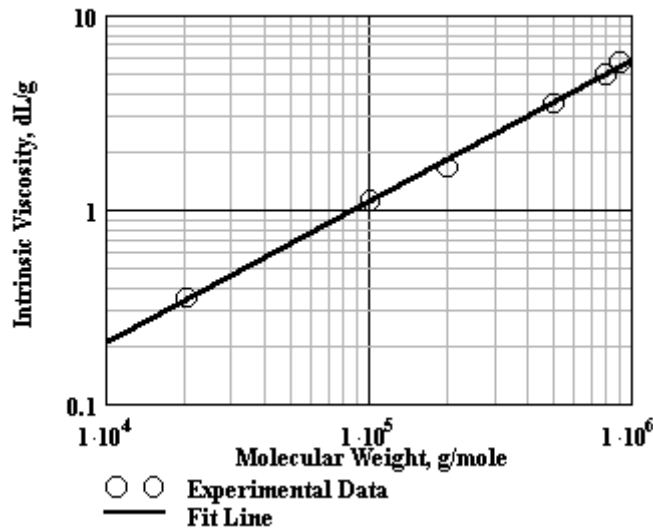


Figure 2-1 Logarithmic Plot of $[\eta]$ vs. M (Schematic) [28].

The slope contains information about the shape of molecules, as illustrated below

- $a = 1/2$ (for flexible polymer chains in an "ideal" (theta) solvent).
- $0.5 < a < 0.8$ (for flexible polymer chains in "good" solvent).
- $a > 0.8$ (for "stiff" chain) [30].

Can be related to the concentration dependence of the reduced viscosity by the following three equations of Huggins [31, 32].

$$\frac{\eta_{sp}}{c} = [\eta] + k'[\eta]^2 c \quad (2.3)$$

Where k' , is constant for a given polymer – solvent – temperature systems [33].

2.3 Review of Polyethylene Oxide Intrinsic Viscosity

Bianchi and Peterlin, [34] collected experiment evidence concerning the dependence of the intrinsic viscosity $[\eta]$ on molecular weight M in the low molecular weight rang (from oligomers to $M = 5 \times 10^4$ g/mol) in a variety of solvent for about ten polymers. i.e., polyethylene, poly (ethylene oxide), poly (propyl-ene oxide), polydimethylsiloxane, polyisobutylene, poly (vinylacetate), poly (methyl methacrylate), polystyrene, poly- α -methylstyrene, and some cellulose derivatives. The results showed that Mark-Houwink constant (a) of different polymers depend on : (1) variation of thermodynamic interaction with molecular weight; (2) variation of conformational characteristics (as for instance the ratio, $\langle r_0^2 / nl^2 \rangle$ where $\langle r_0^2 \rangle$ is the unperturbed mean square end-to-end distance and n is the number of bonds each of length L ; (3) hydrodynamic properties of short chains.

Jeon and Chang, [35] investigated the effect of temperature on the conformational properties of poly (ethylene oxide) (PEO) in aqueous and aqueous urea solutions. The values of intrinsic viscosity and Huggins coefficient for the PEO dissolved in water and urea/water mixtures (urea concentration 0.2, 1, and 2 M) were obtained using a viscometric method and discussed with respect to the change of water structure. At low temperature (below 22°C), the PEO-water interaction was favorable and the chain can be extended, whereas at higher temperature (above 25°C), it was less favorable and the chain can be contracted, i.e., the PEO-water interaction became to be unfavorable with the increase in temperature. As the urea was added to system, the PEO chain could be more extended and hugged by the

perturbation of the structured water originating from the unfavorable PEO-water interaction

Abdel-Azim et al.,^[36] measured the intrinsic viscosities of poly (ethylene glycol)/poly (ethylene oxide) (PEG/PEO) blends in benzene as a function of blend composition for various molecular weights of PEO at two different temperatures (293.15 K and 303.15 K). In order to predict the compatibility of polymer pairs in solution, the interaction parameter term, Δb , (which represent the difference between the interaction coefficient between the tow polymers and the theoretical value of this coefficient), and the difference between the intrinsic viscosities of the polymer blends and the weight average intrinsic viscosities, $\Delta[\eta]$, of the two polymer solutions taken separately are used. When the derived values of $[\eta]$ obtained by the linear least-squares analysis and $\Delta[\eta]$ for polymer blends having different compositions measured at different temperatures were used as an alternative mean for determining the compatibility of polymer blends. The compatibility of the blends was found that the only compatible blends were achieved when the molecular weight of PEG and PEO are nearly equal. The compatibility was detected only in case of the blends PEG (75%)/PEO1 (25%) and PEG (10%)/PEO1 (90%). The studied systems revealed that the values of Δb , in all immiscible blends, increase with increasing the total concentration of the blend. The compatibility data obtained by $\Delta[\eta]$ were found in a good accord with that obtained by Δb .

Comanita,^[37] investigated a preparation of a series of 4-arm, 8-arm, and 16-arm poly (ethylene oxide)s (PEO). The PEO arms were grown anionically from the multifunctional cores. The polymers have narrow molecular weight distributions. Analysis of the molecular weight, intrinsic viscosity, and translational diffusion coefficient in methanol confirmed the star structure of the polymers. The aqueous solutions of the star PEOs

appeared normal. Low molecular weight star polymers, however, showed abnormally low intrinsic viscosities and were adsorbed on the size exclusion column hydrogel material.

Chen, ^[38] reported the creation of star-like chain architecture through complexation of a mono-amino terminated poly (ethylene oxide) (PEO-NH₂) with a macrocyclic compound, 4-sulfonic calix[*n*]arene (*n* = 4 and 8) (SCA-*n*). The intrinsic viscosities [η] of the complexes in toluene were 60% higher than that of neat PEO-NH₂, showing that the star-like structure retained in non-polar solvents. On the other hand, PEO arms dissociated from the cores in water, so that the complexes and neat PEO-NH₂ displayed similar [η].

2.4 The Network Solution (Semi-dilute and Concentrated Solution)

In semi-dilute and concentrated solution, polymer molecules are no longer isolated from one another. Chain-chain interactions at and above a critical concentration (*c*) often termed the overlap concentration, lead to increased values of apparent viscosity η . Apparent viscosity can be related to concentration and molecular weight by equation below, in which *b* is scaling constant for dilute solution regain and *d* is scaling constants for concentrated regain ^[39].

$$\eta \propto c^b M^d \quad (2.4)$$

Usually plots of $\ln \eta$ vs. $\ln c$ at constant molecular weight as shown in figure 2-2 are used to measure entanglement onset. Measurements are made at constant shear rate, temperature, and solvent conditions ^[39].

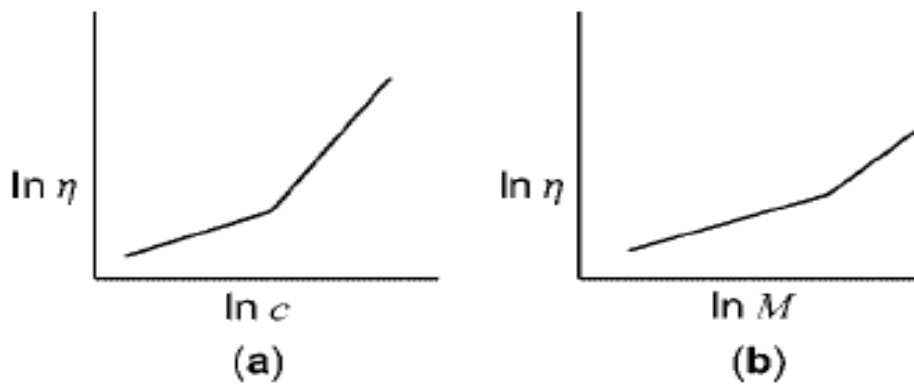


Figure 2-2 Relationship Between Apparent Viscosity and (a) Concentration at Constant Molecular Weight; (b) Molecular Weight at Constant Concentration^[39].

Polymer chains in dilute solutions are isolated and interact with each other only during brief times of encounter. Increasing the polymer concentration in solvent leads to a change at a certain stage, as is schematically indicated in figure 2-3, a limit is reached when the polymers molecules become closely packed because then they begin to interpenetrate^[40].

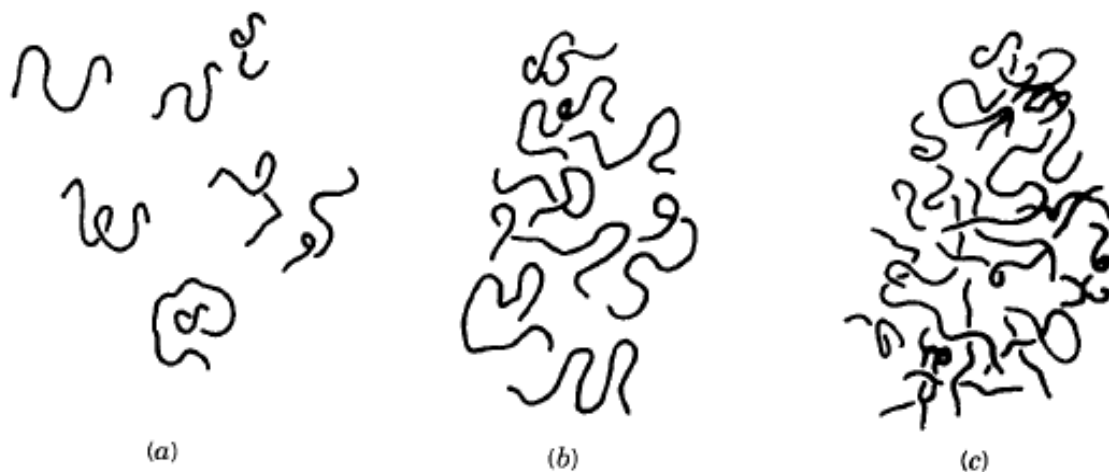


Figure 2-3 Relationships of Polymer Chains in Solution at Different Concentration Regions. (a) Dilute Solution Regime, (b) The Transition Regions, (c) Semi-Dilute Regime^[40].

For network solution, a different description must be used since in this case no individual particles are present, see figure below^[41].

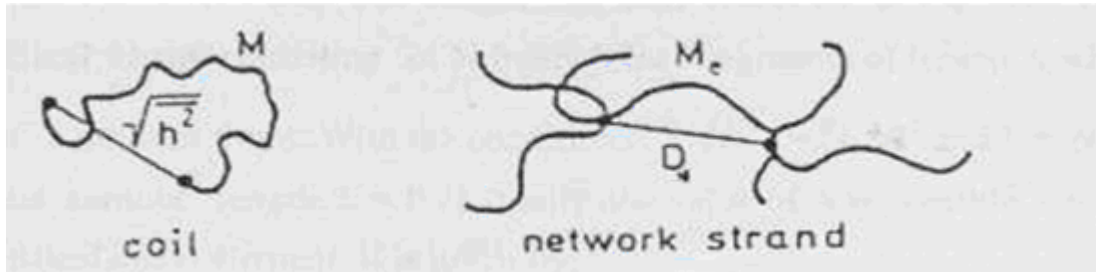


Figure 2-4 The Chain Element Concept^[41].

The critical molecular mass M_c is roughly two times the molar mass of the polymer chain length between two entanglements M_e : $M_c \approx 2 M_e$. The entanglements of different polymer molecules are the origin for the strongly increased sensitivity of the viscosity on molar mass above M_c . Concentrated polymer solutions gives similar results^[42].

2.5 Viscous and Elastic Responses

Viscosity reflects the relative motion of molecules, in which the energy is dissipated by friction. It is a primary characteristic of a liquid. A liquid will always flow until the stress has gone away and it will dissipate energy as it does so. In contrast, elasticity reflects the storage of energy; When a spring is stretched, the energy can be recovered by releasing the deformation. A solid subjected to a small strain is primarily elastic, in that it will remain deformed as long as the force is still applied. In flexible polymers, the elasticity arises from the many conformational degrees of freedom of each molecule and from the intertwining of different chains; it will turn out to be primarily entropic in origin. When the material is subjected to a deformation, the individual

molecules respond by adopting a non equilibrium distribution of conformations. For example, the chains on average may be stretched and/or oriented in the direction of flow; in so doing they lose entropy. Left to themselves, the molecules will relax back to an isotropic, equilibrium distribution of conformation, just like a spring. As they relax, the relative motion of the molecules through the surrounding fluid dissipates the stored elastic energy. It is this interplay of viscous dissipation during elastic recovery that underlies the viscoelastic properties of polymer liquids ^[17].

In experimental measurement of the viscoelastic response, several different time histories are routinely employed. In a transient experiment, at some specific time a strain (or stress) is suddenly applied and held; the resulting stress (or strain) is then monitored as a function of time. The former mode is called stress relaxation and the associated modulus the stress relaxation modulus, $G(t) = \sigma(t)/\gamma$. The latter mode (in parentheses) is called creep and the associated compliance the creep compliance, $J(t) = \gamma(t)/\sigma$. In a steady flow experiment, the strain rate is constant; The resulting steady stress gives the steady flow viscosity. Finally, in what is arguably the most important mode, the sample is subjected to sinusoidally time-varying strain at frequency ω . The resulting dynamic modulus, $G^*(\omega)$, is resolved in to two dynamic moduli: one in-phase with the strain, called G' , reflecting the elastic component of the total response and one -phase with the strain rate, called G'' , reflecting the viscous response ^[17].

2.6 Response of the Maxwell and Voigt Elements

There is a great deal about viscoelastic response through consideration of two simplified models, the so-called Maxwell and Voigt elements. Maxwell model illustrates a viscoelastic liquid, while Voigt model illustrates a viscoelastic solid. Maxwell model will examine the stress relaxation modulus, creep compliance, and dynamic moduli of Maxwell element, which illustrates a viscoelastic liquid. This element will turn out to have a characteristic time, σ , which determines the timescale of its response^[16, 17].

2.6.1 Transient Response: Stress Relaxation

The Maxwell element consists of an ideal, Hookean spring with spring constant G connecting in series with an ideal, Newtonian dashpot with viscosity $\hat{\eta}$, as shown in figure below^[16, 17].

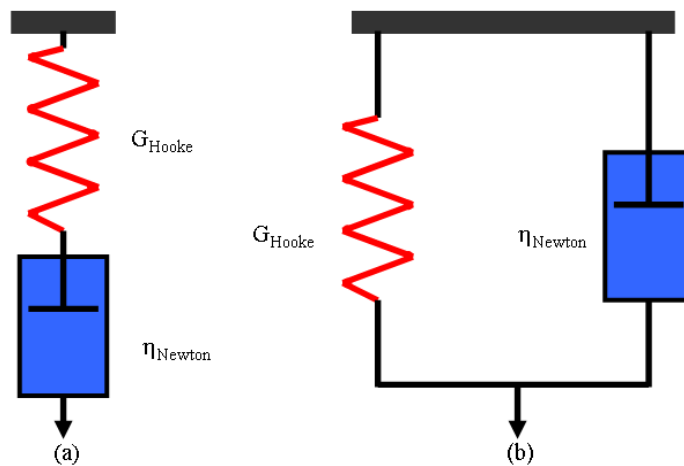


Figure 2-5 Illustration of (a) The Maxwell Element and (b) The Voigt Element^[17].

Thus the stress in the two components is given by:

For the spring

$$\sigma = \hat{G}\gamma \quad (2.5a)$$

And for the dashpot

$$\sigma = \hat{\eta}\dot{\gamma} \quad (2.5b)$$

At time $t = 0$ an instantaneous strain of magnitude γ_0 applies, and hold it indefinitely; if the stress is a function of time, it is a stress relaxation experiment. At very short times, the dashpot will not want to move; that is the whole point of the dashpot (i.e., a shock absorber). The spring, on the other hand, only cares about how much it is stretched, not how rapidly. Thus the initial deformation will be entirely taken up by the spring. However, the stretched spring will then exert a force on the dashpot, which will slowly flow in response. Ultimately, the spring will relax back to its rest length and there will be no more stress; the long time-response is that of a liquid.

To make this argument quantitative, then the total applied strain is distributed between the elements,

$$\gamma_0 = \gamma_{spring} + \gamma_{dashpot} \quad (2.6)$$

And because the strain is constant for $t > 0$,

$$\frac{d\gamma_0}{dt} = 0 = \dot{\gamma}_{spring} + \dot{\gamma}_{dashpot} = \frac{d}{dt} \frac{\sigma(t)}{\hat{G}} + \frac{\sigma(t)}{\hat{\eta}} \quad (2.7)$$

This is a linear, first-order, homogeneous differential equation for $\sigma(t)$:

$$\dot{\sigma} + \frac{1}{\sigma_R} \sigma = 0 \quad (2.8)$$

Where the dot denotes the time derivative, the relaxation time defined as:

$$\sigma_R = \frac{\hat{\eta}}{\hat{G}} \quad (2.9)$$

And from equation (2.7) it is clear that this ratio has units of time.

$$\frac{\hat{\eta}}{\hat{G}} = \frac{\left(\frac{\sigma_R}{\dot{\gamma}} \right)}{\left(\frac{\sigma_R}{\dot{\gamma}} \right)} = \left(\frac{\dot{\gamma}}{\dot{\gamma}} \right) = t \quad (2.10)$$

The relaxation time is a measure of the time required for a system to return to equilibrium after any kind of disturbance.

The solution of equation (2.10) is an exponential decay

$$\sigma(t) = \sigma_o \exp\left(\frac{-t}{\sigma_R}\right) \quad (2.11)$$

At the earliest times the deformation is all in the spring, and therefore $\sigma_o = \hat{G}\gamma_o$. (Note that an instantaneous deformation would make $\dot{\gamma}$ infinite and thus the stress in the dashpot would be infinite if it moved, so it does not.) The stress relaxation modulus is obtained as

$$G(t) = \frac{\sigma(t)}{\gamma_o} = \hat{G} \exp\left(\frac{-t}{\sigma_R}\right) \quad (2.12)$$

The Maxwell model captures the main feature of the stress-relaxation response of any liquid; the material supports the stress for $t \leq \sigma_R$, but flows until the stress has vanished for $t \geq \sigma_R$. Thus the magnitude of the relaxation time is vital in determining the properties that experience ^[17].

2.6.2 Transient Response: Creep

In a Creep experiment, a sample is subjected to a constant force and the resulting deformation is monitored as a function of time. Creep implies that the deformation will be very slow, which in turn suggests that the sample should have a rather high viscosity. Now if the Maxwell element subjected to Creep using σ_0 at time $t = 0$ then $\gamma(t)$ evolve using equation (2.8).

$$\begin{aligned}\gamma(t) &= \gamma_{spring} + \gamma_{dashpot} = \frac{\sigma_0}{\hat{G}} + \frac{1}{\hat{\eta}} \int_0^t \sigma_0 \\ &= \frac{\sigma_0}{\hat{G}} + \frac{\sigma_0}{\hat{\eta}} t\end{aligned}\quad (2.13)$$

Here the strain in the dashpot is obtained by integrating the strain rate $\dot{\gamma}$, where $\dot{\gamma} = \sigma_0/\hat{\eta}$ is a constant. Thus the compliance is given by

$$J(t) = \frac{\gamma(t)}{\tau_0} = \frac{1}{\hat{G}} + \frac{1}{\hat{\eta}} t = J_e^0 + \frac{1}{\hat{\eta}} t \quad (2.14)$$

Figure 2-6 illustrates this behavior, at long time there is a steady-state response, with the strain increasing linearly in time; the slope is the reciprocal of the viscosity. At short times there is a transient response, reflecting the initial deformation of the spring; in this model, it is instantaneous. Consequently, if the long time linear portion is extrapolated back to $t = 0$, there is a finite intercept, J_e^0 , called the steady-state compliance. If the stress is suddenly removed at some instant after steady flow has been achieved, then the spring will retract but the dashpot will stop moving. Consequently there will be an elastic recovery of the fluid; this is also indicated in figure 2-6, the amount of this recovery is called the recoverable compliance and if the flow achieves steady state, the recoverable compliance should be equal to J_e^0 [17].

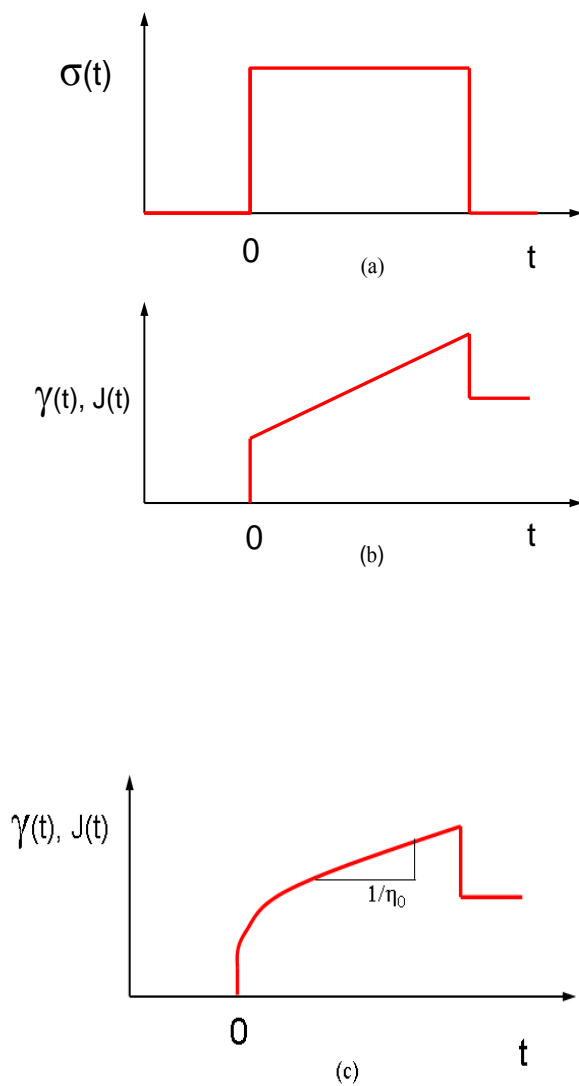


Figure 2-6 Creep experiment: (a) presetting a constant shear stress at time $t=0$ results in a time dependent strain $\gamma(t)$ and compliance $J(t)$ as shown in (b) for a viscoelastic liquid as described by the Maxwell model. The stress τ_0 is removed at some later time. For a real viscoelastic Sample, the shape of the $\gamma(t)$ and $J(t)$ curves is shown in (c). There from the slope at long measuring times, we can obtain the zero shear viscosity η_0 ^[17].

2.6.3 Dynamic Response: Loss and Storage Moduli

Although the step strain and step stress experiments are both useful in characterizing the viscoelastic response of material, the most common experimental approach is to apply a sinusoidally time varying strain (or stress), e. g., $\gamma(t) = \gamma_0 \sin \omega t$ and measure the sinusoidally time varying stress (or strain). One advantage of this approach, so both the viscous and elastic character of the response can be resolved concurrently. Other advantages are technical. In stress relaxation experiment the signal will become smaller and smaller as time evolves. In contrast, the dynamic experiment at each new driving frequency ω the strain amplitude γ_0 can be adjusted to bring the stress signal into the conveniently measurable range.

To see how Maxwell element responds to a strain of $\hat{\gamma} \sin \omega t$, the equation below adapted [17, 18].

$$\begin{aligned} \frac{d\gamma_{tot}}{dt} &= \hat{\gamma} \frac{d}{dt} \sin \omega t = \hat{\gamma} \omega \cos \omega t \\ &= \dot{\gamma}_{el} + \dot{\gamma}_{vis} = \frac{1}{\hat{G}} \dot{\sigma} + \frac{1}{\hat{\eta}} \sigma \end{aligned} \quad (2.15)$$

The solutions of this first-order, linear differential equation is given by:

$$\begin{aligned} \frac{\sigma(t)}{\gamma_0} &= \hat{G} \frac{\omega^2 \sigma^2}{1 + \omega^2 \sigma^2} \sin \omega t + \hat{G} \frac{\omega \sigma}{1 + \omega^2 \sigma^2} \cos \omega t \\ &= G' \sin \omega t + G'' \cos \omega t \end{aligned} \quad (2.16)$$

This last relation defines the elastic or storage modulus, G' , and the viscous or loss modulus, G'' :

$$G' = \hat{G} \frac{\omega^2 \sigma^2}{1 + \omega^2 \sigma^2} \quad (2.17a)$$

$$G'' = \hat{G} \frac{\omega \sigma}{1 + \omega^2 \sigma^2} \quad (2.17b)$$

The former measures the component of the stress response that is in-phase with the strain rate. So the material is viscoelastic if both G' and G'' are significant and when $G' \geq G''$, the material is solid like, and when $G' \leq G''$, the material is liquid like.

The normalized dynamic moduli G'/\hat{G} and G''/\hat{G} for the Maxwell element are plotted versus reduced frequency $\omega\sigma_R$ in figure 2-7, in a double logarithmic format. These functions display the following features. At low frequencies, $\omega\sigma_R \leq 1$, both G' and G'' increase with ω . The former increases as ω^2 and the latter as ω and $G'' > G'$. This scaling with frequency is characteristic of all liquids when the frequency of deformation is much lower than the inverse of the longest relaxation time of the material. Therefore, this is what one would expect to see for all polymer liquids once ω is low enough. At high frequencies, $\omega\sigma_R \geq 1$, $G' > G''$, and G' falls as ω^{-1} . This response is characteristic of a solid: the stress is independent of frequency (or time), and in-phase with the strain. The two functions are equal, $G' = G''$, and G'' shows a maximum when $\omega\sigma_R = 1$. This means when the frequency of deformation is exactly the reciprocal of the relaxation time, the material is equally liquid-like and solid-like. All of these features of G' and G'' will be evident when the detailed molecular models considers for viscoelastic response of polymer liquids [16, 17, 43].

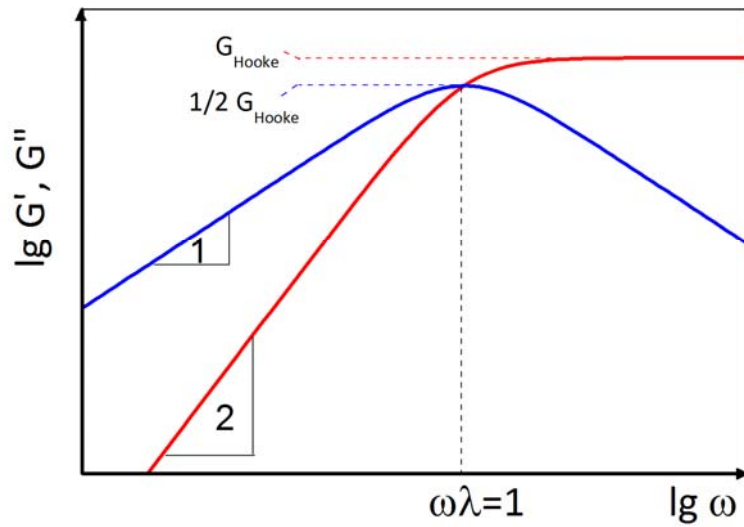


Figure 2-7 Normalized Dynamic Moduli G' and G'' [17, 43].

2.7 Bead-Spring Model

While the Maxwell model is a macroscopic model without any microscopic or molecular meaning, the bead-spring-model [44, 45] gives insight about the molecular physico-chemical origin of the relaxation mechanism. It takes into account the entropic properties of the polymer chain [42].

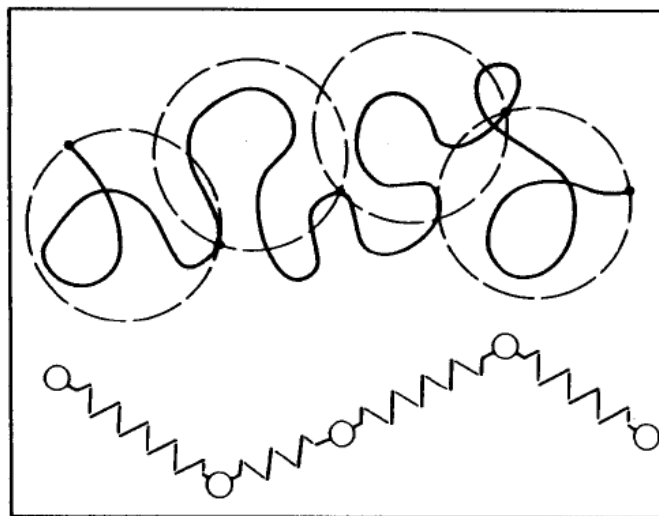


Figure 2-8 Scheme of The Bead-Spring Model [17].

In this model the polymer chain is divided into subsections that are sufficiently large to display rubber like elasticity (springy behavior at small elongations due to entropy elasticity of Gaussian chains). The subsections of the chain have a roughly spherical shape and present a mechanical drag with respect to the remainder of the melt or solution that is quantified with a subsection friction factor. The two elements of a single subsection can be represented in series as a spring of no volume and a rigid bead ^[42].

The calculation for the bead-spring model according to Rouse doesn't account for hydrodynamic interactions between the segments (limit of free draining). The calculation results in an equation which correlates different modes of the relaxation time σ_{Rouse} with the zero shear viscosity η_0 , molar mass M and concentration c of the polymer ^[42]:

$$\sigma_{Rouse, p} = \frac{6}{\pi^2} \frac{[\eta] \eta_s M}{CRT} \quad \text{With } p = 1, 2, 3 \dots \quad (2.18)$$

The longest relaxation time (p=1) is the terminal relaxation time for the total rearrangement of the molecule ^[42].

In the more complex evaluation due to Zimm the hydrodynamic interaction of beads in the same chain is taken into account. A disadvantage of the bead-spring model is the lack of interactions between different polymer molecules. Besides, the model explains linear viscoelastic behavior but not the shear rate dependence of viscosity ^[42].

2.8 Shear Rate Dependence of Viscosity

Newton's law of viscosity, which means a viscosity independent of shear rate can be applied only for few samples, e.g. homogeneous low molecular liquids. Most samples of practical interest like dispersions or entangled polymer solutions and melts, show a strong non-linear relation between shear stress τ and shear rate $\dot{\gamma}$, corresponding to a shear rate dependent viscosity η . In most cases the viscosity decreases with increasing shear rate; this rheological behavior is called shear thinning. The opposite behavior – viscosity increase with shear – is named shear thickening as shown in figure 2-9^[42].

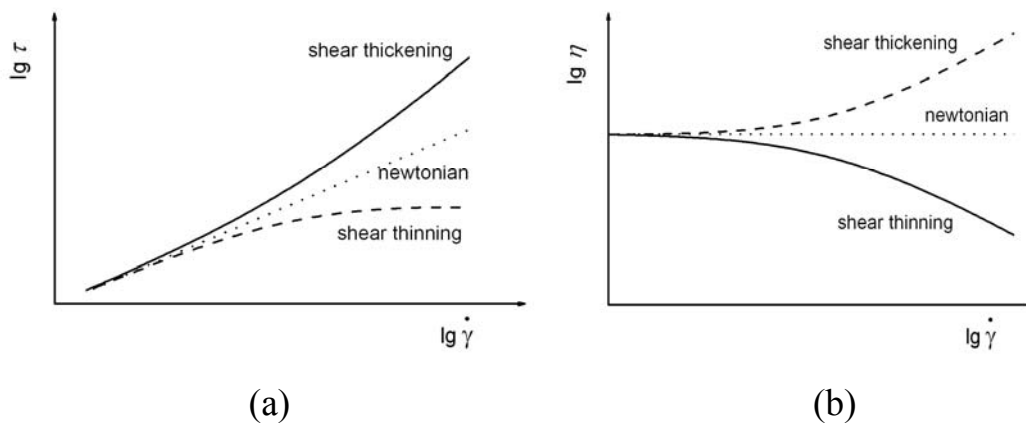


Figure 2-9 Schemes of Flow and Viscosity Curves with Different Flow Behavior (a) Shear Thickening Behavior (b) Shear Thinning Behavior^[42]

The experimental results are depicted in a plot shear stress vs. shear rate (called flow curve) or viscosity vs. shear rate (called viscosity curve or also flow curve). Often logarithmic scaling is used for both axes.

Flow curves are determined by rotational viscometers which are able to measure the viscosity at controlled shear rate or shear stress within a range of several decades^[42].

2.9 Shear Thinning of Polymer

Polymer solutions show at low shear rates a constant viscosity, the plateau value η_0 is called zero-shear viscosity as in figure 2-10. Reaching the critical shear rate $\dot{\gamma} = 1/\sigma_0$ the sample shows shear thinning. This regime is called “power-law regime” and can extend over several decades in shear rate ^[42].

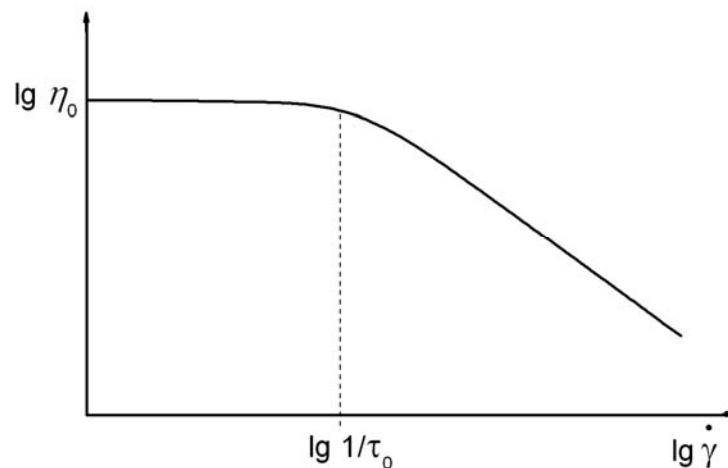


Figure 2-10 Shear Thinning of Polymer Melts and Concentrated Polymer Solutions ^[42].

The shear thinning is caused by the following mechanism: in polymer solutions and polymer melts polymer chains with molecular weights exceeding a critical limit M_c are entangled with each other. In the unperturbed state (no shear), Brownian motion of the polymer segments causes release of some entanglements and formation of new ones, until a thermal equilibrium state with a constant density of entanglements is reached. At low shear rate, the shear motion causes release of the entanglements. Since in this regime the motion due to shear is small compared to the thermal Brownian motion, however, there is sufficient time to allow for reformation of the released entanglements, and the overall entanglement density therefore remains constant. At higher shear rate, the time becomes insufficient for reformation

of all released entanglements, consequently the number density of entanglements decreases with increasing shear rate and the sample shows shear thinning. The critical shear rate $\dot{\gamma}_c$ where shear thinning starts is the reciprocal of the characteristic relaxation time σ_0 , which is the time needed to form a new entanglement at thermal equilibrium^[43].

It is observed that the onset of shear thinning for low to moderately concentrated polymer solutions is governed approximately by the longest bead-spring relaxation time, with $P = 1$. Therefore it is convenient to introduce reduced variables: The viscosity is replaced by η/η_0 and the shear rate by $\eta_0 M \dot{\gamma} / CRT$, which is roughly the product of shear rate and relaxation time of the bead-spring model. Using these reduced variables, most of the observed variation among different samples and systems can be removed^[64], as pointed out by Graessley^[46, 47].

2.10 Review of Viscoelastic Properties of Polyethylene Oxide

The study of the flow behavior of polymeric fluids has recently attracted increasing attention because of their inherent complexity and the increasing number of applications that involve such polymer-based fluids. It is recognized that the rheological properties of polymer solutions are determined by the bulk polymer properties (such as the chemical formulation, the molecular weight, and its distribution, the solvent properties, the polymer concentration, and external variables such as the temperature and the pressure)^[48-52].

Briscoe et al.,^[53] described the rheological properties of certain poly(ethylene oxide)s dissolved in water-based solvents. The experimental results show that the rheological properties in aqueous solutions were significantly affected by the solvent properties, which have been changed by the use of

ethanol–water mixtures and electrolyte solutions and by the variation of the ambient pressure and temperature. The variation of the temperature and pressure was seen to change the polymer chain configuration and also the interactions of polymer segments with the solvent molecules. This gave rise to distinctive and apparently unusual rheological properties for these systems with the variation of the ambient temperature and pressure. The study generally illustrated that the rheology of these systems were, to a large degree, influenced by the hydrogen bonding in the solvent and between the solvent as well as the polymer. At a first-order level, the increase of the pressure and the temperature and also the addition of electrolytes, and the inclusion of an aqueous diluent, produced comparable effects. In essence, these changes seemed to disrupt the hydrogen bonding structure in the solutions and, hence, the solvent quality in a comparable fashion.

Malwitz and Butler, ^[54] investigated the influence of shear on viscoelastic solutions of poly (ethylene oxide) (PEO) and clay [montmorillonite, i.e., Cloisite NA⁺ (CNA)] with rheology and small-angle neutron scattering (SANS). The steady-state viscosity was used to measure the shear-induced orientation and relaxation of the polymer and clay platelets. Anisotropic scattering patterns developed at much lower shear rates than in pure clay solutions. The scattering anisotropy saturated at low shear rates, and the CNA clay platelets aligned with the flow, with the surface normal parallel to the gradient direction. The cessation of shear led to partial and slow randomization of the CNA platelets, whereas extremely fast relaxation was observed for laponite (LRD) platelets. These PEO–CNA network-like solutions were compared with previously reported PEO–LRD networks, and the differences and similarities, with respect to the shear orientation, relaxation, and polymer–clay interactions, were examined.

Niedzwiedz, ^[55] studied the chain dynamics and viscoelastic properties of pure poly (ethylene oxide) (PEO) were studied covering a wide range of molecular weights (1000-932000 g/mol) and temperatures. Two experimental techniques were used: rheology, in order to study the large scale viscoelastic properties, and neutron spin-echo (NSE) spectroscopy, to investigate the chain dynamics at the molecular level. This study aimed to explore the characteristic dynamical parameters of the pure homopolymer system and describe its dependence on the polymer molecular weight and temperature, and observed that, after accounting for the molecular weight dependence of the glass transition temperature, the dynamics observed for the different molecular weight samples can be consistently described by the Vogel-Tammann-Fulcher (VTF) temperature dependence.

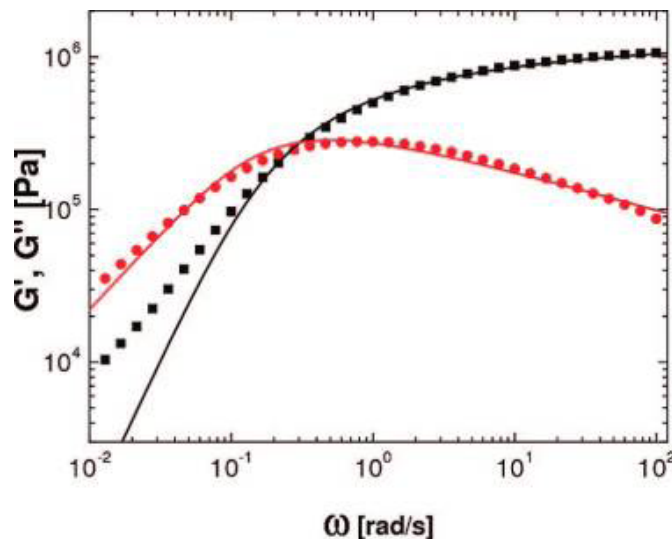


Figure 2-11a Rheology Data for the PEO Sample with $M_w = 932$ kg/mol Measured at Temperature $T = 378$ K. Black Squares Belong to the Storage Modulus, Red Circles to the Loss Modulus ^[55].

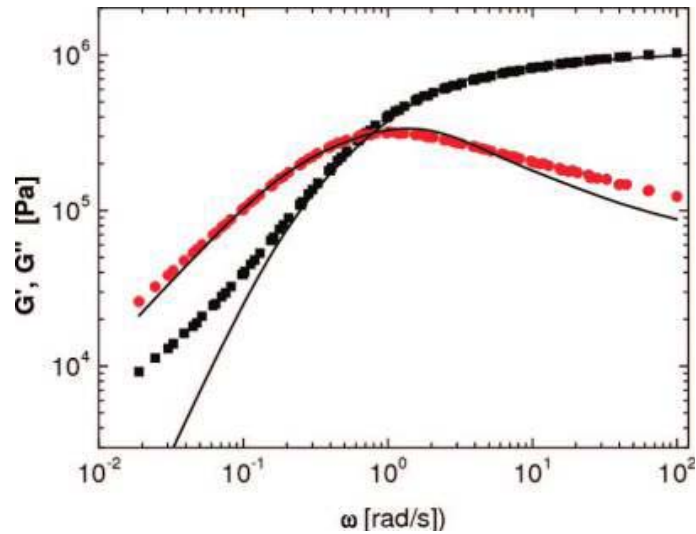


Figure 2-11b Rheology Data for the PEO Sample with $M_w = 610$ kg/mol Measured at Temperature $T = 348$ K. Black Squares Belong to the Storage Modulus, Red Circles to the Loss Modulus ^[55].

2.11 Drag Reduction Phenomenon and Applications

The presence of very small amounts of high-molecular-weight polymeric substances in turbulent flow can cause drastic reduction of frictional drag ^[22]. This turbulent drag reduction (DR) phenomenon implies that pipe flow of solution containing these polymer additives requires a lower pressure drop than the pure solvent for a given flow rate. Ever since the discovery of the drag-reduction phenomenon, efforts have been made for its industrial applications. In the last five decades, the range of applications of drag reduction has increased tremendously. The possible areas include oil-well fracturing operations, crude oil and refined petroleum product transport through pipelines ^[55-65]; oil well fracturing operations ^[66]; closed-circuit pumping installations (e.g. central-heating systems)^[59, 67]; sewage systems to prevent overflow during heavy rain ^[68]; hydraulic transportation of solid particle suspensions ^[69]; increasing the output of the water jet during firefighting and in water supply and irrigation systems ^[59, 67], transport of

suspensions and slurries, water heating and cooling systems, airplane tank filling, and biomedical systems including blood flow ^[70].

Synthetic polymers, biopolymers ^[71] and surfactants ^[72] have been widely used as drag reducers. Among these, the most effective drag-reducing polymers, in general, possess a flexible linear structure with a very high molecular weight. A high-molecular-weight water- soluble poly (ethylene oxide) (PEO), which has been widely used as a drag reducer in aqueous systems, was adopted for our study. Although DR was discovered half a century ago, a satisfactory theoretical interpretation is still not available. Nonetheless, it is accepted that both the non- Newtonian rheological behavior of polymer solutions and the interaction between polymer molecules and turbulence are responsible for turbulent DR ^[22].

Oldroyd and Tom, ^[73, 74] proposed the idea of a shear thinning layer at the wall having an extremely low viscosity. However, the rheograms of drag-reducing polymer solutions demonstrate that they were, in fact, not shear thinning, by considering the viscoelastic behavior of drag-reducing polymer solutions near a wall.

Little, ^[75] suggested that the critical polymer concentration, defined as the concentration where random coils begin to touch, might be used to normalize the drag reduction data since the same critical concentration appeared to produce the same degree of drag reduction, irrespective of the molecular weight of the polymer.

The three-parameter empirical relationship between the drag reduction (DR) and the concentration (*C*) to provide a universal correlation for drag reduction data are:

$$\lim_{c \rightarrow 0} DR = 0 \tag{2.19}$$

$$\lim_{c \rightarrow 0} (DR/C) = [DR] \tag{2.20}$$

$$\lim_{C \rightarrow \infty} DR = DR_{\max} \quad (2.21)$$

Where DR_{\max} is the maximum percent drag reduction for a given polymer solution. $[DR]$ is the intrinsic drag reduction which implies a measure for drag-reducing efficiency of the initial increments of polymer, and C is the polymer concentration (wppm, parts per million based on weight).

Where the drag reduction efficiency can obtain from the relation below

$$DR(\%) = \frac{\tau_{\text{solvent}} - \tau_{\text{solution}}}{\tau_{\text{solvent}}} \times 100 \quad (2.22)$$

Where τ_{solvent} is the torque in the pure solvent and τ_{solution} is the torque required when the polymer is added, that is, the torque in the dilute polymer solution. The rotational Reynolds number N_{Re} is defined as

$$N_{Re} = \frac{\rho r^2 u}{\mu} \quad (2.23)$$

Where ρ and μ are the density and the viscosity of the fluid, r is the radius of the disk, and u is the rotational speed of the disk. Using the RDA, turbulence is produced for $N_{Re} > 3 \times 10^5$ or equivalently 1050 rpm for the rotational disk velocity.

The drag reduction can be model in the following simplified form.

$$DR = \frac{a_0 + a_1 C}{b_0 + b_1 C} \quad (2.24)$$

From equations (2.19), (2.20), and (2.21) the four parameters (a_0 , a_1 , b_0 , and b_1) can easily determine, and (by setting $b_0 = 1$)

$$a_0 = 0, \quad a_1 = [DR], \quad b_1 = \frac{[DR]}{DR_{\max}} \cong \frac{1}{[C]}$$

Therefore an empirical relationship can be written as

$$DR = \frac{DR_{\max} [DR] C}{DR_{\max} + [DR] C} \quad (2.25)$$

Where $[DR]$ is the intrinsic drag reduction and $[C]$ is the intrinsic concentration. To interpret drag reduction data, one can write equation (2.25) as

$$\frac{C}{DR} = \frac{[C]}{DR_{max}} + \frac{C}{DR_{max}} \quad (2.26)$$

Where $[C]$ is the intrinsic concentration which can be calculate using equation below.

$$[C] = \frac{DR_{max}}{\lim_{c \rightarrow 0} \left(\frac{DR}{C} \right)} \quad (2.27)$$

A plot of DR/C vs. C usually gives a straight line, the slope of this line is the $1/DR_{max}$ value and the intercept is equal to the $[C]/DR_{max}$ value and the universal curve for drag reduction when normalized by the hydrodynamic volume fraction of the polymer solution ($\%DR[\eta]C$ verses $[\eta]C$)^[76].

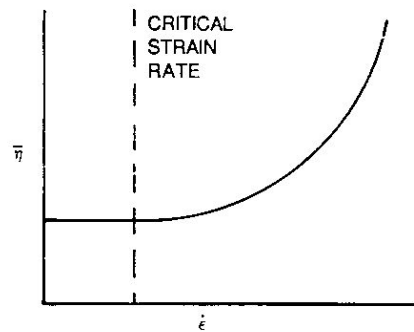
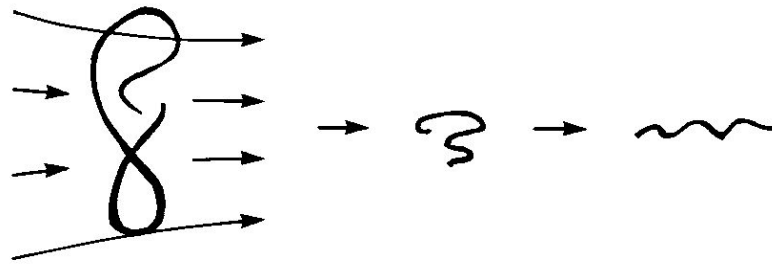
Ruckenstein,^[77] proposed that drag reduction is due to two effects of viscoelasticity: (1) Using a Maxwell model as the constitutive equation for a viscoelastic fluid, he showed that the instantaneous shear stress at the wall is smaller in the viscoelastic fluid than in a corresponding Newtonian fluid. (2) The replacement of the elements of liquid following short paths along the wall takes place as a result of turbulent fluctuations. In order to be replaced by other elements, an element moving along the wall must first relax its elastic stresses to enable viscous deformations required for its replacement to occur. This introduces a delay in the replacement process as compared to a Newtonian fluid. As the instantaneous shear stress at the wall decreases for increasing contact times with the wall, the average shear stress at the wall decreases.

Armstrong and Jhon, ^[78] adopted a simple model to study both the turbulence and dissolved polymer molecules; they related the molecular dissipation to friction factors by constructing a self-consistent method. For polymer molecules they used a variant of the dumbbell model. The dumbbell model represents a polymer molecule dissolved in a solvent by considering the polymer molecule as two spherical beads connected together by a central spring, immersed in an otherwise Newtonian fluid. Turbulence was also modeled by keeping a kinetic energy budget on the overall flow. They found that a polymer molecule grows by a factor of 10 or more from its equilibrium conformation.

Tabor, De Gennes, and Cadot, ^[79-81] proposed an energy cascade and scaling theory, which relates polymer length and deformation to turbulent energy dissipation. They suggested that friction reduction occurs primarily as a consequence of the elastic behavior of polymer molecules. Each polymer molecule (represented as a coil) behaves like a spring and, when deformed, stores part of its elastic energy. When the elastic energy of the molecule was equal to the kinetic energy of the turbulent disturbance, the disturbance was suppressed. A dispute still existed, however, as to whether the dominant DR mechanism occurs in the bulk flow or only at or near the system boundary.

Larson, ^[82] proposed that the high extensional stress in dilute polymer solutions figures prominently in the earliest phenomenological explanations of drag reduction including a “viscous” mechanism and an “elastic” mechanism.

In the viscous mechanism, turbulent flow unravels the polymer molecules, once the local strain rate exceeds the inverse of the polymer relaxation time. This is the “time-scale criterion” for the onset of drag reduction. The unraveled polymer molecules increase the extensional viscosity, causing drag reduction.



STRAIN THICKENING
BEHAVIOR OF FLEXIBLE POLYMER CHAIN
DURING EXTENSIONAL FLOW

Figure 2-12 Extensional Flow^[83].

In the elastic mechanism, the onset of drag reduction occurs when the polymer relaxation time exceeds the time scale associated with the smallest eddies in the flow. This is again the “time scale criterion” alluded to earlier. When the elastic energy stored in the polymer becomes comparable to the turbulent kinetic energy contained in an eddy of a certain size, all eddies smaller than it are suppressed, leading to drag reduction.

2.12 Review of Polyethylene Oxide as Drag Reduction Agent

Poly (ethylene oxide) (PEO) is an important commodity polymer used as a dilute additive in applications such as turbulent drag reduction, oil drilling and recovery ^[84-90]. Fundamental understanding of PEO solution structure, dynamics and rheology may be fruitfully applied to advance these applications. However, the dilute solution properties of PEO have generated controversy because of significant differences between experimental observations and well-established classical theories of polymer science. For example the aqueous solubility of PEO is unexpected: the closest counterparts of PEO in the homologous series of polyethers, poly (methylene) oxide and poly (propylene) oxide, are both practically insoluble in water ^[91]. Aqueous solutions of PEO display a temperature dependence of solvent quality that is the inverse of typical polymer solvent pairs. The aqueous PEO phase diagram also contains closed loop regions ^[92-94]. These anomalous solubility properties are a consequence of hydrogen bonding between the ether oxygen atom in PEO and the hydrogen in the water molecule ^[92, 95-97].

An important feature of dilute aqueous solutions of high molar mass PEO is their ability to reduce friction drag in flow. It is well known that the addition of a small amount of high molar mass polymer to a turbulent Newtonian fluid flow results in drag reduction ^[86, 98]. High molecular weight PEO is the most commonly used polymer for turbulent drag reduction in aqueous solutions since significant drag reduction can be achieved at very small concentrations ^[99, 100]. However, the drag reduction capacity of dilute PEO solutions appears to be much greater than predicted by dilute solution constitutive equations ^[101].

Virk et al., ^[102] observed the extent of DR induced by a homologous series of PEO in water flowing in a pipe and proposed a universal DR relationship, between the drag reduction and the polymer solution properties which was later simplified by little ^[75]. The universal DR equation effectively correlates concentration, molecular weight, and flow geometry.

Choi and Jhon, ^[103] investigated the concentration dependence of DR for PEO in water and polyisobutylene (PIB) in kerosene using a rotating disk apparatus (RDA), and correlations between polymer concentration, DR index, and viscosity-average molecular weight were obtained.

Choi and Kim, ^[104] investigated the Polymer-induced turbulent drag reduction in a rotating disk apparatus using nonionic poly (ethylene oxide) (PEO) in a synthetic saline solution with novel application to ocean thermal energy conversion technology. A maximum total (skin friction plus form) drag reduction of 30% was obtained with 50 wppm of PEO with molecular weight 5.0×10^6 g/mol. The concentration dependence of the percentage drag reduction for the PEO/saline solution system, a universal correlation for various molecular weights and Reynolds numbers are presented. Furthermore, hydrodynamic volume fraction was introduced to correlate drag reduction efficiency with molecular parameters in this PEO/saline solution system.

Chapter Three

Experimental Work

3.1 Materials

The studied polymer was polyethylene oxide with different molecular weights and types in water (with conductivity $< 0.5 \mu\text{S}/\text{cm}$) (deionized water). The samples of average molecular weights 1, 3, 10, 20, and 35 kg/mol (group A) were obtained from Physical Chemistry Institute, Mainz University, Germany. The samples of average molecular weights 100, 300, 1000, 4000, and 8000 kg/mol (group B) were purchased from Sigma – Aldrich Company, Germany, and the branched polyethylene oxide of molecular weight 0.55 and 40 kg/mol was purchased from Creative PEGWorks, Winston Salem, NC, USA, all samples were used as received. The molecular weights given by Sigma – Aldrich were checked by viscometric measurement at 30°C because the samples specifications were quite imprecise. The various molecular weights of polyethylene oxide were used in the present work to see the difference in their behaviors and how the higher molecular weights are more effective than the lower ones for industrial application, especially for drug reduction ^[105-109]. High-molecular-weight linear PEO 8000 kg/mol was chosen because of its excellent DR capabilities and it was the highest molecular weight available ^[104]. The polymer was studied to determine its intrinsic viscosity, critical molecular weight, viscoelastic properties, and drag reduction depending on the molecular weight and concentration.

Note: This work carried out in the Physical Chemistry Institute laboratories at Mainz University, Germany

3.2 Dissolving Process

For capillary viscometry the dissolving of polymers was normally carried out by taking a certain amount of each molecular weight relied on the equation below ^[110] to get solution with specific viscosity η_{sp} of about 1. The intrinsic viscosity in the following equation can be roughly estimated by Mark-Houwink constants ^[16]. From the starting concentration, by further dilution solutions with specific viscosities η_{sp} in the range of 0.2 to 1 were obtained which are suitable for the determination of intrinsic viscosities according to ISO 1628-1.

$$[\eta] = kM^a \approx 0.0499 \cdot M^{0.67} \quad (3.1)$$

$$c = \frac{1}{[\eta]} \quad (3.2)$$

For the capillary viscometers, a total volume of about 20 ml solution was needed. The polymer was dissolved completely and left at laboratory temperature. A homogeneous solution was obtained as shown in table below.

Table 3-1 Dissolving Times of PEO Solutions for Dilute Concentrations

No.	Molecular Weight(kg/mol)	Time of dissolving
1	Linear PEO 1	1.5 hours
2	Linear PEO 3	2 hours
3	Linear PEO 10	5 hours
4	Linear PEO 20	8 hours
5	Linear PEO 35	1 day
6	Linear PEO 100	1 day
7	Linear PEO 300	1 day
8	Linear PEO 1000	2 days
9	Linear PEO 4000	5 days
10	Linear PEO 8000	6 days
11	Branch PEO 0.55	1 hours
12	Branch PEO 40	1 day

Then 15 ml of the homogenous solution was injected inside the capillary and diluted to different concentrations by adding a certain amount of water to the capillary such as 5, 5, 5, 10, 10, 10, and 10 ml H₂O.

For the viscoelastic measurements, the method of the concentrated solution preparation is the same as for diluted solution; a certain amount of polymer per 5 ml water is taken at laboratory temperature to prepare 1% and 5% concentrations. A homogenous solution was obtained as show in Table below.

Table 3-2 Dissolving Times of PEO Solutions for Concentrated Concentrations

No.	Molecular Weight (kg/mol)	Time of dissolving	
		1% conc.	5% conc.
1	Linear PEO 100	4 days	9 days
2	Linear PEO 300	4 days	9 days
3	Linear PEO 1000	5 days	12 days
4	Linear PEO 4000	8 days	18 days
5	Linear PEO 8000	10 days	21 days

For drag reduction measurements, a certain amount from the samples of molecular weights 100 kg/mol were dissolved in 1000 ml of water at laboratory temperature to prepare a solution of 10000 ppm. After obtaining a homogeneous solution, this sample was diluted to 7000, 5000, 3000, 1500, 1000, 700, and 500 ppm, while for the molecular weight 300 kg/mol the first solution was 5000 ppm then the solution were diluted to 3000, 1500, 1000, 700, 500, 300, 150, 100, 50, and 30 ppm.

For the molecular weights 1000 kg/mol, first a solution of (1000 ppm) was prepared and then this sample was diluted to 700, 500, 300, 150, 100, 50, 30, 15, 10, 5, 3, and 1 ppm.

For the molecular weights 4000 and 8000 kg/mol, first a solution of 500 ppm was prepared and then this sample was diluted to 300, 150, 100, 50, 30, 15, 10, 5, 3, and 1 ppm by adding water to the stock solution. A homogenous solution was obtained as shown in table below.

Table 3-3 Dissolving Times of PEO Solutions for Drag Reduction

No.	Molecular Weight(kg/mol)	Time of dissolving
1	Linear PEO 100	2 days
2	Linear PEO 300	3 days
3	Linear PEO 1000	4 days
4	Linear PEO 4000	6 days
5	Linear PEO 8000	10 days

3.4 Operating Procedure

a) Intrinsic Viscosity Measurement:

1. The flow times (t) were measured for aqueous solutions of the PEO compositions. Different concentrations of each composition as well as pure water were measured.
2. A water bath of type Messgeraetewerk LAUDA, Germany, with double thermostat type (D-60-S) has been thermostated at temperature (25°C) as shown in figure 3-1.



Figure 3-1 Viscometric Measurement System.

3. A Schott Ubbelohde viscometer size (0a, 0c, 1c) for dilute system as shown in figure 3-2 was used to measure the flow time of the solvent (t_0) and flow time of polymer solutions (t).

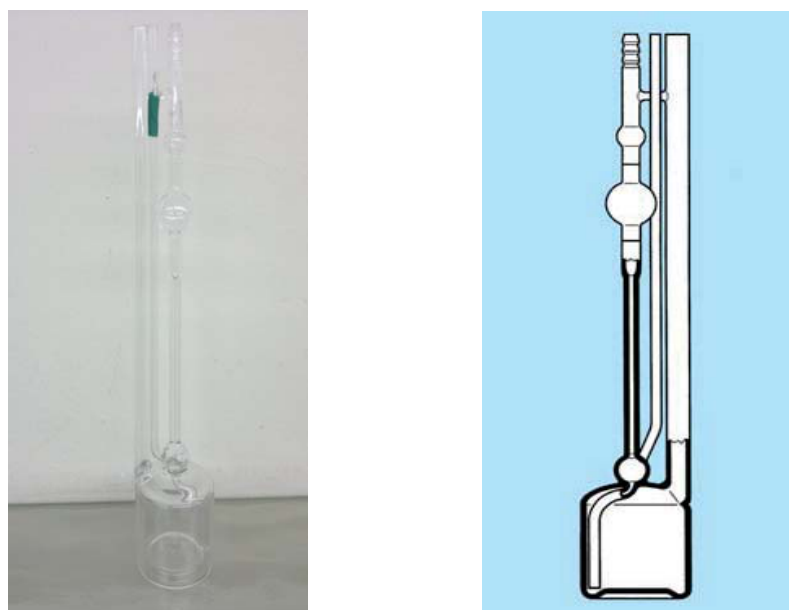


Figure 3-2 Schott Ubbelohde Capillary Viscometer.

Using of the Viscometer

This method is used for dilute solutions. Ubbelohde viscometer has been used of different sizes. The procedure is as follows:

- The viscometer was cleaned using suitable solvents (mixture of sulphuric acid H_2SO_4 (95 – 97%) and nitric acid HNO_3 65% then with water then with acetone (CH_3COCH_3) and then dried by oven for one day.
- The definite volume (normally 15ml) of solution is placed in the capillary viscometer
- The viscometer is placed into the holder, and inserted to the constant temperature bath, (25°C) as shown in figure 3-3.



Figure 3-3 Water Bath with Viscometer.

- The solution was allowed approximately 10-15 minutes to come to bath temperature and become free of air bubbles.
- The solution was pumped automatically by pressing air so that the meniscus of the liquid passes the upper light barrier. Then

automatically the liquid flow through the capillary (narrow diameter section of viscometer) because of the height difference of the liquid in the two arms of the viscometer; so there is a hydrostatic driving pressure.

- The flow times and concentrations are used to calculate the intrinsic viscosity for solutions.

The time required for the solutions to flow from the high barrier to the low barrier is greater than of the solvent. If the flow occurs rapidly (t is small), the liquid is moving fast and kinetic energy will be significant. In this case it is important to correct the kinetic energy.

b) Linear Viscoelastic Measurement:

The linear viscoelastic measurements and steady shear measurements were carried out using rotational rheometer type UDS200, Anton Paar GmbH, Graz, Austria, as shown in figure 3-4 for concentrations of 5%, 1%, 0.2%, and 0.05%, for the high molecular weights PEO.



Figure 3-4 UDS200 Rotational Rheometer.

The instrument can be equipped with different measuring geometries. For the viscoelastic measurements, cone/plate and double gap geometries were used as shown in figure 3-5.

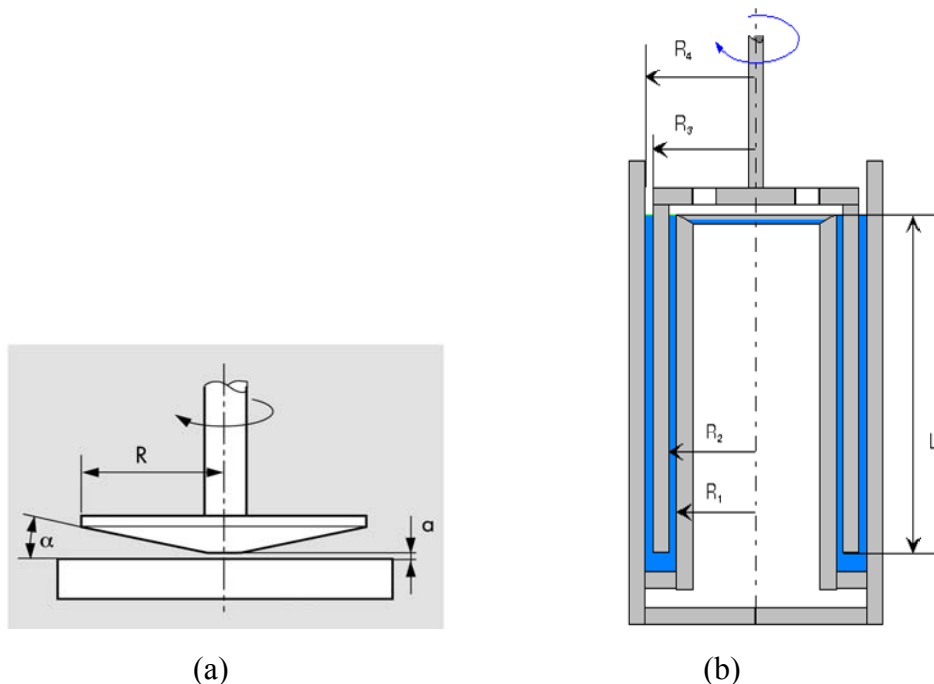


Figure 3-5 Rotational Rheometer Geometries (a) Cone/Plat (b) Double Gap.

Generally, the higher the viscosity of the sample the smaller the measuring geometry, the measurements were carried out by using three different geometries: For high concentrations and high molecular weights, a cone/plate MK21 with 25 mm diameter and 2° cone angle was used. For lower concentrations and/or lower molecular weights, a cone MK22 with 50 mm diameter and 1° cone angle was used. For very low viscosities, the double gap geometry Z1 was used.

The procedure of measurement of the linear viscoelastic properties is as follows:

- The temperature of system was kept constant at 25°C
- The calibration was done before using any geometry.
- The zero position was done before starting the measurements.
- For measurements with cone/plate, silicon oil (viscosity 2 cSt) was used to cover the sample at the edge of the high concentrated solutions to avoid the evaporation of water. For some measurements, additionally

polyisobutylene was used to prepare a ring around the cone which avoided the flowing of the low viscose silicon oil. The silicon oil can be used for this purpose because it is immiscible with aqueous solutions and does not contribute to the measured torque of the Rheometer because of the low viscosity, as shown in figure 3-6.



Figure 3-6 Set up of cone/plat measurements

- For oscillatory measurements, first an amplitude sweep is performed: Here the frequency is kept constant (10 rad/s) while the strain is varied from 0.1 to 100 %. In this measurement, the linear viscoelastic (LVE) regime is determined. This means that the range of strains in which the measured shear moduli G' and G'' is constant.
- The most important measurements are frequency sweeps at constant strain. The strain was chosen in the LVE regime, normally 1% to 30%. The frequency range normally is 0.1 to 600 rad/s.
- For some highly gelly samples (5% solutions of high molecular weight PEO samples), the zero shear viscosity was not obtained by the above described frequency sweeps because of the high relaxation times. For these samples, creep measurements at constant shear stress were

performed. From these creep measurements at long measuring times the zero shear viscosity were determined.

Mechanical Equations of Cone and Plate Geometry

The cone-and-plate apparatus (CPA) consists of a shallow rotating cone on top of a stationary plate, both surrounded by a circular cylinder, see Figure above. Liquid is flowing inside the device. When the angle α between the cone and plate is very small and the rotational speed ω is low, the flow is basically azimuthal, i.e. streamlines are concentric circles, the velocity profile is linear and the shear-rate is constant. Thus the most well-known motivation for the use of CPA has been a viscometer, mainly used for very viscous or viscoelastic fluids ^[111].

In fact the flow pattern is only approximately azimuthal: as the angle α and rotational rate ω increase, the fluid near the cone experiences an increasing centrifugal force that promotes radial fluid motion towards the periphery of the device. Thus a radial secondary flow develops, streamlines turn into spirals, until the onset of turbulence. The appearing of secondary flow was shown to be controlled by a single parameter $Re \epsilon^2$, with $\epsilon = \tan \alpha$ and Re the Reynolds number. From a mathematical view point CPA has been much less studied than Couette flow between cylinders. Indeed the cone-plate geometry gives rise to a quite different picture: whereas in Couette flow there is an exact analytical solution that becomes unstable, in CPA flow no analytical solution is available but only an approximate one, which is stable, at least in the small gap limit. Due to a discontinuity located at the intersection of the cylinder and the cone, the solution cannot belong to $W^{1,2}(\Omega)$ ^[111].

Problem setting and scaling

Let Ω_ϵ be the domain filled by the fluid, which suppose to be Newtonian, of kinematics' viscosity ν , constant density ρ and $\epsilon = \tan \alpha$. The radius of the outer cylinder is denoted by R . Let O be the cone apex, Oy_3 its axis, Oy_1y_2 the plane in a rectangular Cartesian coordinate system (y_1, y_2, y_3) and corresponding basis (e_1, e_2, e_3) ^[111].

The incompressible Navier–Stokes equations with no-slip Dirichlet boundary condition read: Given an initial function U_0 , find a velocity field $U = (U_1, U_2, U_3)$ and a pressure field P , such that for $\tau > 0$

$$\partial\tau U + (U \cdot \nabla)U - \nu\Delta U + 1/\rho \nabla P = 0 \quad \text{in } \Omega_\epsilon, \quad (3.3a)$$

$$\text{div}U = 0 \quad \text{in } \Omega_\epsilon, \quad (3.3b)$$

$$U = 0 \quad \text{on } ((y_3 = 0) \cup (r = R)), \quad (3.3c)$$

$$U = r\omega \cdot e_\theta \quad \text{on } (y_3 = r \cdot \epsilon), \quad (3.3d)$$

$$U(\cdot, 0) = U_0 \quad \text{in } \Omega_\epsilon. \quad (3.3e)$$

Here and in the following, ω is the angular velocity of the cone, r the distance to the vertical axis and e_θ the azimuthal direction. In order to bring (3.3a)–(3.3e) into non dimensional form and to make the domain independent of ϵ , it was set ^[111].

$$x_1 = y_1/R, \quad x_2 = y_2/R, \quad x_3 = y_3/R_\epsilon, \quad t = \omega\tau$$

So that $\Omega = \{(x_1, x_2, x_3) \in \mathbb{R}^3; 0 < r < 1, 0 < x_3 < r \text{ with } r = \sqrt{x_{21}^2 + x_{22}^2}\}$ is the new fixed domain. Define the different parts of the boundary

$$\Gamma_1 := \{x \in \partial\Omega; r = x_3\}, \quad \Gamma_2 := \{x \in \partial\Omega; x_3 = 0\}, \quad \Gamma_3 := \{x \in \partial\Omega; r = 1\}.$$

The corresponding kinematic scaling is

$$u_1 = U_1/R\omega, \quad u_2 = U_2/R\omega, \quad u_3 = U_3/R\omega\epsilon, \quad p = P/R^2\omega^2\rho, \quad (3.4)$$

So that $u = (u_1, u_2, u_3)$ is the new unknown velocity and p the new pressure.

As corresponding Reynolds number define

$$Re = R^2\omega/\nu$$

With the above considerations, problem (3.3a) – (3.3e) transforms into the following anisotropic Navier–Stokes equations: Find $\mathbf{u} = (u_1, u_2, u_3)$ and p , such that for $t > 0$

$$\partial_t u_i + \mathbf{u} \cdot \nabla u_i - 1/Re \Delta_{\varepsilon} u_i + \partial_i p = 0 \quad \text{in } \Omega, i = 1, 2 \quad (3.5a)$$

$$\varepsilon^2 (\partial_t u_3 + \mathbf{u} \cdot \nabla u_3 - 1/Re \Delta_{\varepsilon} u_3) + \partial_3 p = 0 \quad \text{in } \Omega, \quad (3.5b)$$

$$\operatorname{div} \mathbf{u} = 0 \quad \text{in } \Omega, \quad (3.5c)$$

$$\mathbf{u} = \mathbf{g} \quad \text{on } \partial\Omega, \quad (3.5d)$$

$$\mathbf{u}(\cdot, 0) = \mathbf{u}_0 \quad \text{in } \Omega, \quad (3.5e)$$

Where Δ_{ε} is an anisotropic Laplacian, defined by

$$\Delta_{\varepsilon} := \sum_{k=1}^2 \frac{\partial^2}{\partial x_k^2} + \frac{1}{\varepsilon^2} \frac{\partial^2}{\partial x_3^2},$$

And the boundary data is collected in

$$\mathbf{r} \cdot \mathbf{e}_{\theta} \text{ on } \Gamma_1,$$

$$\mathbf{g} := 0 \quad \text{on } \Gamma_2,$$

$$0 \quad \text{on } \Gamma_3.$$

Notations and auxiliaries

Hereafter, $\|\cdot\| = \|\cdot\|_{\Omega}$, and for $G \subseteq \Omega$, $\|w\|_G = (\int_G |w|^2)^{1/2}$ denotes the usual

$L^2(G)$ -norm for scalar as well as vector- and matrix-valued functions on G , (\cdot, \cdot) is the L^2 -inner product. To avoid confusion, vector-valued functions will always be denoted with boldface characters ^[111].

For $0 < r_0 < 1$ define $\Omega_{r_0} := \{x \in \Omega; r < r_0\}$.

This will need the following function spaces.

$$V = \{\boldsymbol{\varphi} \in C_0^{\infty}(\Omega); \operatorname{div} \boldsymbol{\varphi} = 0\}.$$

V (resp. H) is defined as the closure of V in $H_0^{\infty}(\Omega)$ (resp. $L^2(\Omega)$).

Acylindrical coordinates shall frequently use (r, θ, x_3) . Some formulas recall, which will be used below. The cylindrical coordinates are defined by

$$r = \sqrt{x_1^2 + x_2^2}, \quad x_1 = r \cos \theta, \quad x_2 = r \sin \theta$$

With the corresponding basis

$$\mathbf{e}_r = \frac{1}{r} (x_1 \mathbf{e}_1 + x_2 \mathbf{e}_2), \quad \mathbf{e}_\theta = \frac{1}{r} (-x_2 \mathbf{e}_1 + x_1 \mathbf{e}_2), \quad \mathbf{e}_3.$$

Thus a 3D vector field \mathbf{w} can be decomposed as

$$\mathbf{w} = w_r \mathbf{e}_r + w_\theta \mathbf{e}_\theta + w_3 \mathbf{e}_3.$$

Furthermore, define the horizontal part \mathbf{v}_H of a 3D vector field \mathbf{v} by

$$\mathbf{v}_H := v_1 \mathbf{e}_1 + v_2 \mathbf{e}_2$$

Likewise $\nabla_H := \mathbf{e}_1 \partial_1 + \mathbf{e}_2 \partial_2$ and

$$\|\mathbf{w}\|_G^2 := \|\mathbf{w}_H\|_G^2 + \epsilon^2 \|w_3\|_G^2.$$

In the sequel same notation will use for a function f depending on the Euclidean basis or cylindrical coordinates: $f(x_1, x_2, x_3) = f(r, \theta, x_3)$. This abuse of notation will not lead to confusion. The following differential operators transform like:

$$\nabla = \mathbf{e}_r \partial_r + \frac{1}{r} \mathbf{e}_\theta \partial_\theta + \mathbf{e}_3 \partial_3, \quad \partial_\theta \mathbf{e}_\theta = -\mathbf{e}_r, \quad \partial_\theta \mathbf{e}_r = \mathbf{e}_\theta,$$

$$\text{Div } \mathbf{w} = \frac{1}{r} \partial_r (r w_r) + \frac{1}{r} \partial_\theta w_\theta + \partial_3 w_3,$$

$$\Delta w = \frac{1}{r} \partial_r \left(r \frac{\partial w}{\partial r} + \frac{1}{r^2} \frac{\partial^2 w}{\partial \theta^2} + \frac{\partial^2 w}{\partial x_3^2} \right),$$

$$\Delta \mathbf{w} = \left(\Delta w_r - \frac{2}{r^2} \partial_\theta w_\theta - \frac{w_r}{r^2} \right) \cdot \mathbf{e}_r + \left(\Delta w_\theta + \frac{2}{r^2} \partial_\theta w_r - \frac{w_\theta}{r^2} \right) \cdot \mathbf{e}_\theta + \Delta w_3 \cdot \mathbf{e}_3.$$

Formal asymptotics

Multiplying (3.5a) by ϵ^2 , sending ϵ to zero and then formally equating (3.5a) yields

$$\frac{\partial^2 u_H}{\partial x_3^2} = 0$$

So that u_H is linear in x_3 :

$$u_H = A_H(x_1, x_2)x_3 + B_H(x_1, x_2).$$

Taking into account the boundary conditions on Γ_1 and Γ_2 we formally get

$$u_1 = x_3 (-x_2/r), \quad u_2 = x_3 (x_1/r).$$

Plugging this in the incompressibility equation (3.5c) gives

$$\partial_3 u_3 = 0,$$

Which, with the boundary condition on Γ_2 allows us to derive

$$u_3 = 0.$$

Hence the velocity field is completely characterized within the device:

$$\mathbf{u} = x_3 \cdot \mathbf{e}_\theta \quad (3.6)$$

This is what is called the primary flow and will be denoted by \bar{u} .

The primary flow has only a θ -component (swirl), i.e. is purely azimuthal. Its modulus depends on x_3 only. It satisfies the no-slip boundary conditions on the cone Γ_1 and on the plane Γ_2 but violates the boundary condition at the outer cylinder Γ_3 . In the physical variables, the primary flow is

$$\bar{U} = \frac{w y_3}{\varepsilon} \cdot \mathbf{e}_\theta.$$

The resulting shear stress has constant magnitude:

$$\sigma_{\theta y_3}(\bar{U}) = \rho \nu \partial_{y_3} \bar{U} = \rho \nu \frac{w}{\varepsilon} \cdot \mathbf{e}_\theta. \quad (3.7)$$

This basic flow is indeed observed in physical experiments and the shear stress (3.7) is used to measure fluid viscosity, provided that $Re \varepsilon^2$ is small enough. Now, the surprising fact is that the primary flow is not a solution of the Navier–Stokes equations (3.5). Indeed, it compute

$$-\frac{1}{Re} \Delta_\varepsilon \bar{u} + (\bar{u} \cdot \nabla) \bar{u} = \frac{1}{Re} \frac{x_3}{r^2} \cdot \mathbf{e}_\theta - \frac{x_3^2}{r} \cdot \mathbf{e}_r. \quad (3.8)$$

It is easy to see that (3.8) is not a gradient, so the above term cannot be balanced by a pressure gradient alone. Furthermore, if the limit of (3.5a) – (3.5b) take in the sense that we set $\mathbf{u} = \bar{u}$ and then formally send $\varepsilon \rightarrow 0$ we get for the pressure ^[111].

$$\partial_r p = \frac{x_3}{r^2}, \quad (3.9)$$

$$\partial_{\theta} p = -\frac{1}{\text{Re}} \frac{x_3}{r}, \quad (3.10)$$

$$\partial_3 p = 0. \quad (3.11)$$

Of course (3.9) – (3.11) cannot hold simultaneously.

For the same reason, as

$$-\frac{1}{\text{Re}} \Delta_{\epsilon} \bar{u} = \frac{1}{\text{Re}} \frac{x_3}{r^2} \cdot \mathbf{e}_{\theta}, \quad (3.12)$$

Neither is the primary flow solution of Stokes equations. The estimate for the shear stress is now a direct consequence of the above bounds: From the equations above can derive the equation below

$$\frac{\partial}{\partial t} |||v|||^2 + \frac{1}{2\text{Re}\epsilon^2} |||\partial^3 v|||^2 \leq C_3^2 \text{Re} \epsilon^2 \quad (3.13)$$

Integrating this relation with respect to time from 0 to t and using the estimate for $|||v(t)|||$ represents the stated result ^[111].

c) Drag Reduction Measurement:

Drag reduction measurement was carried out by using a rotating rheometer UDS200 that used for linear viscoelastic measurement. To measure the drag reduction, a special big plate measuring geometry made of brass was manufactured in the physical chemistry institute, Mainz University, Germany, with a diameter of 120 mm as shown in figure 3-7.

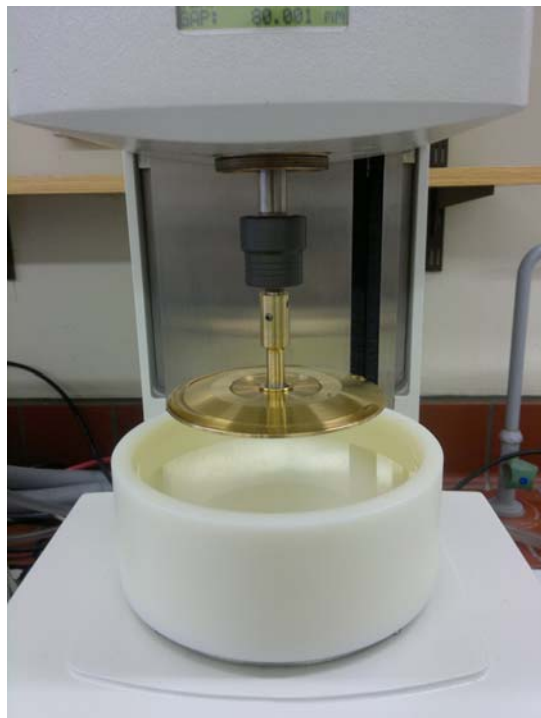


Figure 3-7 Drag Reduction Geometry.

Additionally, a special container with a cover made of polyamide was also manufactured. The dimensions are: inner diameter = 160 mm, height = 50 mm). The geometry was constructed according to ^[83] as shown in figure 3-8.

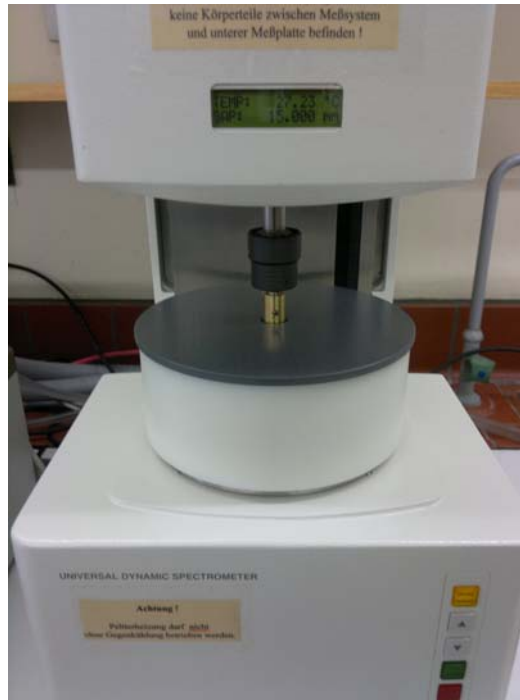


Figure 3-8 Drag Reduction's Container.

Because of the large diameter, the maximum angular velocity of 1200 rpm leads to a high speed at the plate rim of 7.54 m/s. This high velocity leads to turbulent flow as described in the literature ^[83].

The procedure of measurement of the Drag reduction factor is as follows:

- The temperature of system was kept constant at the range (23.3-23.8 °C)
- The zero position was determined before starting the measurements. The measuring position of the plate was at a height of 15 mm from the bottom of the container.
- The measuring procedure at the rheometer: First increase of the rotational speed to 1200 rpm in 1 minute, then 5 data points (measuring point duration: 3 s) were obtained at this speed.
- The value of the torque is used to determine the drag reduction factor.
- The value of viscosity of the solution was checked by using a capillary measurement by using Schott Ubbelohde viscometer size (1) which filled with (15-20 ml) of solution at 23.6°C as shown in figure 3-9.

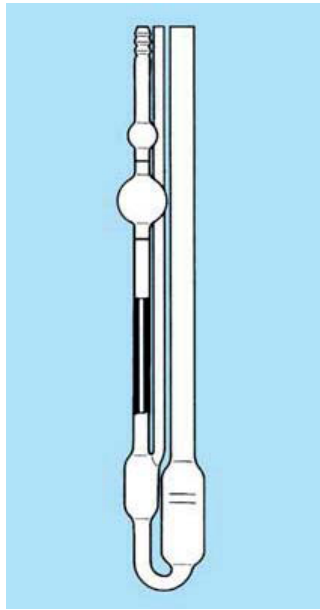


Figure 3-9 Schott Ubbelohde Capillary Viscometer.

Figures 3-2 and 3-4 show that there are two types of viscometers, one type is a capillary viscometer which is used for Newtonian and diluted solution, and the second type is the rotational viscometer which is used for non-Newtonian and concentrated solution.

3.4 Calculations

a) Capillary Viscometer Measurements:

1- The times of the solvent (t_0) and solution (t) was measured.

2- The relative viscosity was calculated from $\eta_{rel} = \frac{t}{t_0}$.

3- The specific viscosity was calculated from $\eta_{sp} = \frac{t-t_0}{t_0}$.

4- The reduced viscosity was also calculated $\eta_{red} = \frac{\eta_{sp}}{c}$.

5- The $\eta_{red} = \frac{\eta_{sp}}{c}$ was plotted with each concentration to get intrinsic Viscosity $[\eta]$ as shown in figure below.

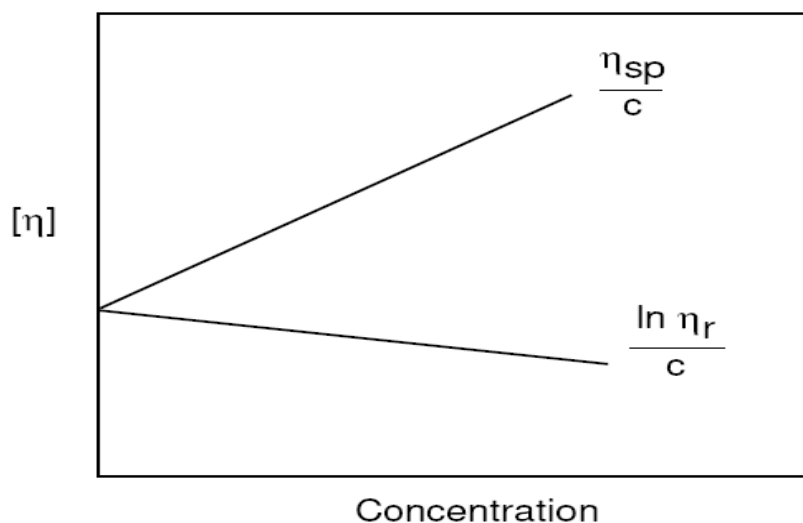


Figure 3-10 $\frac{\eta_{sp}}{c}$ or $\frac{\ln \eta_r}{c}$ versus Concentration.

b) Linear Viscoelastic Measurement:

The basic rheometric calculations, as conversion of the measured torque into shear stress or the calculation of strain and shear rate from the rotational speed is done by the rheometer software Rheoplus V3.40, Anton Paar GmbH, Graz, Austria.

From the creep measurements, the zero shear viscosity is calculated from the plot strain versus time by dividing the applied shear stress by the final stationary slope, which is the stationary shear rate, by the σ : $\eta_0 = \frac{1}{\tau} \frac{d\gamma}{dt}$.

c) Drag Reduction Measurement:

1. The torque of the pure solvent (τ_0) and solution (τ_p) were measured.
2. The percentage drug reduction was calculated from $DR\% = \frac{\tau_0 - \tau_p}{\tau_0} * 100$.
3. The intrinsic drag reduction was calculated from the initial slope of the percentage drag reduction curves according to the following equations.

$$\lim_{c \rightarrow 0} DR = 0$$

$$\lim_{c \rightarrow 0} (DR/C) = [DR]$$

4. The drag reduction value was calculated by using the formula.

$$DR = \frac{DR_{\max} [DR] C}{DR_{\max} + [DR] C}$$

5. The value of the intrinsic concentration of the drag reduction estimated from the slope according to the following equation.

$$\frac{C}{DR} = \frac{[C]}{DR_{\max}} + \frac{C}{DR_{\max}}$$

Chapter Four

Results and Discussion

4.1 Introduction

The present work deals with intrinsic viscosity, Mark-Houwink constants, critical molecular weight parameters, viscoelastic properties, and drag reduction factors and concentrations for different molecular weights of polyethylene oxide in water.

4.2 Intrinsic Viscosity of Polyethylene Oxide in Water

The relative, specific and reduced viscosities were measured using Schott Ubbelohde capillary viscometer for dilution sequences to determine the intrinsic viscosity for PEO for twelve different molecular weights, at temperature 25°C. Polyethylene oxide stock solutions were diluted in the capillaries with pure water to different concentrations by adding a certain amount of water to the capillary, and the effect of concentration on specific and reduced viscosity are represented graphically at 25°C.

4.2.1 Intrinsic Viscosity Measurements for Group A Samples at 25 °C

The measurements of the intrinsic viscosity were carried out for the samples (1, 3, 10, 20, 35 kg/mol) that obtained from physical chemistry institute as shown in figure 4-1, and the results in tables from 4-1 to 4-5 and in appendix A.

Table 4-1 Specific and Reduced Viscosity of 1 kg/mol Molecular Weight PEO at 25 °C

Concentration (g/ml)	$\eta_{sp} = (t/t_0) - 1$	$\eta_{red} = \eta_{sp}/conc.$ (ml/g)
0.158	0.73	4.61
0.119	0.527	4.432
0.095	0.411	4.322
0.079	0.336	4.246
0.059	0.255	4.301
0.048	0.199	4.203
0.04	0.168	4.25

Table 4-2 Specific and Reduced Viscosity of 3 kg/mol Molecular Weight PEO at 25 °C

Concentration (g/ml)	$\eta_{sp} = (t/t_0) - 1$	$\eta_{red} = \eta_{sp}/conc.$ (ml/g)
0.062	1.453	23.34
0.047	1.036	22.193
0.037	0.806	21.584
0.031	0.673	21.608
0.023	0.446	19.094
0.019	0.362	19.384
0.016	0.291	18.693

Table 4-3 Specific and Reduced Viscosity of 10 kg/mol Molecular Weight PEO at 25 °C

Concentration (g/ml)	$\eta_{sp} = (t/t_0) - 1$	$\eta_{red} = \eta_{sp}/\text{conc.}$ (ml/g)
0.036	1.309	36.779
0.027	0.951	35.652
0.021	0.732	34.284
0.018	0.575	32.333
0.013	0.394	29.544
0.011	0.313	29.317
0.009	0.252	28.272

Table 4-4 Specific and Reduced Viscosity of 20 kg/mol Molecular Weight PEO at 25 °C

Concentration (g/ml)	$\eta_{sp} = (t/t_0) - 1$	$\eta_{red} = \eta_{sp}/\text{conc.}$ (ml/g)
0.023	1.332	57.689
0.017	0.879	50.738
0.014	0.663	47.852
0.012	0.535	46.333
0.009	0.385	44.435
0.007	0.292	42.215
0.006	0.248	42.995

Table 4-5 Specific and Reduced Viscosity of 35 kg/mol Molecular Weight PEO at 25 °C

Concentration (g/ml)	$\eta_{sp} = (t/t_0) - 1$	$\eta_{red} = \eta_{sp}/\text{conc.}$ (ml/g)
0.011	0.657	61.469
0.008	0.474	59.06
0.006	0.368	57.416
0.005	0.302	56.578
0.004	0.223	55.636
0.003	0.177	55.32
0.002	0.146	54.773

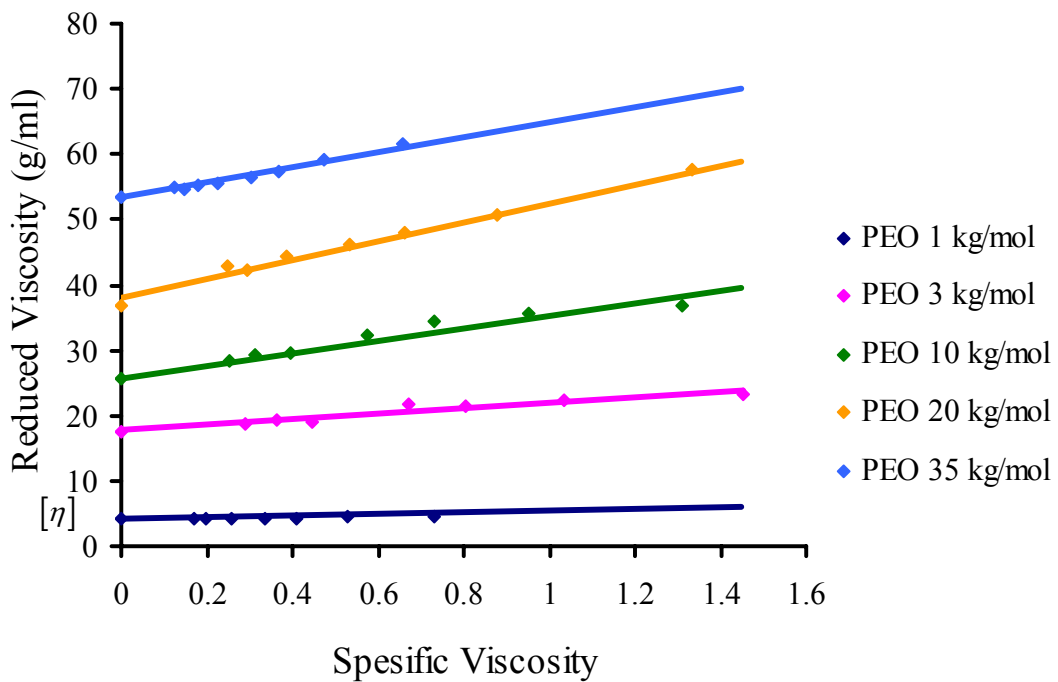


Figure 4-1 Reduced Viscosity vs. Specific Viscosity for PEO Samples that Obtained from Physical Chemistry Institute at 25°C.

Figure 4-1 shows that the polyethylene oxide (PEO) behaves as neutral polymer in water. Neutral polymers have the property that the reduced viscosity increases with increasing of the specific viscosity and polymer concentration, because the structure of PEO may not contain ionic groups^[133]. Otherwise if the polymer contains e.g. a carboxyl groups the reduced viscosity would decrease with increasing the specific viscosity and concentration of the polymer: in dilute solution the effective electrostatic repulsion extends the polymer coil, while in more concentrated solution the electric charge of the chain are shielded by counter ions^[113].

4.2.2 Intrinsic Viscosity Measurements for Group B Samples at 30 °C

The measurements were done at 30 °C in water to check the value of high molecular weights samples of polyethylene oxide obtained from Sigma-Aldrich company because only a very broad molecular weight range was given in the specification. At 30 °C reliable values of k and a can be taken from the literature^[16] which cover the whole molecular weight range of polyethylene oxide from 20 kg/mol to 5000 kg/mol^[16], when the value of k equal to 0.0125 ml/g and the value of a equal to 0.78 by using the equation:

$$[\eta] = kM^a$$

The values of intrinsic viscosities were obtained by capillary measurements using Schott Ubbelohde capillary viscometer size (0a, 0c, 1c) as shown in figure 4-2, and the results are shown in tables from 4-6 to 4-10 and appendix A.

Table 4-6 Specific and Reduced Viscosity of 100 kg/mol Molecular Weight PEO at 30 °C

Concentration (g/ml)	$\eta_{sp} = (t/t_0) - 1$	$\eta_{red} = \eta_{sp}/\text{conc.}$ (ml/g)
0.01	1.333	137.592
0.007	0.917	126.174
0.006	0.726	124.849
0.005	0.567	117.03
0.004	0.41	112.761
0.003	0.32	110.15
0.002	0.263	108.422

Table 4-7 Specific and Reduced Viscosity of 300 kg/mol Molecular Weight PEO at 30 °C

Concentration (g/ml)	$\eta_{sp} = (t/t_0) - 1$	$\eta_{red} = \eta_{sp}/\text{conc.}$ (ml/g)
0.0029	1.001	344.7
0.00218	0.697	320.101
0.00174	0.537	308.465
0.00145	0.462	318.052
0.00109	0.325	298.437
0.00087	0.255	293.136
0.00073	0.211	291.158

Table 4-8 Specific and Reduced Viscosity of 1000 kg/mol Molecular Weight PEO at 30 °C

Concentration (g/ml)	$\eta_{sp} = (t/t_0) - 1$	$\eta_{red} = \eta_{sp}/\text{conc.}$ (ml/g)
0.0007	0.509	726.251
0.00053	0.368	700.363
0.00042	0.291	692.939
0.00035	0.239	682.99
0.00026	0.174	663.215
0.00021	0.137	650.994
0.00018	0.113	645.659

Table 4-9 Specific and Reduced Viscosity of 4000 kg/mol Molecular Weight PEO at 30 °C

Concentration (g/ml)	$\eta_{sp} = (t/t_0) - 1$	$\eta_{red} = \eta_{sp}/\text{conc.}$ (ml/g)
0.00032	0.549	1698.237
0.00024	0.396	1633.557
0.00019	0.306	1576.909
0.00016	0.247	1528.132
0.00012	0.173	1425.607
0.0001	0.136	1402.19
0.00008	0.111	1370.445

Table 4-10 Specific and Reduced Viscosity of 8000 kg/mol Molecular Weight PEO at 30 °C

Concentration (g/ml)	$\eta_{sp} = (t/t_0) - 1$	$\eta_{red} = \eta_{sp}/\text{conc.}$ (ml/g)
0.00032	0.8788	2725.308
0.00024	0.6542	2705.293
0.00019	0.5167	2670.776
0.00016	0.4220	2617.64
0.00012	0.3052	2523.961
0.0001	0.2384	2464.559
0.00008	0.1935	2400.53

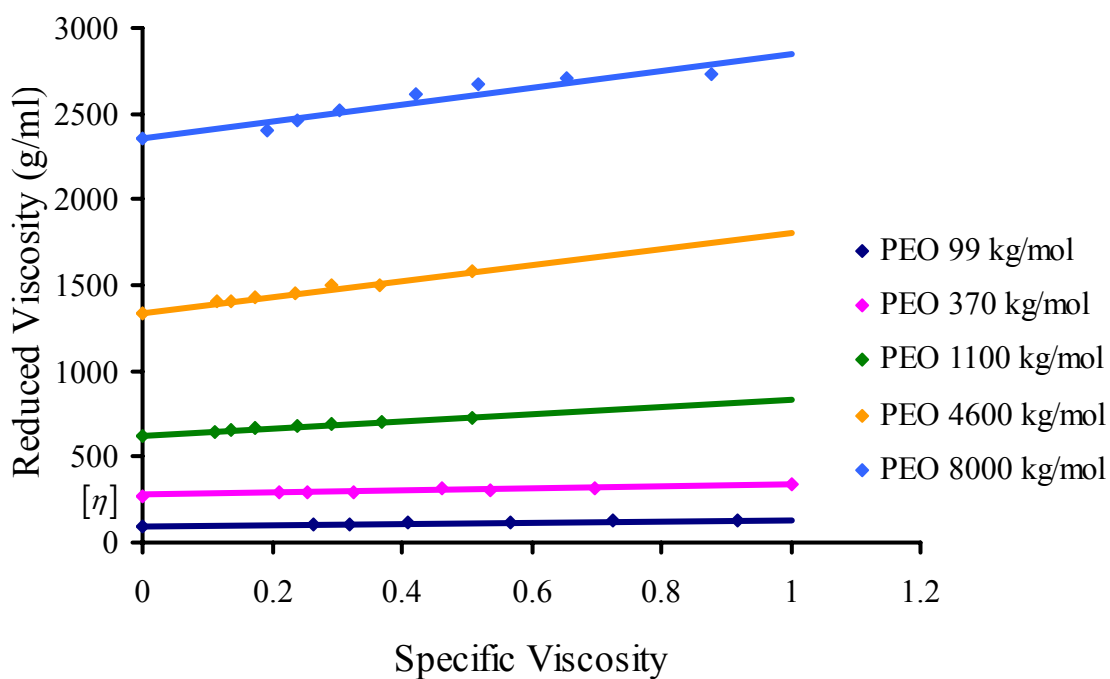


Figure 4-2 Reduced Viscosity vs. Specific Viscosity for PEO Samples that Obtained from Sigma-Aldrich at 30°C.

The results of the measurement of the capillary viscometer at 30 °C give values of molecular weights which are approximately the same that were obtained from Sigma Aldrich, company as shown in table below:

Table 4-11 Calculated Molecular Weight and Intrinsic Viscosity of Group B of PEO Samples at 30 °C

Obtained Molecular Weight (kg/mol)	Intrinsic Viscosity $[\eta]$ (ml/g)	Calculated Molecular Weight (kg/mol)
Linear PEO 100	98.6	99
Linear PEO 300	274.1	370
Linear PEO 1000	622.8	1100
Linear PEO 4000	1273.2	4600
Linear PEO 8000	2353.3	8000*

* All the measurements at 30 °C show results close to what were obtained from Sigma-Aldrich Company expect these for 8000 kg/mol sample which were in a wide range of error, so they were used as they are because the other results were reasonable.

4.2.3 Intrinsic Viscosity Measurements for Group B Samples at 25 °C

The measurements of the intrinsic viscosity were carried out for the measured values of the samples that obtained from Sigma-Aldrich, company shown in figure 4-3, and the results in figures from 4-12 to 4-16 and in appendix A.

Table 4-12 Specific and Reduced Viscosity of 99 kg/mol Molecular Weight PEO at 25 °C

Concentration (g/ml)	$\eta_{sp} = (t/t_0) - 1$	$\eta_{red} = \eta_{sp}/\text{conc.}$ (ml/g)
0.0098	1.306	132.883
0.0074	0.904	122.63
0.0059	0.685	116.125
0.0049	0.55	111.902
0.0042	0.459	108.902
0.0033	0.342	104.266
0.0027	0.273	101.898
0.0023	0.224	98.778
0.002	0.189	96.084

Table 4-13 Specific and Reduced Viscosity of 370 kg/mol Molecular Weight PEO at

25 °C

Concentration (g/ml)	$\eta_{sp} = (t/t_0) - 1$	$\eta_{red} = \eta_{sp}/\text{conc.}$ (ml/g)
0.0026	0.975	374.303
0.002	0.691	353.578
0.0016	0.535	342.551
0.0013	0.438	336.322
0.0011	0.369	330.457
0.0009	0.282	325.301
0.0007	0.23	323.232
0.0006	0.192	319.865
0.0005	0.167	319.854

Table 4-14 Specific and Reduced Viscosity of 1100 kg/mol Molecular Weight PEO at

25 °C

Concentration (g/ml)	$\eta_{sp} = (t/t_0) - 1$	$\eta_{red} = \eta_{sp}/\text{conc.}$ (ml/g)
0.00068	0.495	729.956
0.00051	0.351	690.285
0.00041	0.271	666.768
0.00034	0.22	647.924
0.00029	0.183	630.832
0.00023	0.137	606.39
0.00018	0.109	590.658
0.00016	0.091	580.689
0.00014	0.078	571.758

Table 4-15 Specific and Reduced Viscosity of 4600 kg/mol Molecular Weight PEO at 25 °C

Concentration (g/ml)	$\eta_{sp} = (t/t_0) - 1$	$\eta_{red} = \eta_{sp}/\text{conc.}$ (ml/g)
0.00032	0.536	1664.512
0.00024	0.39	1614.418
0.00019	0.302	1561.717
0.00016	0.243	1510.713
0.00012	0.174	1437.77
0.0001	0.137	1412.081
0.00008	0.111	1377.241
0.00007	0.094	1363.639

Table 4-16 Specific and Reduced Viscosity of 8000 kg/mol Molecular Weight PEO at 25 °C

Concentration (g/ml)	$\eta_{sp} = (t/t_0) - 1$	$\eta_{red} = \eta_{sp}/\text{conc.}$ (ml/g)
0.00031	0.695	2245.485
0.00023	0.49	2109.9
0.00019	0.376	2024.748
0.00015	0.3	1940.018
0.00012	0.208	1795.416
0.00009	0.153	1642.818
0.00008	0.12	1545.548

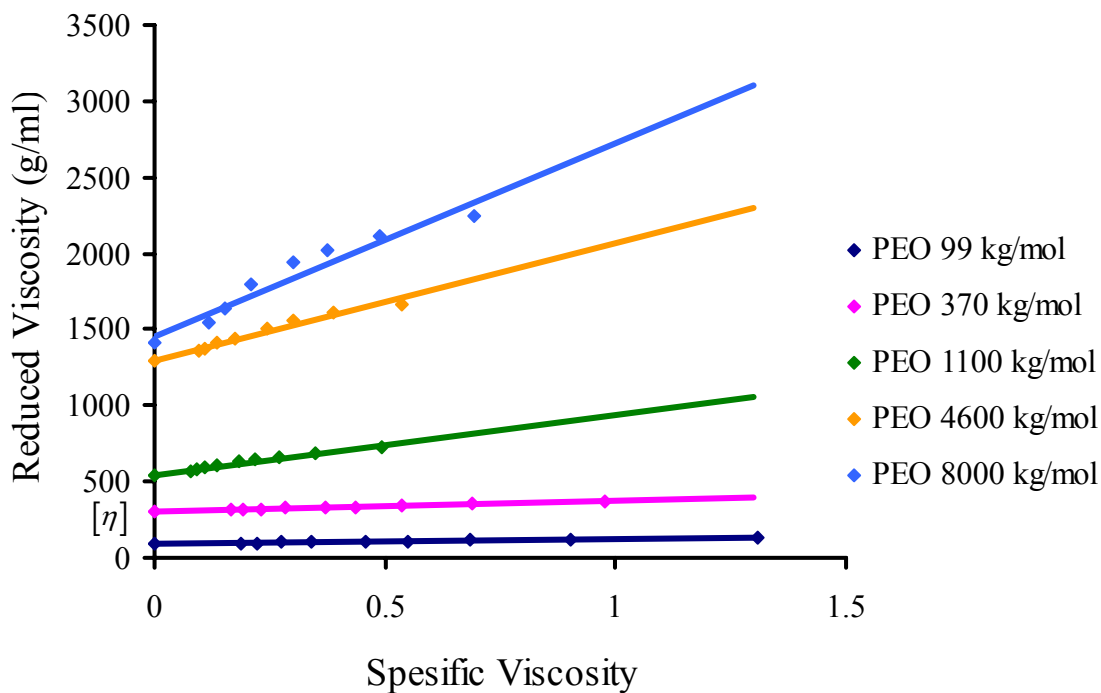


Figure 4-3 Reduced Viscosity vs. Specific Viscosity for PEO Samples that Obtained from Sigma-Aldrich at 25°C.

Figure 4-3 shows that polyethylene oxide (PEO) with high molecular weight also behaves as neutral polymers in water. The reduced viscosity is a linear function of specific viscosity as for the concentration where it increases with increasing the specific viscosity of the polymer, while for 8000 kg/mol molecular weight the reduced viscosity shows a non-linear increasing with the specific viscosity. This special behavior for the highest molecular weight sample can be due to aggregation effects or shear thinning which was observed in measurements with the rotational viscometer.

4.2.4 Intrinsic Viscosity Measurements for the Branched Polyethylene Oxide at 25 °C

For the branched polyethylene oxide the measured values are shown in figure 4-4, and the results in tables 4-17 and 4-18 and in appendix A.

Table 4-17 Specific and Reduced Viscosity of 0.55 kg/mol Molecular Weight PEO at 25 °C

Concentration (g/ml)	$\eta_{sp} = (t/t_0) - 1$	$\eta_{red} = \eta_{sp}/\text{conc.}$ (ml/g)
0.093	0.51	5.457
0.07	0.354	5.045
0.056	0.271	4.834
0.047	0.216	4.62
0.035	0.16	4.561
0.028	0.121	4.313
0.023	0.098	4.188

Table 4-18 Specific and Reduced Viscosity of 40 kg/mol Molecular Weight PEO at 25 °C

Concentration (g/ml)	$\eta_{sp} = (t/t_0) - 1$	$\eta_{red} = \eta_{sp}/conc.$ (ml/g)
0.0163	0.579	35.611
0.0122	0.41	33.653
0.0098	0.316	32.409
0.0081	0.256	31.542
0.0061	0.186	30.582
0.0049	0.146	29.951
0.0041	0.12	29.418

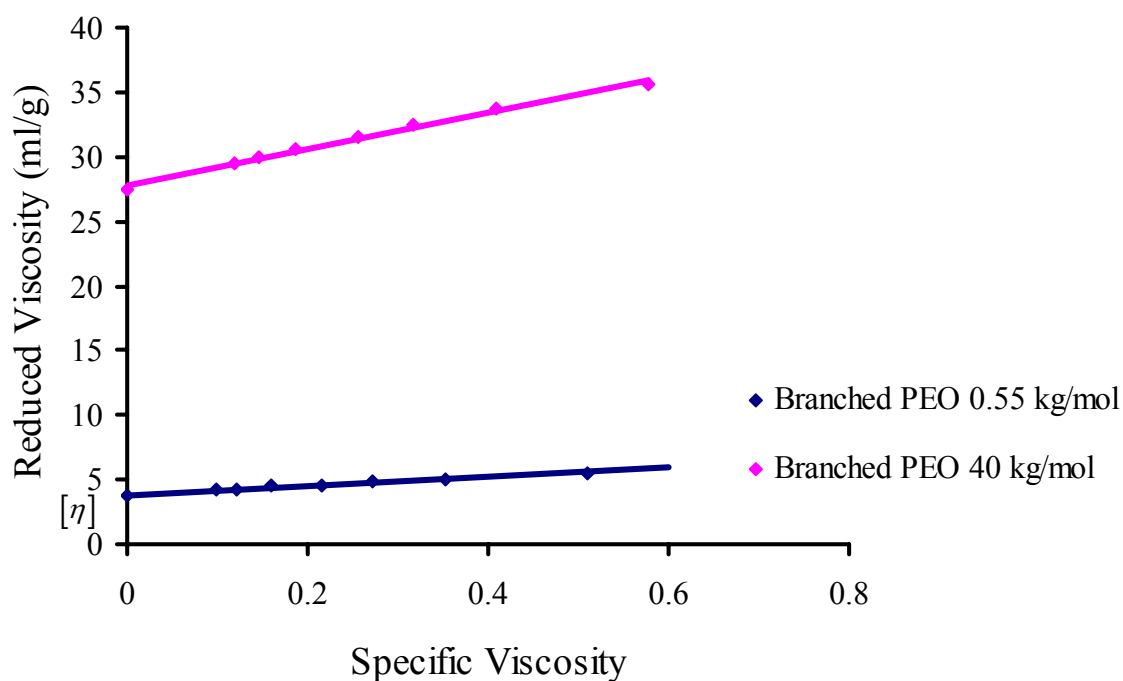


Figure 4-4 Reduced Viscosity vs. Specific Viscosity for Branched PEO Samples at 25°C.

Figure 4-4 for the branched polyethylene oxide shows the same influence for reduced viscosity with the specific viscosity where it increases with increasing the concentration as the linear polyethylene oxide.

By using equation, $\frac{\eta^{sp}}{c} = [\eta] + k'[\eta]^2 c$ and reduced viscosity equal to $\frac{\eta^{sp}}{c}$, from figures 4-1 to 4-4 the relation of reduced viscosity against specific viscosity, usually gives a straight line, the slop of this line is equal to $k'[\eta]^2$ and the intercept is equal to $[\eta]$, so that Huggin's constant K' can be determined from the slope, the values of intrinsic viscosity shown in table 4-19.

Table 4-19 Intrinsic Viscosity of PEO Solution with Different Molecular Weights at 25°C

Molecular Weight (kg/mol)	Intrinsic Viscosity (ml/g)
Linear PEO 1	4.1
Linear PEO 3	17.4
Linear PEO 10	25.8
Linear PEO 20	36.8
Linear PEO 35	53.3
Linear PEO 99	88.9
Linear PEO 370	303.5
Linear PEO 11×10^2	539.1
Linear PEO 46×10^2	1290.4
Linear PEO 8×10^3	1410.4
Branch PEO 0.55	3.8
Branch PEO 40	27.5

Figures 4-1 to 4-4 show that the hydrodynamic volume which proportional to $[\eta]$ of PEO in water increase with increasing the molecular weight for both linear and branched polyethylene oxide.

The branched samples show a much smaller intrinsic viscosity than the linear samples which close to them molecular weight. This effect is explained by the decrease of hydrodynamic volume with increase of branching.

By using equation 2.2, $[\eta] = KM^a$ a plot of the $\log[\eta]$ versus $\log M_{wt}$ for PEO in water at 25°C usually gives a straight line, the intercept of this line is equal to k and the slope is equal to "a" as shown in figure 4-5, and table 4-20.

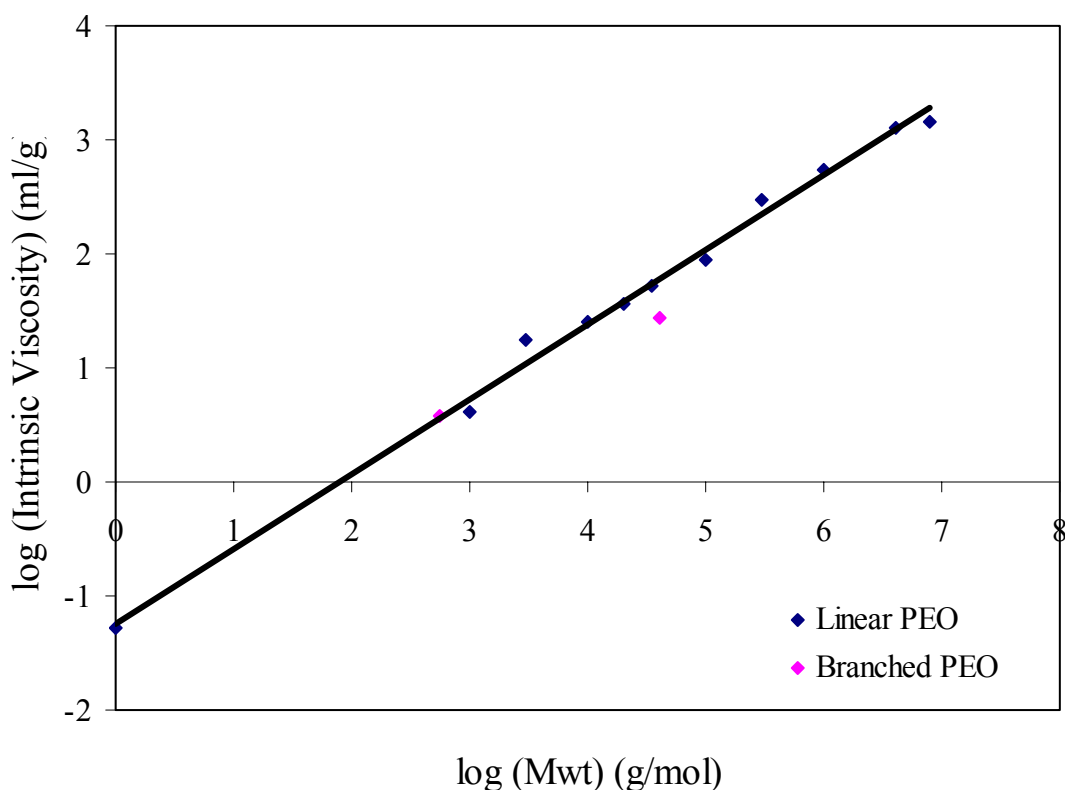


Figure 4-5 log (Molecular Weight) vs. log (Intrinsic Viscosity) for Different PEO in Water at 25°C.

Table 4-20 Huggin's Constant and Mark-Houwink Parameters of PEO in Water at 25°C

Molecular Weight (kg/mol)	Huggin's Constant (K')	k (ml/g)	a
Linear PEO 1	0.179	0.0068	0.667
Linear PEO 3	0.335		
Linear PEO 10	0.513		
Linear PEO 20	0.683		
Linear PEO 35	0.289		
Linear PEO 99	0.577		
Linear PEO 370	0.284		
Linear PEO 1100	1.016		
Linear PEO 4600	0.757		
Linear PEO 8000	1.477		
Branch PEO 0.55	1.174		
Branch PEO 40	0.67		

4.3 Transition Condition from Particle to Network (Critical Molecular Weight)

The zero shear viscosity is measured by using the rheometer to estimate the critical molecular weight for PEO at 25°C in solutions of different concentration. Polyethylene oxide solutions were prepared for 1% and 5% concentration for different molecular weights, and the effect of the molecular weight on the polymer structure is represented graphically in figures 4-6 and 4-7 which show the change from the particle region to network region at a certain molecular weight, and the results are shown in tables 4-21 and 4-22.

Table 4-21 Zero Shear Viscosity of 1% PEO Solution at 25°C

Molecular Weight (kg/mol)	Zero Shear Viscosity (pa.s)
Linear PEO 99	0.002
Linear PEO 370	0.007
Linear PEO 1100	0.034
Linear PEO 4600	3.15
Linear PEO 8000	118

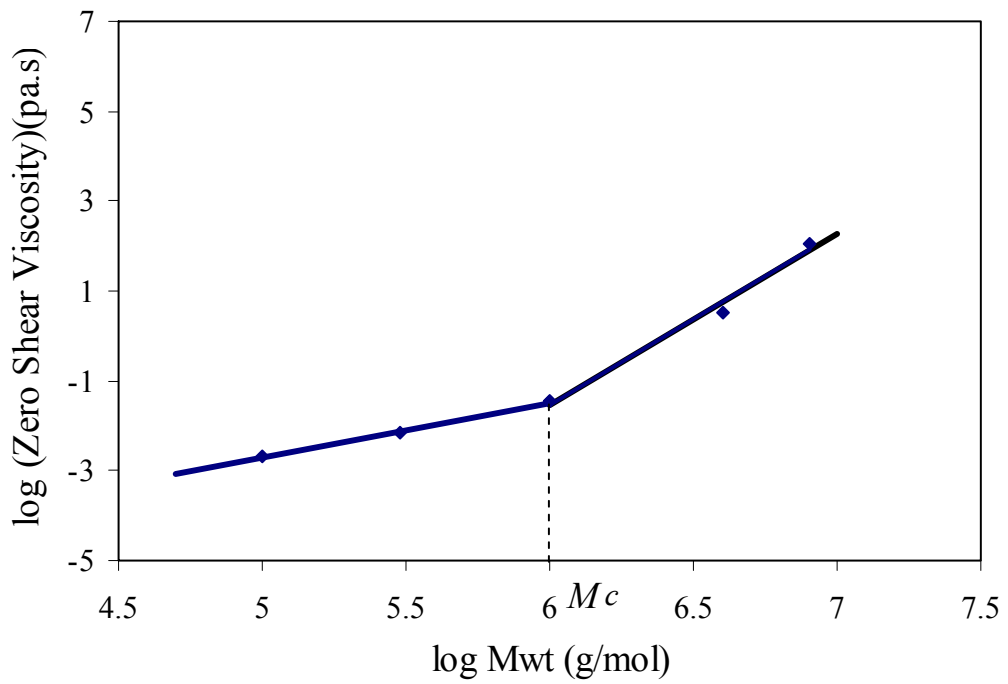


Figure 4-6 log (Molecular Weight) vs. log (Zero Shear Viscosity) for 1% PEO Solutions at 25°C.

Table 4-22 Zero Shear Viscosity of 5% PEO Solution at 25°C

Molecular Weight (kg/mol)	Zero Shear Viscosity (pa.s)
Linear PEO 10	0.003
Linear PEO 20	0.008
Linear PEO 35	0.013
Linear PEO 99	0.019
Linear PEO 370	0.364
Linear PEO 1100	23.8
Linear PEO 4600	9100
Linear PEO 8000	35000

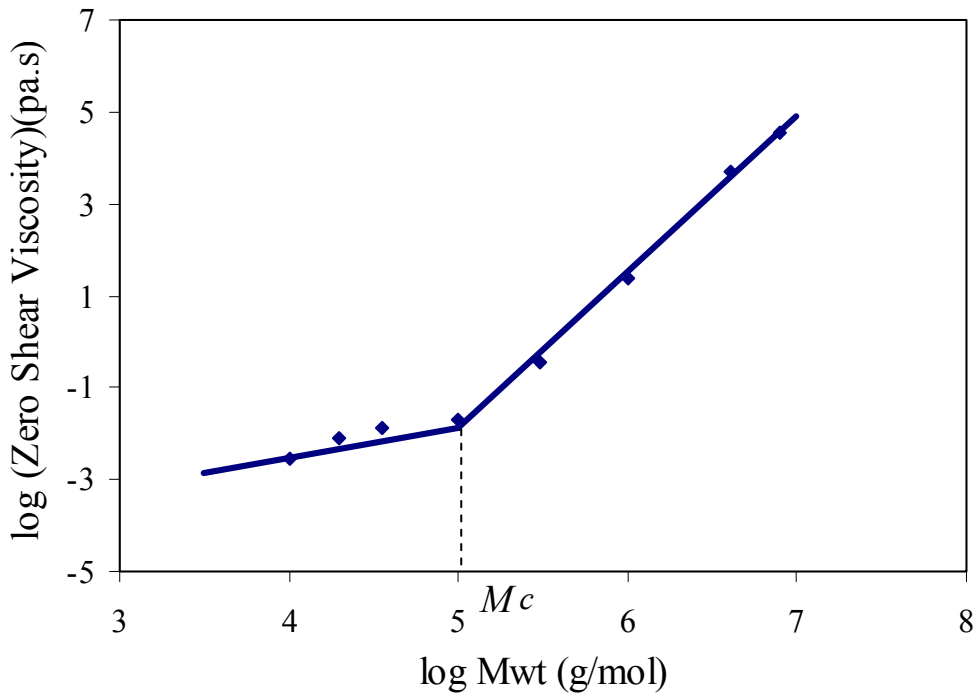


Figure 4-7 \log (Molecular Weight) vs. \log (Zero Shear Viscosity) for 5% PEO Solutions at 25°C.

Figures 4-6 and 4-7 show the plotting of η_0 versus M_{wt} in log-log scale to determine the critical molecular weight (M_c) from the discontinuity which appears clearly at a certain point for both concentrations. In figure 4-6 the slope change from 1.03 to 4.67 at a molecular weight of about 10^6 g/mol which represents the critical molecular weight for 1% concentration while in figure 4-7 the slope changes from 0.353 to 3.33 at a molecular weight of about 10^5 g/mol which indicates the critical molecular weight that shows the transition from a semi-dilute solution (particle) to an entangled concentrated solution (network). The results in table 4-21 and 4-22 show that for the high concentration low molecular weight samples were required to get this break point otherwise the measurements are in the concentrated, entangled region only.

The value of M_e is calculated from M_c by using the relation $M_c \approx 2M_e$ where for 1% PEO solution it is equal to 500,000 g/mol and for 5% PEO solution it is equal to 50,000 g/mol.

4.4 Viscoelastic Properties of Polyethylene Oxide

The viscoelastic properties of polyethylene oxide like shear rate, shear stress, shear viscosity, relaxation time, torque, and many other parameters were measured using a rotational rheometer with three different measuring geometries: cone/plat 25 mm diameter/ 2° , cone/plat 50 mm diameter/ 1° , and double gap. For these measurements the high molecular weights samples ≥ 1100 kg/mol were used at two different concentrations of 1% and 5% PEO at 25°C as shown in figures 4-8 to 4-15.

4.4.1 The Flow Behavior of Polyethylene Oxide

The measured shear viscosities of polyethylene oxide solutions are plotted versus the shear rate in log-log scale as shown in figures 4-8 and 4-9.

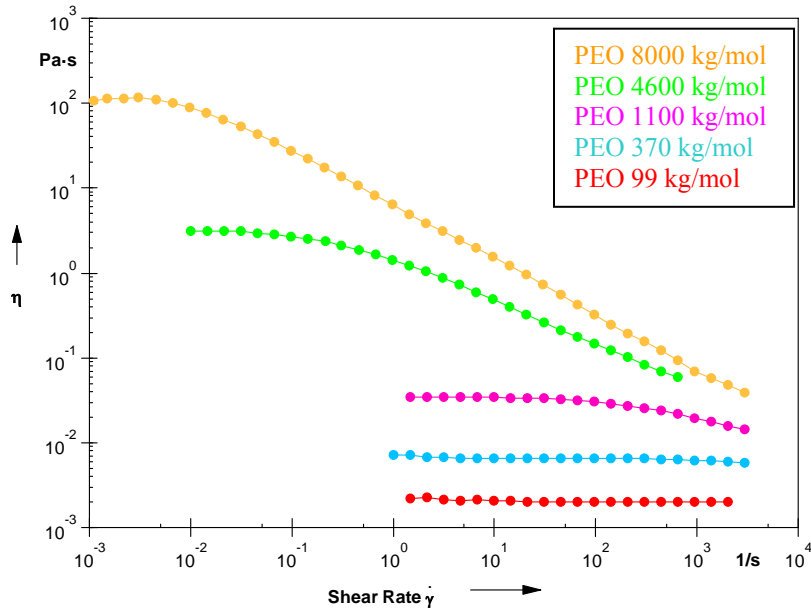


Figure 4-8 Flow Curve for 1% PEO Solutions at 25°C.

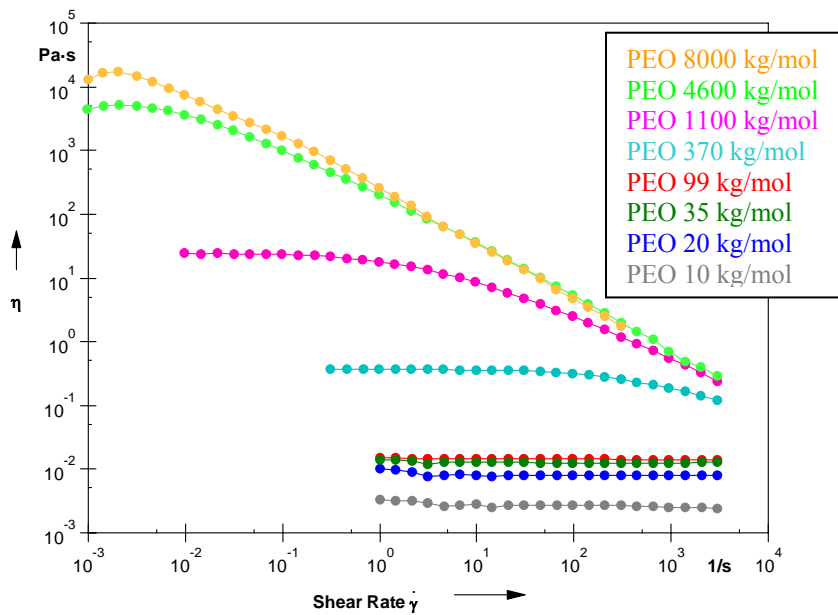


Figure 4-9 Flow Curve for 5% PEO Solutions at 25°C.

In figure 4-8 for 1% PEO solution the Newtonian behavior can be observed for the samples 99 and 370 kg/mol which have the same value of the viscosity for all the shear rate values while for the samples 1100, 4600 and 8000 kg/mol PEO the value of the viscosity started to decrease with increasing the shear rate values due to the decrease in the entanglement density during the flow which represents the shear thinning behavior.

Figure 4-9 for 5% PEO solution shows the Newtonian behavior for the samples 10, 20, 35 and 99 kg/mol where the value of the viscosity is constant, while for the 370 and 1100 kg/mol the samples have a Newtonian behavior at low shear rate (zero shear viscosity) followed by a shear thinning behavior at a certain shear rate value where the viscosity starts to decrease. For the samples 4600 and 8000 kg/mol PEO samples no clear zero shear viscosity was measured at low shear rate, but a maximum close to the lowest shear rate followed by a strong shear thinning behavior for all higher shear rates. The maximum of the viscosity at these very low shear rates is probably caused by transient effects which means that no stationary shear state was attained during the measurement to get the right values of the zero shear viscosity, creep measurements were done for these two samples as described in chapter two.

The difference in the flow behavior in the two figures is due to change in concentration. The values of the zero shear viscosity obtained from the flow curves are shown in tables 4-21 and 4-22.

4.4.2 Creep diagram of polyethylene oxide

The $J(t)$ of polyethylene oxide is plotted in figure 4-10 as a function of time in log-log scale for the molecular weights 4600 and 8000 kg/mol to estimate the right value of the zero shear viscosity which was not clearly determined in the flow curve measurements for 4600 and 8000 kg/mol PEO samples at 5% concentration.

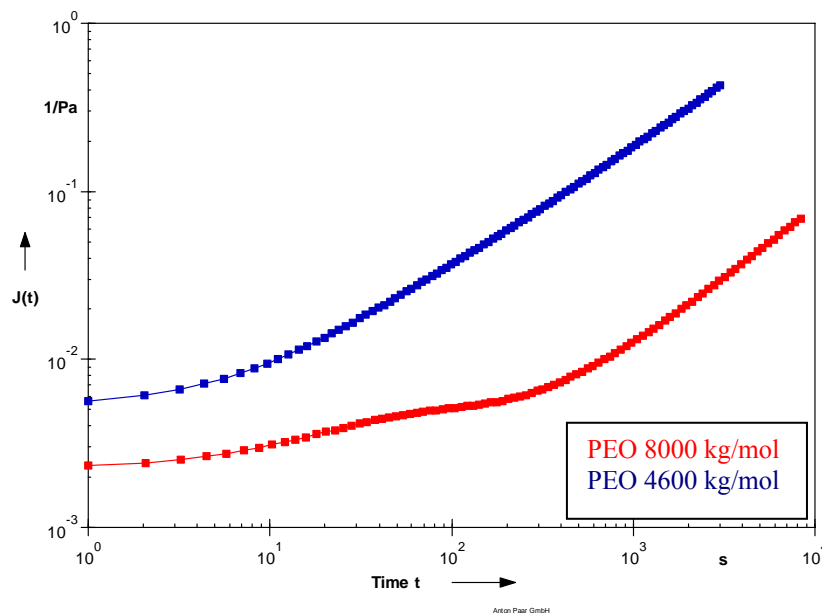


Figure 4-10 Creep Diagram for 5% PEO Solutions at 25°C.

Figure 4-10 shows the relation between the steady-state compliance and time for PEO which is called Creep diagram. The value of zero shear viscosity in this diagram is equal to the inverse slope of the compliance at the steady state (at long measuring times) which for 4600 kg/mol sample is equal to 9100 Pa.s while for 8000 kg/mol is equal to 35,000 Pa.s.

4.4.3 Graessley Diagram of Polyethylene Oxide

The reduced presentation of the flow curve, reduced viscosity η/η_0 , versus reduced shear rate $\dot{\gamma}\sigma$, here mentioned as Graessley diagram is shown for the two concentrated solutions of polyethylene oxide 1% and 5% in figure 4-11. The required relaxation time σ was obtained from the following formula.

$$\text{The relaxation time} = \frac{\eta_0 M}{CRT}$$

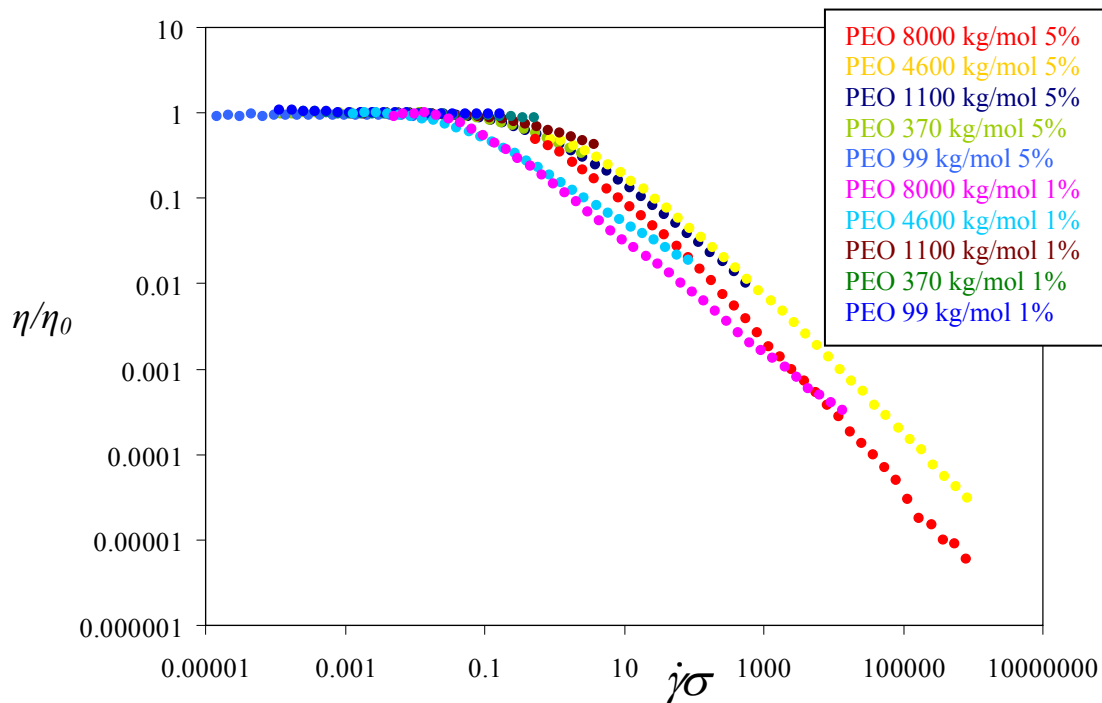


Figure 4-11 Graessley Diagram for 1% and 5% PEO Solutions at 25°C.

Figure 4-11 shows to what extent the shear thinning behavior of PEO solutions of very different molar masses can be reduced to a single curve just by using Rouse relaxation time without any further fit parameters. Taking into consideration that the relaxation times of the different molar masses and concentrations span a broad range of nearly 9 decades from 10^{-6} to 10^3 seconds as shown in table 4-23, the reduced presentation shows reasonable

concordance regarding the beginning of shear thinning which can be located in only one decade at $\sigma \dot{\gamma} = 0.1 \dots 1$. The remaining difference between the different samples is mainly due to the lack of the bead-spring-model which is based on single molecules and ignores intermolecular interactions, especially entanglements. Therefore for a better description of the relaxation mechanism of the high molar mass samples, the reptation of the molecules across the entanglements should be taken into account.

Nevertheless the results confirm that the simple Rouse formula can be used to calculate at least the scale of the relaxation time for the onset of shear thinning also at quite high concentrations and entanglement densities.

4.4.4 Storage and Loss Modulus and Maxwell and Bead-Spring Model

The measurement of storage and loss modulus was carried out by using a rotational rheometer at 25°C by using three different measuring geometries for different molecular weights PEO solution at different concentrations 5%, 1%, 0.2 %, and 0.05% as shown in figures 4-12 to 4-14.

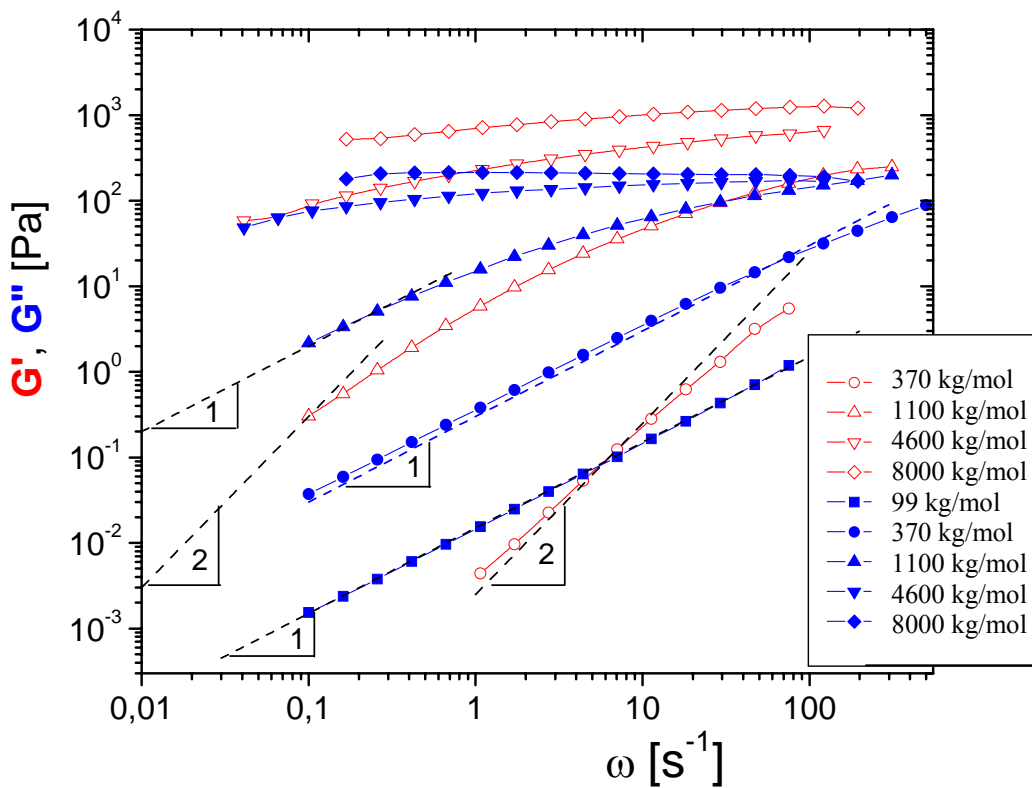


Figure 4-12 Shear Moduli vs. Frequency of 5% PEO Solutions of Different Molar Mass at 25 °C. Red and Open Symbols: Storage Modulus; Blue and Filled Symbols: Loss Modulus.

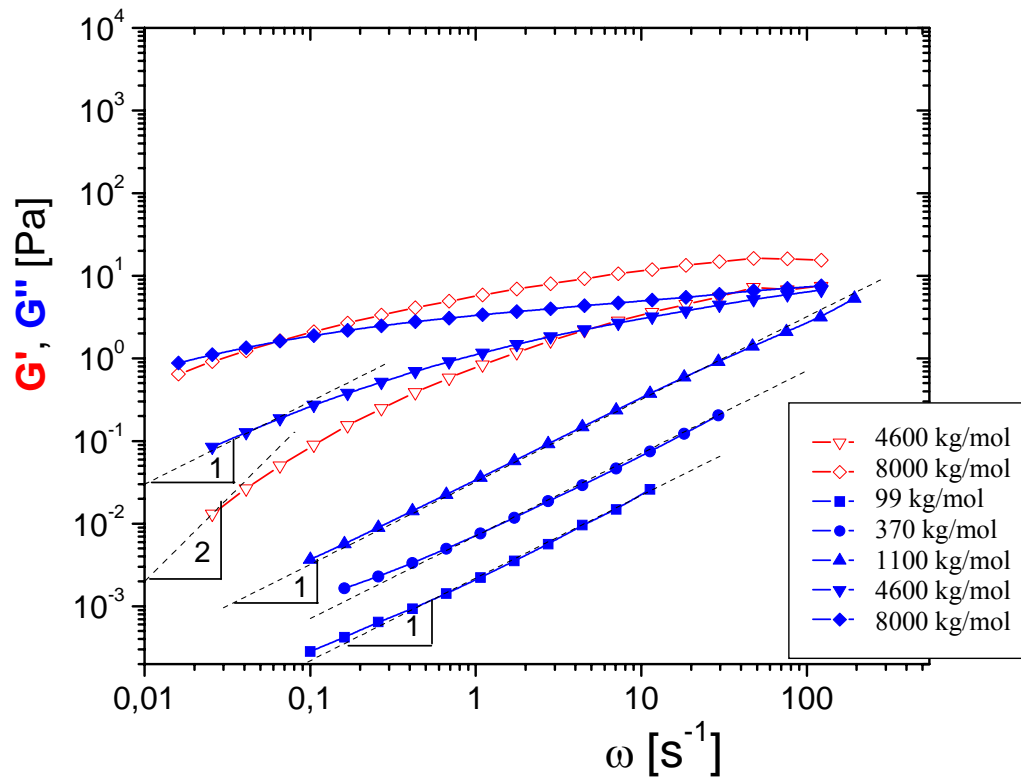


Figure 4-13 Shear Moduli vs. Frequency of 1% PEO Solutions of Different Molar Mass at 25 °C. Red and Open symbols: Storage Modulus; Blue and Filled Symbols: Loss Modulus.

Figures 4-12 and 4-13 show the dependence of both shear moduli, G' and G'' , with frequency for PEO solutions of 5% and 1%, respectively. In figure 4-12 for 5%-Solutions: For the highest molecular weight, 8000 kg/mol, the storage modulus G' is higher than the loss modulus G'' for all frequencies. This means that the sample behaves rheologically like a viscoelastic gel. The 4600 kg/mol solution shows similar behavior, but has a crossover point of G' and G'' at the lowest measuring frequencies. This means, that the long time behavior changes from gelly to liquid. The 1100 kg/mol sample shows $G'' > G'$ for nearly all frequencies (without the highest) which shows the behavior of a viscoelastic liquid in this frequency range. For the lowest frequency, the limiting slopes of 1 and 2 for G'' and G' were obtained, respectively, which would show the behavior of a pure liquid.

Therefore, this sample still shows some elastic behavior even at the lowest measuring frequencies. The 370 kg/mol sample shows this scaling behavior of both moduli of a sample in the flow regime, which means nearly pure viscous but no gelly behavior. While for this sample G' can still be measured, there are no reasonable results for G' for the 99 kg/mol sample any more, despite of using the double gap measuring geometry. This means pure liquid-like rheological behavior, no elastic component.

By comparison to the 5% solutions, in figure 4-13 the rheological behavior of the 1% solutions shifts towards more liquid-like behavior and towards lower values for both shear moduli. Only for the 8000 kg/mol and the 4600 kg/mol PEO solutions a reasonable storage modulus was able to measure. These samples show viscoelastic behavior. The other samples of lower molar masses show only pure viscous behavior.

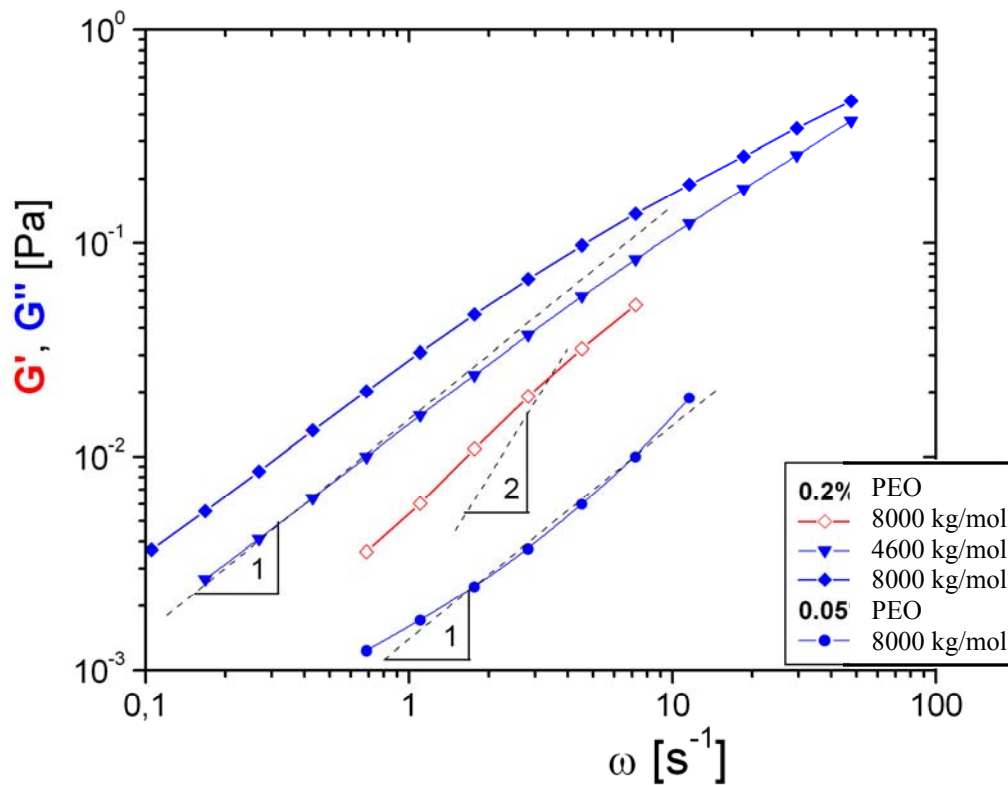


Figure 4-14 Shear Moduli vs. Frequency of 0.2% and 0.05% PEO Solutions of Different Molar Mass at 25 °C. Red and Open Symbols: Storage Modulus; Blue and Filled Symbols: Loss Modulus. Due to the Low Viscosity all Measurements were performed with a Double Gap Geometry Z1.

Figure 4-14 shows that for the 0.2% PEO solutions, only the 8000 kg/mol and the 4600 kg/mol solutions were measured because the viscosity of the lower molecular weight samples of these concentrations were too small. Both samples show liquid like behavior, and only the 8000 kg/mol sample exhibit some viscoelastic contribution (small G' values). For 0.05% solutions, only the 8000 kg/mol sample was measured. It shows pure liquid-like behavior with very low viscosity close to the viscosity of water. The upwards bending of the curve G'' versus frequency is probable an artifact due the very low viscosity of this sample.

The shift of the crossover point of G' and G'' with molar mass and concentration of PEO is related to a corresponding shift of the relaxation times: The smaller the molecular weight and the smaller the concentration, the smaller there is also the relaxation time. It can be calculated according to the Rouse model (bead-spring-model), equation (2.18), $\sigma_{Rouse} = \frac{6}{\pi^2} \frac{[\eta] \eta_s M}{CRT}$. The calculated values for certain concentrations and molecular weights are given in Figure 4-15, and the results are shown in table 4-23.

Table 4-23 Relaxation Times for Different Concentrations of PEO Solution at 25°C

M _{wt} (kg/mol)	IV [η]	Concentration (kg/m ³)				
		50	10	2	0.5	Inf. Dilution
99	88.9	9.0E-06	3.3E-06	-	-	2.2E-06
370	304	5.3E-04	5.0E-05	-	-	2.2E-05
1100	539	1.2E-01	8.4E-04	-	-	1.3E-04
4600	1290	1.8E+02	3.1E-01	7.4E-03	-	1.3E-03
8000	1410	1.4E+03	2.3E+01	3.4E-02	6.3E-03	2.8E-03

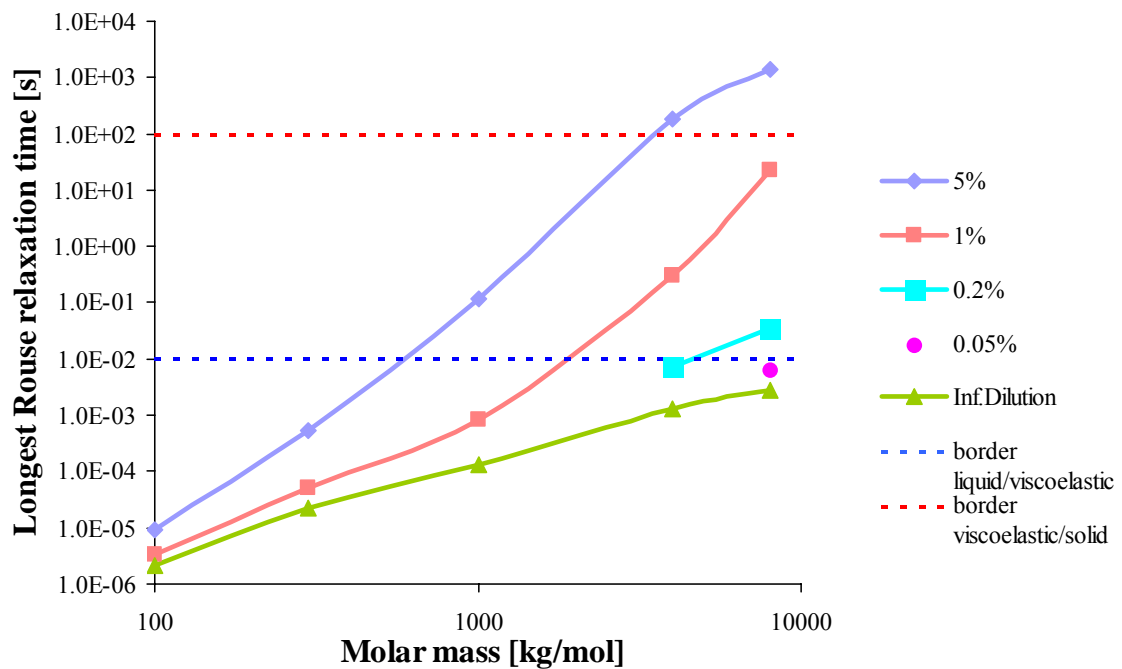


Fig 4-15 Calculated Relaxation Time Due to the Rouse Model for Different Molecular Weights and Concentrations. The Horizontal Lines at 10 ms and 100 s Correspond to the Highest and Lowest Frequency Which can be measured in the Frequency Sweep.

As shown in Figure 4-15, the Rouse calculation for the concentrated solutions (5% and 1%) of the highest molecular weight 8000 kg/mol gives relaxation times higher than 100 s. This time is related to the lowest frequency 0.01 rad/s measured in the frequency sweeps. For these samples with longer relaxation times we expect gelly-like behavior, $G' > G''$, for the whole frequency range. In fact this is shown by these samples.

For lower concentrations of the 8000 kg/mol sample and for the high concentrations of the lower molecular weight PEO, the calculated relaxation time is between 10 ms and 100 s. Both values correspond to the border lines of highest and lowest frequency, respectively, in the frequency sweep. Therefore these samples should show viscoelastic behavior in this frequency

range, $G' \approx G''$ with a crossover at a certain frequency. Really this is confirmed by the experiments.

For the very low concentrations of all polymers, the Rouse calculation gives relaxation times smaller than 10 ms. Therefore, the samples should have liquid-like behavior, $G'' > G'$, as again confirmed by the frequency sweep experiments. Therefore, it can be concluded that the calculation of the Rouse relaxation time gives reasonable results for all PEO samples with different molecular weights and concentrations.

For the very low concentrations of a few ppm, which are interesting for drag reduction, the relaxation times are smaller than 0.01 s. Therefore, it becomes clear that in the standard frequency range all very dilute PEO solutions are well within the flow regime $\omega > 1/\sigma_{max}$ with the scaling $G' \sim \omega^2$ and $G'' \sim \omega$. To measure elastic behavior of dilute PEO solutions, frequencies of 1000 rad/s or higher would be required.

The importance of viscoelastic behavior of the high molecular weight PEO solutions for drag reduction can be described as follows: The viscoelastic behavior is established at a time scale of σ_{max} or at even shorter times. The relaxation time at infinite dilution is in the range of 1 ms or less, due to the bead-spring-model calculation. This relaxation time is important for drag reduction, both in the "viscous" and in the "elastic" mechanism: Drag reduction takes place when the local strain rate in eddies or vortices exceeds the inverse of the polymer relaxation time. Due to the viscous mechanism, at this high shear rates the polymer is unraveled. The unraveled molecules increase the extensional viscosity, causing drag reduction. In the elastic mechanism the elasticity conferred to instabilities that leads to smaller length scale flows or eddies. Therefore, here also the onset of drag reduction occurs when the polymer relaxation time exceeds the time scale associated with the smallest eddies in the flow^[101].

The time for one revolution of eddies – or inverse frequency – gives a number for the time scale for eddies and inverse shear and extensional rate, respectively. The frequency of eddies depends on the eddy size and the Reynolds number ^[114]. In water for Reynolds numbers in the range of 10^4 to 10^5 the typical eddy frequency f is in the range of 100 Hz to 10000 Hz for the small eddies which dissipate the energy.

Therefore, the relaxation time of the polymer must exceed $1/f = 0.1$ ms ...10 ms to unravel the polymers in eddies and to become effective for drag reduction according to the viscous mechanism.

This polymer relaxation time is in accordance with the results of the Rouse calculations for high molar mass polymers and the viscoelastic experiments and confirms, that high molar masses of polymer are required to be effective in drag reduction: Only the high molar masses starting from about 1000 kg/mol exhibits relaxation times higher than 0.1 milliseconds as shown in figure 4-15.

4.5 Drag Reduction

The drag reduction measurements of polyethylene oxide were performed by using a rheometer equipped with a measuring plate with big diameter. The temperature of the measurements was set to (23.3-23.8 °C). This range is quite board because the measurements were carried out by using an external container, added to the rheometer as shown in figure 3-8, which made the controlling of the temperature difficult. The value of the torque were determined for PEO solutions of the molecular weights 99, 370, 1100, 4600, 8000 kg/mol because they are the only samples which gave a reasonable values for the drag reduction efficiency. First a relatively concentrated stock solution was prepared where of the other concentrations were prepared by

dilution. The results are shown in figures from 4-16 to 4-20, and shown in tables 4-24 to 4-28.

Table 4-24 Torque Values of PEO Solutions at (23.3-23.8 °C)

Concentration (ppm)	Torque (μNm)				
	8000 kg/mol	4600 kg/mol	1100 kg/mol	370 kg/mol	99 kg/mol
10000	-	-	-	-	47,260
7000	-	-	-	-	43,260
5000	-	-	-	49,860	42,320
3000	-	-	-	42,740	41,600
1500	-	-	-	38,840	42,560
1000	-	-	41,840	37,520	42,940
700	-	-	39,300	38,440	42,040
500	46,920	48,540	38,780	37,900	40,780
300	44,020	47,560	36,660	38,620	-
150	40,040	42,340	35,600	39,900	-
100	37,420	38,900	35,480	40,600	-
50	35,620	36,640	35,380	39,860	-
30	34,860	35,480	35,920	41,780	-
15	33,060	35,360	37,880	-	-
10	32,460	34,700	38,720	-	-
5	34,480	34,740	40,080	-	-
3	35,660	35,060	40,000	-	-
1	38,880	38,140	41,280	-	-

Table 4-24 shows the values of the torque for different concentrations which start from different values for each sample depending on the value of the molecular weight. The value of the torque for water was 40,640 μNm and the measurements were stopped for the samples 370 and 99 kg/mol at concentrations when the measured torque required to rotate the disk was

equal to that need for water in the range of error because of the viscosity of the solution which start be equal to the viscosity of water for the low molecular weight in 1000 ml of water. The value of the percentage drag reduction (%DR) was calculated by using equation (2.22).

$$DR(\%) = \frac{\tau_{solvent} - \tau_{solution}}{\tau_{solvent}} \times 100$$

Results of percentage drag reduction (%DR) are shown in table 4-25 and represented graphically in figure 4-16.

Table 4-25 Percentage Drag Reduction of PEO Solutions at (23.3-23.8 °C)

Concentration (ppm)	Percentage drag reduction (%DR)				
	8000 kg/mol	4600 kg/mol	1100 kg/mol	370 kg/mol	99 kg/mol
10000	-	-	-	-	-16.289
7000	-	-	-	-	-6.447
5000	-	-	-	-22.687	-4.134
3000	-	-	-	-5.167	-2.362
1500	-	-	-	4.429	-4.876
1000	-	-	-2.953	7.677	-5.659
700	-	-	3.297	5.413	-3.445
500	-15.453	-19.439	4.577	6.742	-0.345
300	-8.317	-17.028	9.793	4.971	-
150	1.476	-4.183	12.402	1.821	-
100	7.923	4.282	12.697	0.098	-
50	12.352	9.843	12.943	1.919	-
30	14.222	12.697	11.614	-2.805	-
15	18.652	12.992	6.791	-	-
10	20.128	14.616	4.724	-	-
5	15.157	14.518	1.378	-	-
3	12.254	13.73	1.575	-	-
1	4.331	6.152	-1.575	-	-

Table 4-25 shows the values of the %*DR* for the four samples which were chosen because they have the higher molecular weights which are important for drag reduction. As shown, the drag reduction started with negative values at high concentrations increases towards lower concentrations, a maximum value reached is called the maximum drag reduction (DR_{max}), and this has different values for different molecular weights. For lower concentrations, this value starts to decrease again. For the high molecular weight samples 8000, 4600 kg/mol the values of %*DR* still have small positive values down to concentration of 1 ppm. At this concentration the measurements were stopped because the drag reduction values were in the range of error. For the samples 1100 and 370 kg/mol the maximum of drag reduction is shifted towards higher concentrations, and in the case of 370 kg/mol sample less pronounced. For 99 kg/mol, all percentage drag reduction values were negative which conforms a high molecular weight of the polymer is required for the drag reduction which agrees with the literature. The results are plotted in figure 4-16.

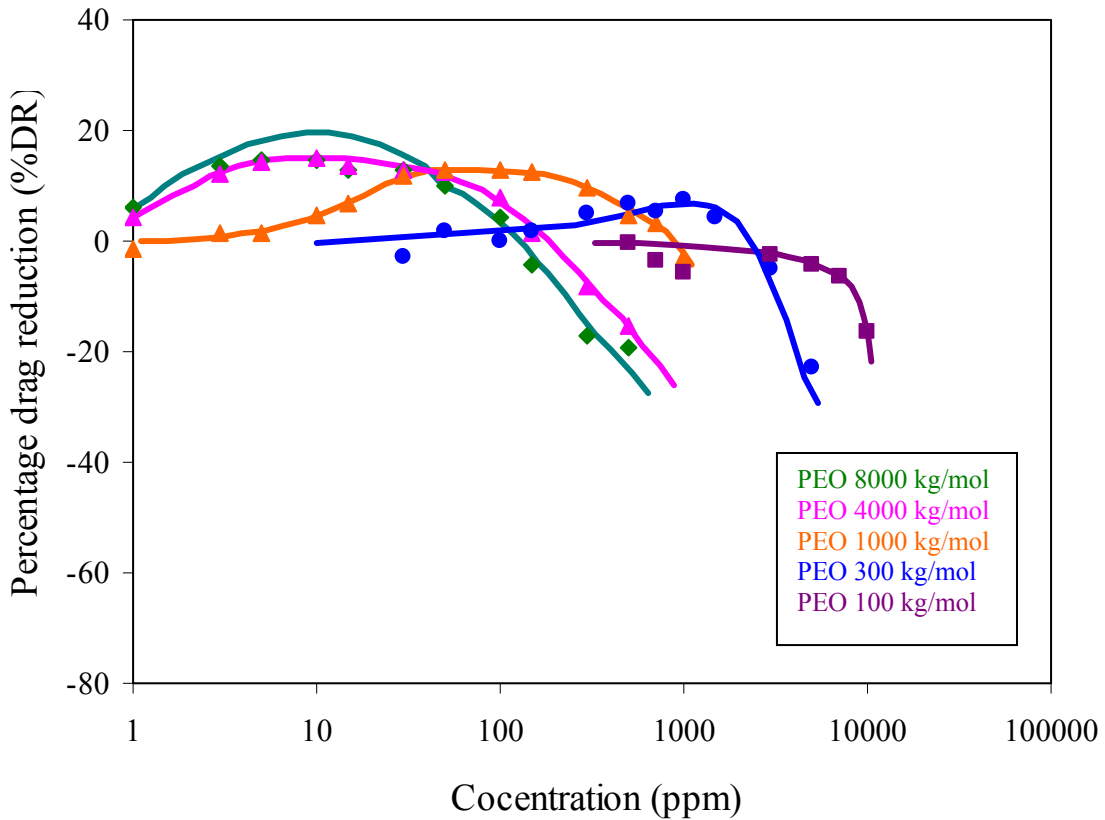


Figure 4-16 Percentage Drag Reductions vs. Concentration of PEO Solutions at (23.3-23.8 °C).

Figure 4-16 shows the dependence of the percent drag reduction of five different molecular weights of PEO as a function of polymer concentration up to 10,000 ppm at a rotational speed of 1200 rpm. The concentrations having the maximum drag reduction at each different molecular weight can be obtained from this figure and called optimum concentration. The data clearly indicate that the concentration required for maximum drag reduction decreases with increasing molecular weight. The maximum in the drag reduction-concentration data is due to the combination of the two following factors: the drag-reducing property of the solute and the increasing viscosity of the solutions, which becomes

increasingly significant at higher molecular weight of the polymer ^[83]. The values of the maximum drag reduction are shown in table 4-26.

Table 4-26 Maximum Drag Reduction of PEO Solutions at (23.3-23.8 °C)

Molecular Weight (kg/mol)	Maximum Drag Reduction (DR _{max})
8000	20.13
4600	14.62
1100	12.94
370	7.68

From equation (2.25), $DR = \frac{DR_{max} [DR]C}{DR_{max} + [DR]C}$ the value of the drag reduction determined where the value of intrinsic drag reduction $[DR]$ was obtained from the initial slope for each sample from figure 4-16. The results are shown in figures 4-27 and 4-28.

Table 4-27 Intrinsic Drag Reduction of PEO Solutions at (23.3-23.8 °C)

Molecular Weight (kg/mol)	Intrinsic Drag Reduction [DR]
8000	3.962
4600	3.789
1100	0.413
370	0.034

Table 4-28 Drag Reduction Values of PEO Solutions at (23.3-23.8 °C)

Concentration (ppm)	drag reduction (DR)			
	8000 kg/mol	4600 kg/mol	1100 kg/mol	370 kg/mol
10000	-	-	-	-
7000	-	-	-	-
5000	-	-	-	7.51
3000	-	-	-	7.44
1500	-	-	-	7.35
1000	-	-	12.55	7.146
700	-	-	12.389	6.684
500	19.916	14.504	12.18	6.278
300	19.778	14.431	11.72	5.824
150	19.44	14.25	10.708	5.311
100	19.113	14.073	9.857	4.406
50	18.195	13.569	7.959	3.089
30	17.1	12.951	6.333	2.378
15	14.864	11.626	4.192	-
10	13.145	10.547	3.133	-
5	9.759	8.251	1.782	-
3	7.264	6.394	1.132	-
1	3.189	3.01	0.401	-

The value of DR/C is plotted versus concentration by using equation (2.26), $\frac{C}{DR} = \frac{[C]}{DR_{max}} + \frac{C}{DR_{max}}$, where the relation of DR/C against concentration gives a straight line, the slope of this line is equal to $1/DR_{max}$ and the intercept is equal to $[C]/DR_{max}$, where the value of the intrinsic concentration [C] can be estimated from the intercept, as shown in figures from 4-17 to 4-20.

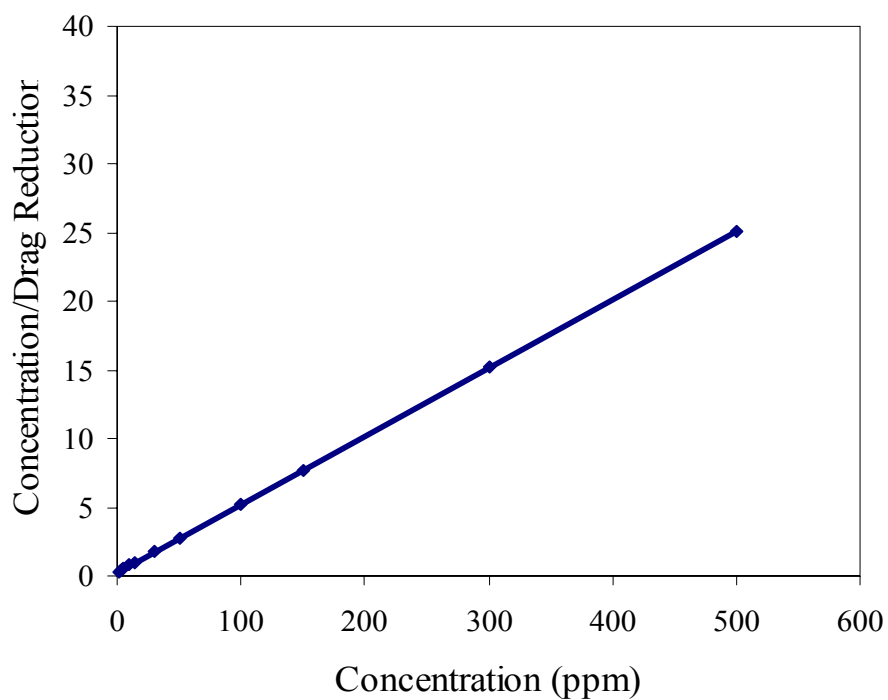


Figure 4-17 C/DR vs. Concentration of 8000 kg/mol PEO Solutions at (23.3-23.8 °C).

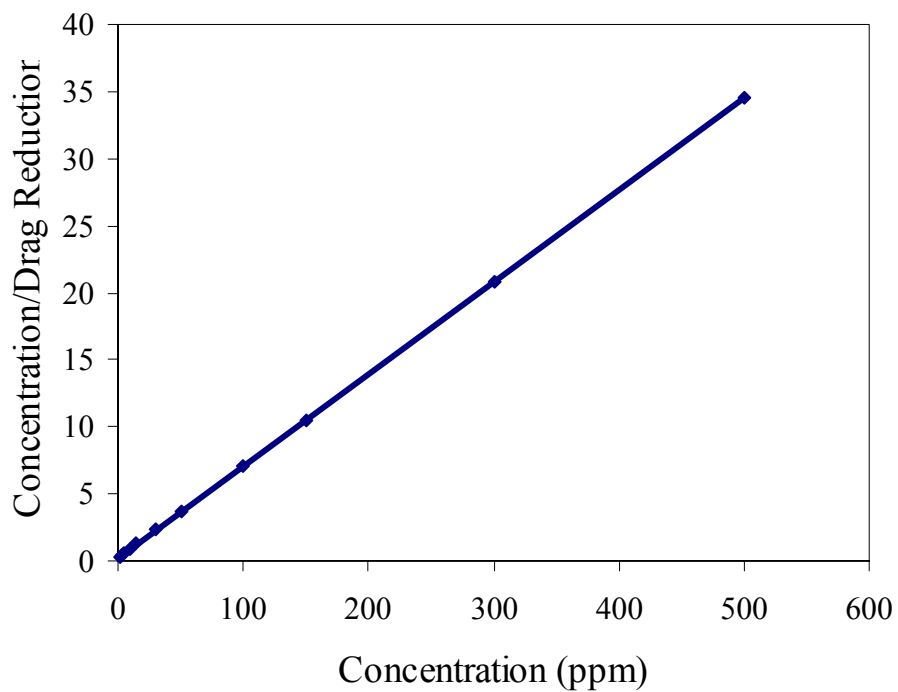


Figure 4-18 C/DR vs. Concentration of 4600 kg/mol PEO Solutions at (23.3-23.8 °C).

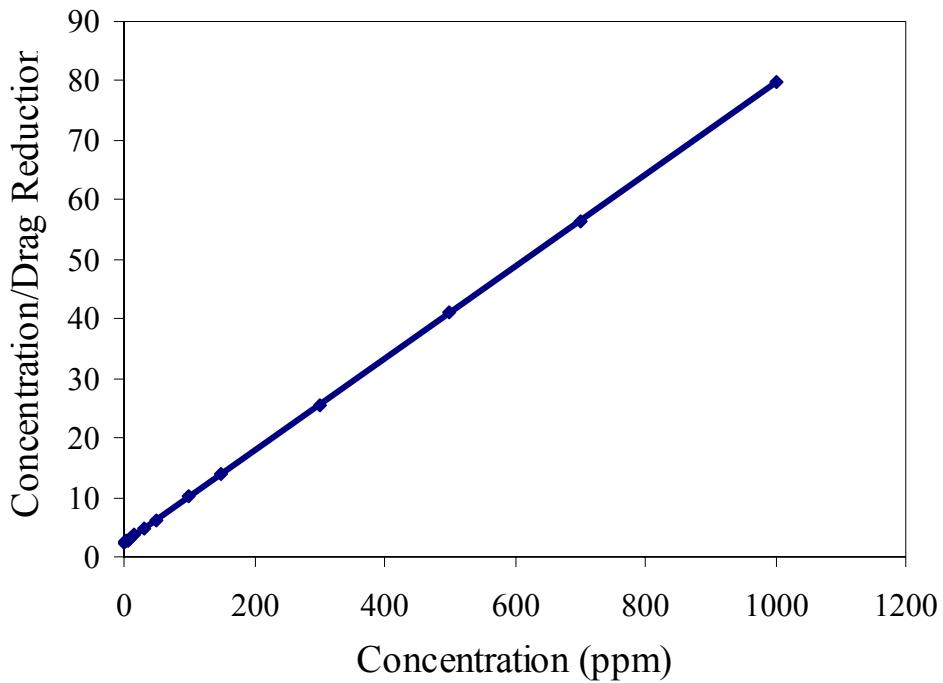


Figure 4-19 C/DR vs. Concentration of 1100 kg/mol PEO Solutions at (23.3-23.8 °C).

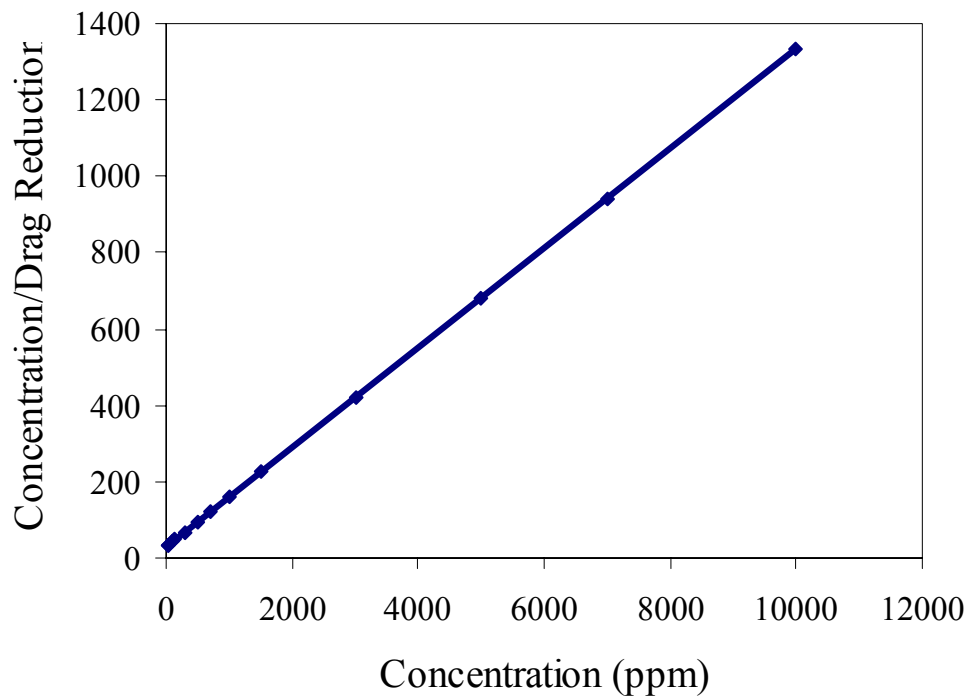


Figure 4-20 C/DR vs. Concentration of 370 kg/mol PEO Solutions at (23.3-23.8 °C).

Figures 4-17 to 4-20 show the linear correlation between the polymer concentration and C/DR for four different molecular weights of PEO, which shows that equation (2.26), can be applied to drag-reduction polymer-solvent systems. The intercept value at $C/DR=0$ yields the intrinsic concentration $[C]$, as shown in table 4-28.

Table 4-29 Intrinsic Concentration of PEO Solutions at (23.3-23.8 °C)

Molecular Weight (kg/mol)	Intrinsic Concentration $[C]$ (ppm)
8000	1
4600	3.86
1100	31.31
370	222.79

Table 4-29 shows that the values of intrinsic concentration decreases with increasing the molecular weight of the polymer, where for various polymer-solvent systems, more efficient DR materials have a larger DR_{max} and a smaller $[C]$. $[C]$ is found to be an extremely useful quantity for normalizing the DR data of different molecular weight compounds into one homologous series

Chapter Five

Conclusions and Recommendations

5.1 Conclusions

Several conclusions have been extracted from the present work:

- 1- For dilute solution of polyethylene oxide in water, the reduced viscosity increases with increasing concentration as well as the intrinsic viscosity increases with increasing the molecular weight. The PEO behaves as neutral polymer.
- 2- k and a (Mark-Houwink constants) were determined for polyethylene oxide in water at temperature 25°C also for high molecular weight up to 8000 kg/mol , which has not been mentioned in the literature so far.
- 3- Critical molecular weights were determined for concentrated polyethylene oxide solutions at a wide range of molecular weights. Critical molecular weight increases with increasing the concentration at constant temperature.
- 4- The zero shear viscosity increases with increasing molecular weight of polyethylene oxide in water at constant concentration.
- 5- Polyethylene oxide solution behaves as a Newtonian fluid for the low molecular weights then the behavior changes to shear thinning behavior for the high molecular weights depending on the concentration.
- 6- The results of polyethylene oxide in water at 25°C were discussed in term of Maxwell and Bead-Spring models. The relaxation time of PEO calculated by the Bead-Spring model for high and moderate concentrated solutions complies with the experimental figures: the start of shear thinning behavior of flow curves as well as their viscoelastic properties, measured with frequency sweeps.

7- A new set-up to measure drag reduction was developed. The set-up is based on commercial rotational rheometer equipped with especial measuring plate with high diameter to enter the region of turbulent flow (high Reynolds numbers). Unlike other standard motors drives, the rheometer exhibits a very high precision of torque and speed measurement.

8- Percentage Drag reduction, intrinsic drag reduction, drag reduction, and intrinsic concentration were determined for polyethylene oxide in water at temperature range (23.3-23.8°C) for high molecular weights up to 8000 kg/mol ,and this has not been mentioned in the literature.

9- High molecular weight polymer is more sufficient for drag reduction process than low molecular weight ones.

5.2 Recommendation

1- Determination of intrinsic viscosity and Mark-Houwink constants (k and a) of polyethylene oxide and other polymers like polyisobutlene, polystyrene in different solvents like methanol at different temperature.

2- Determination of the critical molecular weight and viscoelastic properties for different polymers in different solvents and at different temperatures and classify the behavior of these polymers in each solvent.

3- Determination of the drag reduction efficiency for other polymers with high molecular weight in different suitable solvents, which is important for different industries especially oil industry.

References

1. Martin Hubbe, Associate Professor of Wood and Paper Science, NC State University.
2. "Polyethylene Oxide", Encyclopedia of Polymer Science and Technology the free incyclopedia.htm, 2011.
3. High Purity Discrete PEG Oligomer Crystals Allow Structural Insight A.C. French, A.L. Thompson, B.G. Davis Angew. Chem. Intl Ed., Vol. 48, 1248-1252, 2009.
4. "Poly (ethylene glycol) and Poly (ethylene oxide)", <http://www.Sigma-Aldrich/Co.com> , 2011.
5. "Polyethylene Oxide", <http://www.Reference:table.com> : "description and solubility-P.htm".
6. Bailey Jr FE, Koleske JV. Poly (ethylene oxide), New York: Academic Press; 1976.
7. Finch CA, editor, Chemistry and technology of water soluble polymers. New York: Prenum Press; 1983.
8. Jun H. S., Dong C. L., Hyun J. P., "Conformational characteristics of poly (ethylene oxide) (PEO) in methanol" polymer, Vol. 48, 4205-4212, May 2007.
9. "Final Report on the Safety Assessment of PEG-2, -3, -5, -10, -15, and -20 Cocamine". International Journal of Toxicology, Vol. 18 (3): 43–50. 1999.
10. Y. Chen, Journal of Polymer Science: Part A: Polymer Chemistry, Vol. 42, 2263–2271, 2004.
11. P.J. Carreau, POLYM. ENG. SCI., Society of Plastics Engineers, Vol. 45:1385–1394, 2005.
12. Y. Fang, P.J. Carreau, and P.G. Lafleur, Polym. Eng. Sci., 43, 1391,

- 2003.
13. I.W. Hamley, *Angew. Chem. Int. Ed.*, Vol. 42, 1682, 2003.
 14. S. Hou, D. Taton, M. Saule, J. Logan, E. Chaikof, Y. Gnanou, *Polymer*, Vol. 44, 5067, 2003.
 15. Macromol, "Multiarm star polymer (PEO)", *Chem. Phys.*, Vol. 211, 35–44, 2010.
 16. R. Byron Bird, *Dynamics of Polymeric Liquids*, Vol. 1, Fluid Mechanics, 112-114, 1948.
 17. J. D. Ferry, *Viscoelastic Properties of Polymers*, 3rd Ed, John Wiley, New York, 1980.
 18. F. C. MacKintosh and C. F. Schmidt, *Curr. Opin. Colloid Interface Sci.*, Vol. 4, 300, 1999.
 19. K. S. Choi, K. K. Prasad, and T. V. Truong, *Emerging Techniques in Drag Reduction*, Mechanical Engineering Publications Ltd., London, U.K., 1996.
 20. B. A. Toms, *Proceedings of the 1st International Rheological Congress, Part 2*, North Holland Publishing Co., the Netherlands, pp. 135–142, 1949.
 21. J. G. Savins, *Rheol. Acta*, Vol. 6, 323–330, 1967.
 22. A. Gyr and H. W. Bewersdorff, *Drag Reduction of Turbulent Flows by Additives*, Kluwer Academic Publishers, Dordrecht, the Netherlands, 1995.
 23. M. Gad-El-Hak, *Flow Control*, Cambridge University Press, Cambridge, U.K., 2000.
 24. T. Mousa and C. Tiu, *Chemical Engineering Science*, Vol. 49, 1681–1692, 1994.
 25. "View of the Structure of Rheologh" <http://www.google.com>

26. Ghosh, p., and Haltu, P.P.," Fundamental of polymer science, Molecular Weights of Polymers", <http://nsdl.niscair.in/bitstream/123456789/406/2/molecular+weights+of+polymers.Pdf>, 2006.
27. Flory, P.J., and T. G. Fox, JR, "Treatment of Intrinsic Viscosities", J. Am, Chem, Soc., Vol. 73, pp. 1904-1908, 1951.
28. "Macrolab Experiment Dilute Solution Viscosimetry, Molecular weight Determination by Dilute solution viscosity Measurements", <http://www.pslc.ws/macrog/lab/dsvh.htm>.
29. Cowie, J.M.G., "Polymer Chemistry and polymer science of Modern Materials", New York, 1973.
30. "Intrinsic viscosity", <http://www.google.it/search?hl=en&q=intrinsic+viscosity&btnG=Google+search>.
31. "Determination of Molecular Weight of polymers", http://74.125.113.132/search?q=cache:pkz6w_zqfkQJ:www.polymer.hacett, 2009.
32. Rodriguez, F., "Principles of polymer systems", second edition, McGraw –Hill Book Company, 1985.
33. Gowariker, V.R., N.V. Viswanathan and J. Sreedhar, "Polymer Science", John Wiley and Sons, New York, 1987.
34. Bianchi, U., and A. Peterlin, "Intrinsic Viscosity of Polymers of Low Molecular Weight", Vol. 6, 1759-1772, 1968.
35. Jeon, S. I., and G. D. Chang, "Temperature Dependence of the Intrinsic Viscosity for polyethylene oxide-Water and –Aqueous urea systems", Journal of the Korean Chemical Society, Vol. 40, No.12, 1996.
36. AbdeI-Azim A. AbdeI-Azim, Wagdy Y. Boutros, and El-Sayed M. AbdeI-Bary, Polymer, Vol. 39, No. 12, pp. 2543-2549, 1998.

37. B. Comanita, B. Noren, and J. Roovers, American Chemical Society Macromolecules, Vol. 32, 1069-1072, 1999.
38. Hsin-Lung Chen, Chung-Chi Ko, Wen-Chung Ou-Yang and Tsang-Lang Lin Journal of Polymer Research, Vol. 9: 221–226, 2002.
39. Cormick Mc. L., “Water-Soluble Polymers”, Encyclopedia of Polymer Science and Technology, Vol. 12, P. 452, 2005.
40. Sperling L.H., “Introduction to Physical Polymer Science”, 4th edition, Canada, 2006.
41. Buche F., Physical Properties of Polymers; Interscience, New York, 1962.
42. A. Eich, Viscosity of Polymer Solutions, Exp. 5, 1-19, 2011.
43. William W. Graessley, Advances in Polymer Science, Vol. 16, 125-138, New York, 1974.
44. Rouse, P. E., Jr., J. Chem. Phys., Vol. 21, 1872, 1953.
45. Zimm, B. H., J. Chem. Phys., Vol. 24, 269, 1956.
46. Mezger, T. G.; the Rheology Handbook, 2nd ed.; Vincentz Network: Hanover, Chapter 3, pp 29–73, 2006.
47. A. Varesano, A. Aluigi, C. Vineis, C. Tonin, Journal of Polymer Science: Part B: Polymer Physics, Vol. 46, 1193–1201, 2008.
48. L. Nielson, Polymer Rheology, Marcel Dekker, New York, 1997.
49. E. Kiran and Z. Gokmenoglu, J. Appl. Polym. Sci., Vol. 58, 2307, 1995.
50. E. Kiran and Y. Sen, ACS Symp. Series, 514, 104, 1993.
51. Y. Xiong and E. Kiran, Polymer, Vol. 38, 4817, 1997.
52. Y. Xiong and E. Kiran, Polymer, Vol. 38, 5185, 1977.
53. B. Briscoe, and P. Luckham, S. Zhu, Journal of Applied Polymer Science, Vol. 70, 419–429, 1998.

54. Matthew M. Malwitz, Paul D. Butler, Lionel Porcar, Drew P. Angelette, Gudrun Schmidt, *Journal of Polymer Science: Part B: Polymer Physics*, Vol. 42, 3102-3112, 2004.
55. K. Niedzwiedz, A. Wischniewski, W. Pyckhout-Hintzen, J. Allgaier, D. Richter, *Macromolecules*, Vol. 41, 4866-4872, 2008.
56. Burger ED, Chorn LG, Perkins TK, *J Rheol*, Vol. 24:603, 1980.
57. R. P. Singh, *Encyclopedia of Fluid Mechanics*, Vol. 9, Gulf Publishing Co., Houston, Tex., Chapt. 14, pp. 425–480, 1990.
58. R. H. J. Sellin, J. W. Hoyt, and O. Scrivener, *J. Hydraulic. Res.*, Vol. 20, 29–68, 1982.
59. R. H. J. Sellin, J.W. Hoyt, J.W. Pollert, and O. Scrivener, *J. Hydraulic. Res.*, Vol. 20, 235–292, 1982.
60. J.W. Hoyt, in Y. Rabin, ed., *AIP Conference Proceedings Series, Polymer Flow Interaction*, American Institute of Physics, New York, pp. 95–115, 1985.
61. J. L. Zakin, B. Lu, and H.W. Bewersdorff, in N. R. Amundson, D. Luss, and A. Marmur, eds., *Reviews in Chemical Engineering*, Vol. 14: *Surfactant Drag Reduction*, Freund Publishing House Ltd., London, England, pp. 253–320, 1998.
62. R. P. Singh, in P. N. Prasad, J. E. Mark and T. J. Fai, eds., *Polymer and other Advanced Materials: Emerging Technologies and Business Opportunities*, Plenum Press, New York, Vol. 1, pp. 227–250, 1995.
63. J. W. Hoyt, *Encyclopedia of Polymer Science and Engineering*, 2nd ed., Vol. 5, pp. 129–157, 1986.
64. J. Pollert, in G. Gampert, ed., *IUTAM Symposium*, Essen, Germany, 1984, Springer- Verlag, Berlin, pp. 371–395, 1985.
65. J. W. Hoyt, in R. H. J. Sellin and R. T. Moses, eds., *Drag Reduction*,

- University of Bristol, pp. I.1-1–I.1-8, 1984.
66. Ousterhout RS, Hall CD, *J Petroleum Technol*, Vol. 13:217, 1961.
 67. Sellin RH, Ollis M, *J Rheol*, Vol. 24:667-684, 1980.
 68. Golda J, *Chem Eng Commun*, Vol. 43:53-67, 1986.
 69. "Drag Reduction in Flow: Review and Application", *Journal of Industrial and Engineering Chemistry*, Vol. 14, 409-416, 2008.
 70. Kim CA, Choi HJ, Kim CB, Jhon MS, *Macromol Rapid Commun*, Vol. 19:419-422, 1998.
 71. Shenoy AV, *Colloid Polymer Sci*, Vol. 262:319-337, 1984.
 72. Armstrong R, Jhon MS, *J Chem Phys*, Vol. 77:4256-4257, 1982; *J Chem Phys*, Vol. 79:3143-3147, 1983.
 73. Oldroyd, J. G. Suggested Method of Detecting Wall Effects on Turbulent Flow through Tubes. *Proceedings of the 1st Congress on Rheology*; North-Holland: Amsterdam, Vol. 2, p 130, 1948.
 74. Toms, B. A. some Observations on the Flow of Linear Polymer Solutions through Straight Tubes at Large Reynolds-Numbers. *Proceedings of the 1st Congress on Rheology*; North-Holland: Amsterdam, Vol. 2, p 135, 1948.
 75. Little RC, *J Colloid Interface Sci*, Vol. 37:811, 1971.
 76. Choi HJ, Jhon MS, *Ind Eng Chem Res*, Vol. 35:2993-2998, 1996.
 77. Ruckenstein, E. A. Note on the Mechanism of Drag Reduction. *J. Appl. Polym. Sci.*, Vol. 17, 3239, 1973.
 78. Armstrong R, Jhon MS, *Chem Eng Commun* 30:99-111, 1984.
 79. Tabor M, de Gennes PG, *Euro-phys Lett*, Vol. 2(7):519-522, 1986.
 80. De Gennes PG, 1986, *Physica* 140 A: 9; 1990, *Introduction to Polymer Dynamics*, Cambridge University Press, Cambridge, UK.
 81. Cadot O, Bonn D, Douady S, *Phys Fluids*, Vol. 10:426-436, 1998.

82. Anshuman Roy and Ronald G. Larson, *Applied Rheology*, Vol. 15, Issue 6, 370–389, 2005.
83. Rheometric, Inc., "Rheometrics Fluids Analyzer", publication number 902-001118.
84. Baghdadi HA, Sardinha H, Bhatia SR. *Journal of Polymer Science, Part B: Polymer Physics*, Vol. 43(2):233–40, 2005.
85. Morgan SE, McCormick CL. *Progress in Polymer Science*, Vol. 15(1):103–45, 1990.
86. Gil ES, Hudson SA. *Progress in Polymer Science*, Vol. 29(12):1173–222, 2004.
87. Figueredo RCR, Sabadini E. *Colloids and Surfaces A: Physicochemical and Engineering Aspects*, Vol. 215(1–3):77–86, 2003.
88. Kauser N, Dos Santos L, Delgado M, Muller AJ, Saez AE. *Journal of Applied Polymer Science*, Vol. 72(6):783–95, 1999.
89. Rodriguez S, Romero C, Sargenti ML, Muller AJ, Saez AE, Odell JA. *Journal of Non-Newtonian Fluid Mechanics*, Vol. 49(1):63–85, 1993.
90. Addai-Mensah J, Yeap KY, McFarlane AJ. *Powder Technology*, 179(1–2): 79–83, 2007.
91. Toryanik AI. *Journal of Structural Chemistry*, 25(3):385–8, 1984.
92. Straziel C. *Makromolekulare Chemie: Macromolecular Chemistry and Physics*, 119(DEC):50–63, 1968.
93. Saeki S, Kuwahara N, Nakata M, Kaneko M. *Polymer*, Vol. 17(8):685–9, 1976.
94. Malcolm GN, Rowlinson JS. *Transactions of the Faraday Society*, Vol. 53(7):921–31, 1957.
95. Dormidontova EE. *Macromolecules*, Vol. 37(20):7747–61, 2004.

96. Smith GD, Bedrov D, Borodin O. *Physical Review Letters*, 85(26):5583, 2000.
97. Tasaki K. *Journal of the American Chemical Society*, Vol. 118(35):8459–69, 1996.
98. Berman NS. "Annual Review of Fluid Mechanics", Vol. 10:47–64, 1978.
99. Berman NS. *Physics of Fluids*, Vol. 20(5):715–8, 1977.
100. White CM, Mungal MG. *Annual Review of Fluid Mechanics*, Vol. 40:235–56, 2008.
101. Larson RG. *Journal of Rheology*, Vol. 49(1):1–70, 2005.
102. Virk PS, Merrill EW, Mickley HS, Smith KA, Mollo-Christensen EL, *J Fluid Mech*, 30:305, 1967.
103. Hyoung J. Choi, and Myung S. Jhon, *Ind. Eng. Chem. Res.*, Vol. 35, 2993-2998, 1996.
104. H. J. Choi & C. A. Kim .J. H., Sung Department of Polymer Science and Engineering, Inha University Inchon 402-751, Korea, 2000.
105. Slaiman, I.N., "Effectiveness of Polyisobutylene of Drag Reducing Agent in Turbulent Pipe Flow", Ph.D thesis, Al-Nahrain University, Baghdad, 2000.
106. Taofeaq, H. M., "Effect of molecular Weight on Turbulent Drag Reduction with polyisobutylene Additives", M.Sc thesis, Al-Nahrain University, Baghdad, 2006.
107. Mohamed, H.J., "Study of Drag Reduction in Turbulent Flow Using High Molecular Weight Polymers", M.Sc thesis, Al-Nahrain University, Baghdad, 2006.
108. Atshan, A. A., "Turbulent Drag Reduction of polyacrylamide and Xanthan Gum, Experimental and Theoretical Investigation, M.Sc

- thesis, Al- Nahrain University, Baghdad, 2008.
109. Abdul Jabbar, M. F., " The Influence of Mechanical Effects on Degradation of Drag Reducing Agents", M.Sc thesis, Al-Nahrain University, Baghdad, 2008.
 110. Gregory, Huglin, Makromol.Chem., Vol. 187, 1745-1755, (1986).
 111. Pascal Azerad and Eberhard Bansch "Quasi-Stability of the Primary Flow in a Cone and Plate Viscometer" J. math. fluid mech. 6, pp 253–271, 2004.
 112. Lebedeva, O. V., "Technology of Pressure –Sensitive Adhesives and Product", CRC Press, chapter four, 2009.
 113. Zeynali, M. E., A. Rabii, and H. Baharvand, "Synthesis of Partially Hydrolyzed Polyacrylamide and Investigation of Solution Properties (Viscosity Behaviour)", Iranian polymer Journal, Vol. 13, No.6, pp. 479- 484, 2004.
 114. G. Ahmadi, "Turbulence", Klarkson university, pp. 637, 1-5.

Appendix A

Intrinsic Viscosity

Table A-1 Linear Polyethylene Oxide of Molecular Weight 1 kg/mol with Water at
Temperature 25°C, Time of Water = 256.41 sec

Conc. (g/ml)	Time (s)	$\eta_r =$ t/t_0	η_{sp} $= t-t_0/t_0$	η_{red} $= \eta_{sp}/\text{conc.}$	$[\eta]$ (ml/g)	k'
0.158	443.63	1.73	0.73	4.61	4.1	0.179
0.119	391.41	1.527	0.527	4.433		
0.095	361.71	1.411	0.411	4.322		
0.079	342.62	1.336	0.336	4.246		
0.059	321.9	1.255	0.255	4.301		
0.048	307.61	1.199	0.199	4.203		
0.04	299.56	1.168	0.168	4.25		

Table A-2 Linear Polyethylene Oxide of Molecular Weight 3 kg/mol with Water at
Temperature 25°C, Time of Water = 256.41 sec

Conc. (g/ml)	Time (s)	$\eta_r =$ t/t_0	η_{sp} $= t-t_0/t_0$	η_{red} $= \eta_{sp}/\text{conc.}$	$[\eta]$ (ml/g)	k'
0.062	628.25	2.453	1.453	23.34	17.4	0.335
0.047	521.51	2.036	1.036	22.193		
0.037	462.61	1.806	0.806	21.584		
0.031	428.39	1.673	0.673	21.608		
0.023	370.3	1.446	0.446	19.094		
0.019	348.86	1.362	0.362	19.384		
0.016	330.65	1.291	0.291	18.693		

Table A-3 Linear Polyethylene Oxide of Molecular Weight 10 kg/mol with Water at
Temperature 25°C, Time of Water = 256.41 sec

Conc. (g/ml)	Time (s)	$\eta_r =$ t/t_0	η_{sp} $= t-t_0/t_0$	η_{red} $= \eta_{sp}/\text{conc.}$	$[\eta]$ (ml/g)	k'
0.036	591.34	2.309	1.309	36.779	25.8	0.513
0.027	499.84	1.951	0.951	35.652		
0.021	443.62	1.732	0.732	34.285		
0.018	403.49	1.575	0.575	32.334		
0.013	357.12	1.394	0.394	29.544		
0.011	336.3	1.313	0.313	29.317		
0.009	320.56	1.252	0.252	28.272		

Table A-4 Linear Polyethylene Oxide of Molecular Weight 20 kg/mol with Water at
Temperature 25°C, Time of Water = 256.41 sec

Conc. (g/ml)	Time (s)	$\eta_r =$ t/t_0	η_{sp} $= t-t_0/t_0$	η_{red} $= \eta_{sp}/\text{conc.}$	$[\eta]$ (ml/g)	k'
0.023	597.97	2.332	1.332	57.689	36.8	0.683
0.017	481.71	1.879	0.879	50.738		
0.014	426.4	1.663	0.663	47.852		
0.012	393.57	1.535	0.535	46.333		
0.009	355.07	1.385	0.385	44.435		
0.007	331.39	1.292	0.292	42.215		
0.006	320.05	1.248	0.248	42.995		

Table A-5 Linear Polyethylene Oxide of Molecular Weight 35 kg/mol with Water at
Temperature 25°C, Time of Water = 180.67sec

Conc. (g/ml)	Time (s)	$\eta_r =$ t/t_0	η_{sp} $= t-t_0/t_0$	η_{red} $= \eta_{sp}/\text{conc.}$	$[\eta]$ (ml/g)	k'
0.011	299.4	1.657	0.657	61.469	53.3	0.289
0.008	266.23	1.474	0.474	59.06		
0.006	247.21	1.368	0.368	57.416		
0.005	235.31	1.302	0.302	56.578		
0.004	220.97	1.223	0.223	55.636		
0.0032	212.73	1.177	0.177	55.32		
0.0027	207.12	1.146	0.146	54.773		
0.0023	203.38	1.126	0.126	54.866		

Table A-6 Linear Polyethylene Oxide of Molecular Weight 99 kg/mol with Water at
Temperature 30°C, Time of Water = 256.15 sec

Conc. (g/ml)	Time (s)	$\eta_r =$ t/t_0	η_{sp} $= t-t_0/t_0$	η_{red} $= \eta_{sp}/\text{conc.}$	$[\eta]$ (ml/g)	k'
0.0097	598.19	2.333	1.333	137.592	98.6	0.413
0.0073	491.47	1.917	0.917	126.174		
0.0058	442.48	1.726	0.726	124.849		
0.0048	401.76	1.567	0.567	117.03		
0.0036	361.45	1.41	0.41	112.761		
0.0029	338.49	1.32	0.32	110.15		
0.0024	323.74	1.263	0.263	108.423		

Table A-7 Linear Polyethylene Oxide of Molecular Weight 370 kg/mol with Water at
Temperature 30°C, Time of Water = 256.15 sec

Conc. (g/ml)	Time (s)	$\eta_r =$ t/t_0	η_{sp} $= t-t_0/t_0$	η_{red} $= \eta_{sp}/\text{conc.}$	$[\eta]$ (ml/g)	k'
0.0029	512.47	2.001	1.001	344.7	274.1	0.31
0.0022	434.67	1.697	0.697	320.101		
0.0017	393.77	1.537	0.537	308.465		
0.0015	374.4	1.462	0.462	318.052		
0.0011	339.37	1.325	0.325	298.437		
0.0009	321.54	1.255	0.255	293.136		
0.0007	310.27	1.211	0.211	291.158		

Table A-8 Linear Polyethylene Oxide of Molecular Weight 1100 kg/mol with Water at
Temperature 30°C, Time of Water = 256.15 sec

Conc. (g/ml)	Time (s)	$\eta_r =$ t/t_0	η_{sp} $= t-t_0/t_0$	η_{red} $= \eta_{sp}/\text{conc.}$	$[\eta]$ (ml/g)	k'
0.0007	386.46	1.5088	0.5088	726.251	622.8	0.393
0.00053	350.4	1.36797	0.3680	700.363		
0.00042	330.75	1.2913	0.2913	692.939		
0.00035	317.42	1.2392	0.2392	682.99		
0.00026	300.77	1.1742	0.1742	663.215		
0.00021	291.19	1.1368	0.1368	650.994		
0.00018	285.11	1.1131	0.1131	645.659		

Table A-9 Linear Polyethylene Oxide of Molecular Weight 4600 kg/mol with Water at Temperature 30°C, Time of Water = 256.15 sec

Conc. (g/ml)	Time (s)	$\eta_r =$ t/t_0	η_{sp} $= t-t_0/t_0$	η_{red} $= \eta_{sp}/\text{conc.}$	$[\eta]$ (ml/g)	k'
0.00032	386.77	1.51	0.51	1578.972	1339.8	0.407
0.00024	349.5	1.365	0.365	1504.623		
0.00019	330.42	1.29	0.29	1496.325		
0.00016	316.36	1.235	0.235	1455.606		
0.00012	300.37	1.173	0.173	1425.607		
0.0001	290.95	1.136	0.136	1402.19		
0.00008	285.24	1.114	0.114	1406.708		

Table A-10 Linear Polyethylene Oxide of Molecular Weight 8000 kg/mol with Water at Temperature 30°C, Time of Water = 256.15 sec

Conc. (g/ml)	Time (s)	$\eta_r =$ t/t_0	η_{sp} $= t-t_0/t_0$	η_{red} $= \eta_{sp}/\text{conc.}$	$[\eta]$ (ml/g)	k'
0.00032	481.24	1.879	0.879	2725.308	2353.3	0.243
0.00024	423.73	1.654	0.654	2705.293		
0.00019	388.5	1.517	0.517	2670.776		
0.00016	364.25	1.422	0.422	2617.64		
0.00012	334.32	1.305	0.305	2523.961		
0.0001	317.21	1.238	0.238	2464.559		
0.00008	305.71	1.194	0.194	2400.53		

Table A-11 Linear Polyethylene Oxide of Molecular Weight 99 kg/mol with Water at
Temperature 25°C, Time of Water = 289.22 sec

Conc. (g/ml)	Time (s)	$\eta_r =$ t/t_0	η_{sp} $= t-t_0/t_0$	η_{red} $= \eta_{sp}/\text{conc.}$	$[\eta]$ (ml/g)	k'
0.0098	667	2.306	1.306	132.883	88.9	0.577
0.0074	550.69	1.904	0.904	122.63		
0.0059	487.3	1.685	0.685	116.125		
0.0049	448.29	1.55	0.55	111.902		
0.0042	421.91	1.459	0.459	108.902		
0.0033	388.03	1.342	0.342	104.266		
0.0027	368.23	1.273	0.273	101.898		
0.0023	354.03	1.224	0.224	98.778		
0.002	343.85	1.189	0.189	96.084		

Table A-12 Linear Polyethylene Oxide of Molecular Weight 370 kg/mol with Water at
Temperature 25°C, Time of Water = 303.022 sec

Conc. (g/ml)	Time (s)	$\eta_r =$ t/t_0	η_{sp} $= t-t_0/t_0$	η_{red} $= \eta_{sp}/\text{conc.}$	$[\eta]$ (ml/g)	k'
0.0026	598.34	1.975	0.975	374.303	303.5	0.284
0.002	512.25	1.691	0.691	353.578		
0.0016	465.18	1.535	0.535	342.551		
0.0013	435.70	1.438	0.438	336.322		
0.0011	414.76	1.369	0.369	330.457		
0.0009	388.57	1.282	0.282	325.301		
0.0007	372.57	1.23	0.23	323.232		
0.0006	361.26	1.192	0.192	319.865		
0.0005	353.49	1.167	0.167	319.854		

Table A-13 Linear Polyethylene Oxide of Molecular Weight 1100 kg/mol with Water at
Temperature 25°C, Time of Water = 289.22 sec

Conc. (g/ml)	Time (s)	$\eta_r =$ t/t_0	η_{sp} $= t-t_0/t_0$	η_{red} $= \eta_{sp}/\text{conc.}$	$[\eta]$ (ml/g)	k'
0.00068	432.34	1.495	0.495	729.956	539.1	1.016
0.00051	390.72	1.351	0.351	690.285		
0.00041	367.66	1.271	0.271	666.768		
0.00034	352.74	1.22	0.22	647.924		
0.00029	342.23	1.183	0.183	630.832		
0.00023	328.85	1.137	0.137	606.39		
0.00018	320.8	1.109	0.109	590.658		
0.00016	315.49	1.091	0.091	580.689		
0.00014	311.64	1.078	0.078	571.758		

Table A-14 Linear Polyethylene Oxide of Molecular Weight 4600 kg/mol with Water at
Temperature 25°C, Time of Water = 303.022 sec

Conc. (g/ml)	Time (s)	$\eta_r =$ t/t_0	η_{sp} $= t-t_0/t_0$	η_{red} $= \eta_{sp}/\text{conc.}$	$[\eta]$ (ml/g)	k'
0.00031	465.53	1.536	0.536	2245.485	1290.4	0.757
0.00023	421.23	1.39	0.39	2109.9		
0.00019	394.5	1.302	0.302	2024.748		
0.00015	376.77	1.243	0.243	1940.018		
0.00012	355.66	1.174	0.174	1795.416		
0.00009	344.38	1.137	0.137	1642.818		
0.00008	336.64	1.111	0.111	1545.548		
0.00031	331.55	1.094	0.094	2245.485		

Table A-15 Linear Polyethylene Oxide of Molecular Weight 8000 kg/mol with Water at
Temperature 25°C, Time of Water = 289.22 sec

Conc. (g/ml)	Time (s)	$\eta_r =$ t/t_0	η_{sp} $= t-t_0/t_0$	η_{red} $= \eta_{sp}/\text{conc.}$	$[\eta]$ (ml/g)	k'
0.00031	490.16	1.695	0.695	2245.485	1410.4	1.477
0.00023	430.83	1.49	0.49	2109.9		
0.00019	397.93	1.376	0.376	2024.748		
0.00015	376.02	1.3	0.3	1940.018		
0.00012	349.47	1.208	0.208	1795.416		
0.00009	333.32	1.153	0.153	1642.818		
0.00008	323.8	1.12	0.12	1545.548		

Table A-16 Branched Polyethylene Oxide of Molecular Weight 0,55 kg/mol with Water at
Temperature 25°C, Time of Water = 289.22 sec

Conc. (g/ml)	Time (s)	$\eta_r =$ t/t_0	η_{sp} $= t-t_0/t_0$	η_{red} $= \eta_{sp}/\text{conc.}$	$[\eta]$ (ml/g)	k'
0.093	436.69	1.51	0.51	5.457	3.8	1.174
0.07	391.48	1.354	0.354	5.045		
0.056	367.6	1.271	0.271	4.834		
0.047	351.64	1.216	0.216	4.62		
0.035	335.44	1.14	0.14	4.561		
0.028	324.19	1.121	0.121	4.313		
0.023	317.51	1.098	0.098	4.188		

Table A-17 Branched Polyethylene Oxide of Molecular Weight 40 kg/mol with Water at
 Temperature 25°C, Time of Water = 285.95 sec

Conc. (g/ml)	Time (s)	$\eta_r =$ t/t_0	η_{sp} $= t-t_0/t_0$	η_{red} $= \eta_{sp}/\text{conc.}$	$[\eta]$ (ml/g)	k'
0.0163	451.39	1.579	0.579	35.611	27.5	0.67
0.0122	403.21	1.41	0.41	33.653		
0.0098	376.29	1.316	0.316	32.409		
0.0081	359.22	1.256	0.256	31.542		
0.0061	339.23	1.186	0.186	30.582		
0.0049	327.7	1.146	0.146	29.952		
0.0041	320.12	1.12	0.12	29.418		

أخلاصة

لقد تم دراسة اللزوجة الجوهرية، شروط الأنتقال من الحالة الجزيئية الى الحالة الشبكية (الوزن الجزيئي الحرج)، خواص اللزوجة، وعامل تقليل الاحتكاك للبولي أثيلين أوكسايد في الماء لأستخدامة على نطاق واسع في التطبيقات الصناعية. حيث تم أستخدام أنواع وأوزان جزيئية مختلفة من هذا البوليمر، النوع الأول خطي وقد غطى مدى واسع من الأوزان الجزيئية وهي 1- 8000 كغم\مول. اما النوع الثاني المتفرع وقد تم أستخدام الوزنان الجزيئان 0,55 و 40 كغم\مول.

قد تم تحديد اللزوجات الجوهرية وثوابت هاغينز لجميع الأنواع عند درجة حرارة 25 درجه مئوية بأستخدام جهاز قياس اللزوجة الشعرية Capillary Viscometer. وقد وجد أن قيم ثوابت (a, K) Mark-Howink تزداد مع أزدیاد أوزن الجزيئي للبولي أثيلين أوكسايد الخطي والمتفرع. قياسات أوزن الجزيئي الحرج وخواص اللزوجة اجريت للبولي أثيلين أوكسايد الخطي في الماء لتراكيذ مختلفة عند درجة حرارة 25 درحة مئوية بأستخدام جهاز قياس اللزوجة الدوراني، وقد وجد أن أوزن الجزيئي الحرج يقل بأزدیاد التركيز. أما بالنسبة لخواص اللزوجة فقد وجد ان وقت الأسترخاء المقاس يوضح أختلاف كفاءة أوزن الجزيئي لتقليل الأحتكاك الجرياني للأوزان الجزيئية الأواطئة والعالية للبولي أثيلين أوكسايد: فقط الأوزان الجزيئية العالية < 1000 كغم\مول تبدي وقت أسترخاء عالي بصورة تكفي لتنشيط تأثير الدوامات في الجريان الأضطرابي.

قد تم أجراء حسابات تقليل الأحتكاك بأستخدام البولي أثيلين أوكسايد للأوزان الجزيئية للأوزان الجزيئية العالية بأستخدام جهاز قياس اللزوجة الدوراني لكن بأستخدام شكل هندسي وحاوية بأبعاد خاصة تم أضاقتها للجهاز للحصول على الجريان الأضطرابي، حيث وجد ان كمية البولي أثيلين أوكسايد الألازمه لتقليل معامل الاحتكاك للسائل اثناء الجريان تقل بزيادة أوزن الجزيئي.

شكر وتقدير

أضع قلمي بعد أن أنجزت هذا ألبحث لا يسعني إلا ان أشكر من كان وراء هذا
الأنجاز بعد شكر الله تعالى.

ويشرفني أن أتقدم بجزيل الشكر والعرفان لأستاذي الفاضل الدكتور طالب
بهجت عمر كشمولة لما أبداه لي من جهد في التوجيه والإرشاد والمتابعة فجزاة
الله عني خير الجزاء.

أود أيضاً ان أشكر البروفسور فولف وجميع منتسبي مجموعة العلمية في
جامعة ماينز الألمانية لما أبدوه من مساعدة من خلال السماح لي بالعمل في
مختبراتهم وعلى الإرشاد والتوجيه.

أستبرق سعد كامل

أتركيب أريولوجي لمحلول ألبولي أثيلين أوكسايد

رسالة

مقدمة الى كلية الهندسة في جامعة النهرين
وهي جزء من متطلبات نيل درجة ماجستير علوم
في الهندسة الكيمياءوية

من قبل

أستبرق سعد كامل الكرطان
بكلوريوس علوم في الهندسة الكيمياءوية 2009

1433
2012

جمادى الأولى
نيسان